Integrating Comprehensive Air Quality Modeling with Policy Analysis:
Applications for Distributed Electricity Generation

Elisabeth Anne Gilmore

Submitted in partial fulfillment of the requirements for the degree of Doctor of Philosophy in Engineering & Public Policy and Chemical Engineering

Doctoral Committee
Professor Lester B. Lave (Advisor)
Professor Peter J. Adams (Advisor)
Professor Jay Apt
Professor Neil Donahue
Professor Spyros Pandis
Professor Allen Robinson

April 23, 2009

Integrating Comprehensive Air Quality Modeling with Policy Analysis: Applications for Distributed Electricity Generation

Elisabeth Anne Gilmore

Abstract

Small scale and located close to the point of demand, distributed electricity generation (DG) could reduce the cost of electricity, improve grid reliability and support renewable technologies. These facilities also shift the magnitude, timing and location of air quality emissions. The costs from adverse human health effects caused by changes in air quality may outweigh any benefits. In this work, I evaluate the air quality, human health effects and costs for two DG applications. I transform the emissions into ambient concentrations using a chemical transport model, the Particulate Matter Comprehensive Air Quality Model with extensions ($PMCAM_x$), and dispersion plumes. I then translate the concentrations into health effects with concentration-response functions. Finally, I express the health effects as a social cost reflecting the "willingness to pay" to avoid these effects.

First, I investigate using installed backup generators instead of a more expensive peaking turbine for meeting peak electricity demand. Many of generators are uncontrolled diesel engines which have a high social cost. Adding a diesel particulate filter with exhaust gas recirculation to reduce fine particulate matter and nitrogen oxides can mitigate these costs. This result holds in four urban centers over a range of specified health endpoints and when accounting of uncertainty in the representation of the formation of secondary $PM_{2.5}$ in $PMCAM_x$. I conclude that properly controlled generators can be employed for meeting peak electricity demand without substantial harm to human health.

Second, I evaluate the changes in the net and distribution of social cost from integrating a utility-scale battery into the New York State electricity grid. Located in New York City, the battery would discharge when electricity prices are high and charge with cheaper generation during off peak hours. For most types of charging plants, I calculate a net

social benefit from displacing dirtier fuel oil peaking plants, but a net social cost from displacing natural gas peaking plants. In the short term, the upstate population experiences a social cost from the charging plant. In the long term, however, the battery may support renewable generation such as night time wind power resulting in benefits locally and statewide.

Extended Abstract

Small scale and located close to the point of demand, distributed electricity generation (DG) could reduce the cost of electricity, improve grid reliability and support renewable technologies such as wind power. These facilities, however, also shift the magnitude, timing and location of emissions that affect air quality. The costs from adverse human health effects caused by these changes in air quality may outweigh any benefits. In this work, I evaluate the air quality, human health effects and the costs associated with two applications for DG: 1) using installed backup generators for meeting peak electricity demand in Atlanta, Chicago, Dallas and New York City, and 2) integrating utility scale battery storage located in New York City into the New York Independent System Operator (NYISO) grid.

To quantify the costs associated with changes in air quality, I employ an impact pathway approach. First, I develop temporal and spatial emission profiles for the different DG applications. Emissions, however, cannot account for changes in exposure patterns or capture the formation of pollutants that are not emitted directly, such as ozone (O_3) and secondary fine particulate matter ($PM_{2.5}$). These pollutants are linked to the more pernicious health effects. Thus, I transform the emissions into ambient air concentrations using the chemical transport model, the Particulate Matter Comprehensive Air Quality Model with extensions ($PMCAM_x$), and dispersion models. To characterize exposure, I then translate the concentrations into their equivalent human health effects using concentration-response (CR) functions and population distributions. Finally, I express the health outcomes as a social cost reflecting the "willingness to pay (WTP)" to avoid these effects.

From a private cost perspective, using installed backup generators is more cost-effective for meeting peak electricity demand in urban centers than building a new peaking plant. Since the generators are already purchased to address blackout concerns, the additional costs for meeting peak electricity demand are mostly fuel costs and interconnection retrofits so the generators can operate in parallel with the electricity grid. The majority of

these generators, however, are diesel fueled internal combustion engines with significant air quality emissions. Additionally, since the generators are located in urban centers, there is a large potential to harm human health. With the impact pathway approach, I find that uncontrolled diesel generators have a high social cost. Adding emission controls, specifically a diesel particulate filter (DPF) with exhaust gas recirculation (EGR) to reduce $PM_{2.5}$ and nitrogen oxides (NO_x), can mitigate the social costs. The combined private and social cost of a diesel generator with these emission controls is less than a new peaking plant. I conclude that properly controlled generators can be employed for meeting peak electricity demand without substantial harm to human health. This result holds in four urban centers over a range of health endpoints and when accounting of uncertainties in secondary $PM_{2.5}$ formation mechanisms in $PMCAM_x$.

In New York City, sodium sulfur (NaS) batteries could be installed to supply electricity during the afternoon hours while charging with cheaper generation at off peak hours from the rest of the NYISO system. There may, however, be a net benefit or cost to the system depending on the type of generation displaced by the battery and the type used for charging. Using the impact pathway approach, I find that there is a benefit in New York City if the battery displaces dirtier in-city peaking plants. For most charging plants, I calculate a net social benefit if a peaking plant operating on distillate fuel oil is displaced and a net social cost if a peaking plant operating on natural gas is displaced. Further, using estimates of the frequency that each charging plant is used, I find that a system wide benefit occurs when fuel oil generation is displaced and natural gas fueled base-load generation is used to charge. From a distributional perspective, in the short term, the upstate population experiences a social cost from an increase in adverse health effects from the charging plant. In the long term, however, the battery may support renewable generation such as night time wind power resulting in benefits locally and statewide.

Acknowledgements

First and foremost, I would like to thank Dr. Lester Lave. He provided endless support and invaluable advice over the course of this dissertation. I appreciate his guidance and kindness in all matters, and he has had a tremendous impact on my thinking. I am also indebted to Dr. Peter Adams for his patience and his careful reviews of my work. He was a "secondary" advisor in name only. I would like to thank my committee members, Dr. Jay Apt, Dr. Neil Donahue, Dr. Spyros Pandis and Dr. Allen Robinson, as well as Dr. Paul Fischbeck, Dr. David Gerard, Dr. Granger Morgan, Dr. Cliff Davidson and countless other faculty members in the Engineering and Public Policy and Chemical Engineering departments for useful discussions and assistance in focusing my research. I would also like to acknowledge my many colleagues, specifically Dr. Seth Blumsack, Dr. Kathleen Spees and Dr. Jennifer Logue, Dr. Rahul Walawalkar for his work on the battery storage paper, and Dr. Pavan Racherla, Dr. Rob Pinder and Dr. John Dawson for helping me set up my first model runs and providing continued computing support. Additionally, I would like to thank the administrative staff for their help and warmth.

Last but not least, I am grateful for my family and friends who have been a constant source of encouragement and support. Specifically, I would like to thank Matthew Hamilton, Leonardo Reyes-Gonzalez, Jennifer Logue, Abbey Huggan, Amanda Corber, Siobhan Bond, Julie Saragosa and David Michael Wolach. But, most importantly, I would like to thank my father, Dr. Alan Gilmore. This thesis is dedicated to my mother.

This work was supported in part by the Alfred P. Sloan Foundation and the Electric Power Research Institute under grants to the Carnegie Mellon Electricity Industry Center (CEIC), and in part by the Pittsburgh Chapter of Achievement Rewards for College Scientists (ARCS), the Natural Sciences and Engineering Research Council of Canada (NSERC), the Link Energy Fellowship and United States Environmental Protection Agency (EPA) under the Science to Achieve Results (STAR) Graduate Fellowship Program. The research described within does not reflect the views of any of the funders.

Table of Contents

List of Figures

List of Tables

1. Introduction

1.1 Dissertation motivation

Exposure to adverse ambient air quality is linked to premature mortality and chronic and acute morbidity (e.g. cardiovascular and respiratory illnesses, asthma and reduced activity days) (1, 2). For sectors with substantial air emissions, like electricity, accounting for this externality is critical for developing and evaluating the full benefits and costs of different technologies, strategies and policies (3, 4). Presently, the electricity system consists primarily of large centralized generation facilities with substantial transmission and distribution (T&D) infrastructure to transport the electricity to where it is needed. The centralized facilities produce large amounts of emissions that affect air quality at one location, but are normally located far from highly populated areas. An alternative is to employ small-scale generation located close to the point of use (5). Known as distributed electricity generation (DG), this alternative system has the potential to produce significant benefits such as reducing the cost of generation, eliminating the need to site and construct T&D, improving grid reliability and supporting renewable technologies such as wind power. DG will also shift the magnitude, timing and location of air quality emissions with the changes depending on the type of DG (e.g. fossil fuel, renewable, battery, etc…). There is the potential that the cost from adverse human health effects caused by changes in air quality may outweigh any benefits. In this work, I evaluate the air quality, human health effects and costs for two applications for DG: 1) using installed backup generators for meeting peak electricity demand in Atlanta, Chicago, Dallas and New York City, and 2) integrating utility scale battery storage located in New York City into the New York Independent System Operator (NYISO) grid.

To evaluate the human health effects from changes in air quality, it is necessary to convert the emissions to ambient concentrations. Emissions are a poor metric of exposure; most people are exposed to the resulting ambient concentrations. In addition, while some of these pollutants are emitted directly like sulfur dioxide (SO_2) and nitrogen oxides (NO_x), pollutants that are linked to the most pernicious health effects (e.g. premature mortality) such as ozone (O_3) and a portion of the fine particulate matter (e.g.

particulate matter with an aerodynamic diameter less than 2.5 μm, $PM_{2.5}$) are formed by chemical reactions of precursor species. These pollutants also are subject to both short and long range transportation, affecting not only the adjacent population but those downwind. Three dimensional chemical transport models (CTMs) are the most comprehensive tool for capturing all of these features (6). Thus, an important part of this work is using and evaluating the 'state of science' CTM, Particulate Matter Comprehensive Air Quality Model with extensions ($PMCAM_x$) (7).

Converting emissions to ambient concentrations, however, does not provide information that is directly policy relevant. One policy approach is to convert these air quality effects into their equivalent monetary value (8). For air quality, an impact pathway or damage function analysis is the preferred analytical technique for monetization (9). Using concentrations-response (CR) functions derived from epidemiological studies, this technique converts the ambient concentrations to the equivalent changes in human health endpoints in the exposed population. The health effects are then monetized by multiplying the endpoints by a "willingness to pay (WTP)" to avoid these ill health effects (10). The resulting social cost can then be used to evaluate differences in the value of shifting electricity generation from one location to another as well as compared directly to other costs, such as the cost of electricity.

1.2 Dissertation methods, data and tools

The primary tool used in this work is the impact pathway approach with $PMCAM_x$. It is a bottom-up approach which builds the social cost through the following steps (10):

1. Develop spatial and temporal emission scenarios: Emission factors (EF) in grams per kilowatt-hour (g/kWh) for the different technologies and strategies are developed and compiled. These EFs are multiplied by representative operating scenarios.

2. Convert the emissions to ambient concentrations: A CTM or dispersion plumes are used to model the ambient concentrations from the operating emission scenarios. These concentrations are subtracted from baseline concentrations.

3. Translate the concentrations to human health effects: The change in ambient concentration is mapped onto the exposed population and converted to the change in health effects experienced by this population using CR functions. Derived from epidemiological studies, these functions capture the magnitude of the relationship between a pollutant and a health endpoint.

4. Convert the health effects to a social cost: The human health effects are multiplied by a WTP to avoid that effect.

This approach has been used to quantify the externalities from air quality (e.g. the European ExternE project,(11)), for policy evaluation (e.g. the Benefits and Costs of the Clean Air Act, (12, 13)), and other assessments where air quality is a major concern (e.g. the decision to retrofit vehicles with emission controls (14)). A criticism of this method is that it is highly dependent on the present state of understanding of the health effects and WTP estimates. Alternative methods of calculating the social costs are less economically sound. For example, using abatement costs assumes that regulators know the "true" damage costs. The impact pathway approach is also better suited for this analysis as it can provide policy guidance about specific sources and sites (9). I describe each element of this approach in more detail below.

1.2.1 Emission profiles

For electricity generation, emissions for a given pollutant are calculated by multiplying the EF by the amount of electricity generated (as shown in equation 1.1). While total emissions could be expressed for any time period, emissions for $PMCAM_x$ are expressed on an hourly basis.

$$Emissions = EF \cdot Generation \qquad \text{…Eqn 1.1}$$

Where Emissions is the emission rate for a given pollutant (in g/hour);

EF is the emission factor for a pollutant per unit of generation (in g/kWh); and,

Generation is the amount of electricity capacity used (in kW).

I start by collecting EFs relevant to air quality, specifically carbon monoxide (CO), hydrocarbons (HC) or non-methane hydrocarbons (NMHC), NO_x, $PM_{2.5}$ and SO_2. The majority of the EFs for this work are derived from the United States Environmental Protection Agency (USEPA) AP-42 compilation (15). This is supplemented by comprehensive literature reviews to capture a range of values. When measured values are not available for more innovative technologies, such as an integrated gasification combined cycle (IGCC), I use a process-based model, the Integrated Environmental Control Model (IECM), to develop suitable EFs (16). It is important to note that there can be significant variability, uncertainty and differences in quality for EFs for the same type of generator and fuel (17), justifying the use of conservative "worst case" scenarios.

These EFs also need to be further processed for $PMCAM_x$. Most of the factors, except those for $PM_{2.5}$, need to be converted from grams to moles. More importantly, however, EFs need to be disaggregated for comprehensive air quality modeling. For example, an EF for NO_x is divided into nitrogen oxide (NO) and nitrogen dioxide (NO_2) with the ratio of NO to NO_2 depending on the source. The composition of the chemical species that are grouped into the EF for HC is also a function of the emission source. Speciation profiles are available in a USEPA compilation known as SPECIATE (18). However, it would be computationally inefficient to model the chemical reactions for all HC species. As a result, I group the HC species into their chemically reactive functional groups as defined by the Carbon Bond Mechanism, CBM-IV (19, 20). Finally, $PM_{2.5}$ also consists of a range of organic and inorganic compounds, speciated into emissions of elemental carbon (PEC), organic carbon (POC), nitrate (PNO_3) and sulfate (PSO_4). For combustion sources, PEC and POC comprise the majority of the directly emitted $PM_{2.5}$. In addition to the composition, the EF for $PM_{2.5}$ also aggregates different sizes of particulates. In

$PMCAM_x$, the $PM_{2.5}$ is divided into six bins that represent sizes with aerodynamic diameters less than 2.5 μm.

To calculate the total emissions, operating or usage scenarios (e.g. the total amount of electricity generation per hour) are needed. In this work, I use several different data sources and approaches to develop these scenarios. For peak electricity demand, I isolate the peak hours using load data from the Federal Electricity Regulatory Commission (FERC) Form 714 collected from Independent System Operators (ISOs) and other utilities (21). This information is used to identify days with peak electricity demand for simulation and the amount of electricity generation by the backup generators. For the utility scale battery, there are no direct emissions from the battery. Rather, the changes in emissions are from generators being displaced in New York City and off-peak facilities in NYISO used to charge the battery. To estimate which types of generators are displaced and used for charging, I use a range of datasets, including the USEPA's Emissions & Generation Resource Integrated Database 2006 (eGRID2006) (22), the USEPA's National Electric Energy Data System (NEEDS) (23) and the Ventyx Velocity Suite, a private dataset (24). These datasets are discussed in more detail in Supporting Information for Chapter 4 (section 4.5). The emissions are disaggregated by location of electricity generation consistent with the grid resolution in $PMCAM_x$ (e.g. 36 km by 36 km or 12 km by 12 km). The data and techniques for each DG application are discussed in more detail in the individual chapters.

1.2.2 Particulate Matter Comprehensive Air Quality Model with extensions ($PMCAM_x$)

Three-dimensional CTMs that can accurately describe the behavior of the atmospheric pollutants with computational efficiency are crucial for the evaluation of alternative electricity generation strategies (6). In this work, I use the Comprehensive Air Quality Model with extensions and particulate matter modules ($PMCAM_x$). $PMCAM_x$ is a 'state of science' CTM that simulates the emission, advection (convection), dispersion, gas and aqueous phase chemical reactions, and dry and wet deposition for 60 chemical species (35 gaseous species, 12 radical species and 13 aerosol species in 10 size bins with 6 size

bins for aerodynamic diameters less than 2.5 μm) on a 3-D Eulerian grid. Additional modules simulate the dynamic behavior (coagulation, condensation, and nucleation) of aerosol. The gas and aqueous phase chemistry are simulated with the Carbon Bond Mechanism IV (CBM-IV) (19) and the Regional Acid Deposition Model (RADM) (25), respectively. The evaporation and condensation processes are modeled using a bulk equilibrium approach (26, 27). Two product adsorptive partitioning models the formation of secondary organic aerosol (SOA) from semi-volatile organic species (28). The inorganic aerosol behavior is modeled using ISORROPIA, an thermodynamic equilibrium method (29). Meteorological inputs are generated with the MM5 meteorological model with available meteorological files for July 12 – 28, 2001 (30). The baseline emission files are from the Lakeh Michigan Air Directors Consortium (LADCO) (31). For the base model in this work, the domain is discretized into a 36 km by 36 km horizontal grid. I also use an interpolated grid of 12 km by 12 km to better resolve smaller emission changes for the utility scale batteries (Chapter 4). The vertical grid is discretized into 14 vertical layers between the surface and 6 km. The lowest model layer is slightly less than 30 m thick vertically. Additional details and evaluation can be found in Gaydos et al. (2006) (7) and Karydis et al. (2007) (32).

1.2.3 Dispersion models

Since distributed sources are located close to receptors, dispersion on a local scale is also of concern (e.g. 'hot spots' near the source). While this work focuses on using CTMs, I also employ Gaussian dispersion plumes as a screening tool for the installed backup generator analysis (Chapter 2). While dispersion models do not capture the formation of secondary pollutants, chemical reactions are less important over shorter distances and time scales. The form of the dispersion plume in this work is a perfectly reflecting surface producing conservative boundary conditions. Since I am modeling urban centers, I use dispersion parameters for an urban environment from Briggs (1973) (33). The form of the equation (Equation 2.2) and assumptions are presented in section 2.2.

1.2.4 Concentration-response functions and human health effects

Epidemiological research has found a consistent and reproducible statistical association between short and long term exposure to adverse air quality and increases in morbidity and mortality (2). The results from these studies can be transformed into CR functions which relate the change in the number of individuals in a population exhibiting an adverse health effect to a change in an ambient pollutant concentration experienced by that population. The change in health endpoint is then multiplied by the exposed population to yield the total response. I show the most common form of the CR function in Equation 1.2.

$$Response = \left(1 - exp(\beta \cdot \Delta conc)\right) \cdot pop \cdot y_o \quad \ldots \text{ Eqn 1.2}$$

Where β is the strength of the relationship between the change in ambient concentration of a given pollutant and the adverse outcome, derived from epidemiological studies (in cases per averaging period from the study, e.g. 24 hour μg/m^3);

Δconc is the change in ambient concentration of a given pollutant (in the averaging period from the study, e.g. 24 hour μg/m^3);

pop is the population exposed to the change in concentration; and,

y_o is the baseline incidence of the adverse health effect in the absence of the pollutant.

For this work, I employ primarily CR functions from the peer-reviewed compilations in the USEPA retrospective (1997) and prospective (1999) Benefits and Costs of the Clean Air studies (12, 13) with updates from the Environmental Benefits Mapping and Analysis Program (BenMap), version 2.4.85 (34). I also use population and the baseline incidences from BenMap which are discretized to the PMCAMx grid cell resolution. To capture the uncertainty in the strength of these relationships both within and across studies, I use the Monte Carlo implementations in the Fast Environmental Regulatory Evaluation Tool (FERET) (35) and BenMap.

I also evaluate newer and less well characterized health effects. For the sensitivity analysis on backup generators in Chapter 3, I include the relationship between diesel particulate matter (DPM) and cancer. The US Environmental Protection Agency (EPA) estimates a range of 1×10^{-3} to 1×10^{-5} cancer cases for each $\mu g/m^3$ of DPM for continuous exposure over a 70 year lifetime, but concluded that the existing data is insufficient to derive quantitative risk factors (36). By contrast, the California Office of Environmental Health Hazard Assessment (OEHHA) and the Air Resources Board (CARB) established a "reasonable estimate" of 3.0×10^{-4} $\mu g/m^3$ over a 70 year lifetime (37). Also, while this thesis was in progress, the National Research Council of the National Academies (2008) reviewed newer literature linking O_3 to premature mortality, concluding that there is sufficient evidence to support including this relationship in subsequent regulatory analyses (38). I include this relationship in Chapter 3 and Chapter 4. I do not include ecosystem level effects which are smaller and more uncertain.

1.2.5 Valuation of human health effects

Environmental and human health damages arising from electricity can be understood as an externality. Some of the damages are not valued in the market place, and as a result, do not enter into decisions. Others are valued but either no one takes responsibility for these costs or the cost is borne by someone other than the polluter. One solution is to internalize these effects by giving them a monetary value equal to the damage that is incurred (39). For human health effects, the monetary value of these outcomes is the number of cases multiplied by the "willingness to pay" (WTP) to avoid these effects. WTP is defined as the maximum amount of that an individual is willing to pay to be indifferent between having the good and taking the money[1].

For quantifying the adverse health effects from changes in air quality, the most important quantity is the value of premature mortality, known as the value of a statistical life (VSL). VSL is the average WTP for a small reduction in risk of death divided by the risk

[1] The corollary to WTP is willingness to accept (WTA). WTA is the amount of money that the individual would have to be compensated in order to be indifferent to the loss of the good. WTP is dependent on the initial income of the individual whereas WTA is not. In general, however, these two measures are lumped together as WTP.

reduction. There are four common methods in the literature for determining VSLs: 1) labor market or wage premium studies; 2) willingness to pay for safety features; 3) behavior with respect to safety decisions; and, 4) contingent valuation surveys (40). In this work, I use the USEPA estimate which is based on a review of 26 studies: 21 labor market studies and 5 contingent valuation studies. The final model is a Weibull distribution with a mean VSL of $7.5 million (in 2005 dollars) (Weibell scale parameter: 8,300,000; Weibull shape parameter: 1.5096). While the selection of these studies has been criticized as "ad hoc" (41), the USEPA value is widely used. The remainder of the health damages (e.g. cardiovascular and respiratory morbidity, restricted activity days, etc…) are usually measured in terms of medical costs and losses in productivity. Similar to the uncertainty in the relationships in the CR functions, the distribution on the WTP values is captured through Monte Carlo simulations. All values are taken from the USEPA studies and BenMap.

1.3 Summary of thesis chapter and key questions

In this section, I outline the key questions for the thesis chapters. I conclude these chapters with general conclusions and policy recommendations from this work.

1. *The costs, air quality and human health effects of using installed backup generators for meeting peak electricity demand*

   Are installed backup generators cost-effective on a full cost basis for providing peak electricity? What are the private costs of using these generators? Using New York City as a case study, what are the social costs due to the human health effects from the air quality emissions of these generators? Is it cost-effective to control these emissions?

2. *Using backup generators for meeting peak electricity demand: a sensitivity analysis on emission controls, location and health endpoints*

   How sensitive are the social costs from the case study of New York City to the urban center where the generators are located? How does the inclusion of newer and less certain health endpoints influence the social cost? Are additional emission controls warranted? How does uncertainty in the chemical mechanisms in $PMCAM_x$ influence the results?

3. *The air quality and human health effects of integrating utility scale batteries into the New York State electricity grid*

   What are the air quality costs and benefits of displacing turbines installed to peak electricity demand in New York City by installing a utility scale battery? What are the air quality costs and benefits of charging the battery with off peak base-load capacity in the New York Independent System Operator (NYISO) region? What is the net social cost for the system? Can distributional effects from the charging plant be mitigated? What are possible outcomes of this storage interacting with existing regulations affecting the electricity sector (e.g. the Clean Air Interstate Rule and the Renewable Portfolio Standards)?

2. The costs, air quality and human health effects of meeting peak electricity demand with installed backup generators[2]

Abstract

Existing generators installed for backup during blackouts could be operated during periods of peak electricity demand, increasing grid reliability and supporting electricity delivery. Many generators, however, have non-negligible air emissions and may potentially damage air quality and harm human health. To evaluate using these generators, we compare the levelized private and social (health) costs of diesel internal combustion engines (ICE) with and without diesel particulate filters (DPF), natural gas ICEs and microturbines to a new peaking plant in New York, NY. To estimate the social cost, first we calculate the upper range emissions for each generator option from producing 36,000 megawatt-hours (MWh) of electricity over three days. We then convert the emissions into ambient concentrations with a 3-D chemical transport model, $PMCAM_x$, and Gaussian dispersion plumes. Using a Monte Carlo approach to incorporate the uncertainties, we calculate the health endpoints using concentration-response functions and multiply the response by its economic value. While uncontrolled diesel ICEs would harm air quality and health, a generator with a DPF has a social cost, comparable to natural gas options. We conclude on a full (private and social) cost basis that backup generators, including controlled diesel ICEs, are a cost-effective method of meeting peak demand.

[2] This work is published as Gilmore, E.A., Lave, L.B. and Adams, P.J. (2006). "The costs, air quality and human health effects of meeting peak electricity demand with installed backup generators". *Environmental Science & Technology* 40:6887-6893. Minor edits, new fuel cost calculations for Figure 2.1, and references have been updated from the original text.

2.1 Introduction

The US electricity system faces three major problems: 1) meeting demand during periods of exceptional high or peak electricity demand, 2) achieving complete reliability with central station generation and transmission and distribution (T&D), and 3) siting new transmission lines, especially in urban areas. To protect against blackouts, substantial backup capacity has been installed. In New York City (NYC), NY, there is approximately 1,000 MW of backup generation (42). Since blackouts are infrequent, these generators could also be used to meet peak electricity demand when there is otherwise insufficient generation and T&D capacity. This could defer investment in new centralized peaking generation and T&D capacity and enhance grid stability (43). The New York (NYISO) and New England (NEISO) Independent System Operators have investigated and implemented programs using backup generators. California employed backup generators to prevent grid failure during the 2001 electricity shortages. While the private benefits are potentially large, most commercially available, dispatchable backup generators (e.g. a diesel fueled internal combustion engine (ICE)) have non-negligible air emissions. This could result in increased adverse human health effects since these generators are located close to the point of use. Peak electricity days also tend to be hot summer days with compromised air quality. The NYISO excludes diesel ICEs from some of its programs due to concerns about health and violating the National Ambient Air Quality Standards (NAAQS).

Three different approaches have been used to evaluate backup generators' air quality effects: emission inventories, dispersion models, and chemical transport models (CTM). Emissions inventories are the easiest to develop but provide no indication of exposure or attainment issues (44, 45). Dispersion models address some of the limitations of the inventory approach by estimating the ambient concentrations and exposure from one or more point sources. Heath et al. (2005) use Gaussian dispersion plumes to estimate exposure from distributed generation (DG), such as backup generators, in the Southern California Air Basin (SoCAB) (46). They found that DG usage increased exposure compared to centralized power plants. Dispersion models, however, do not address

secondary air pollutants formed by chemical transformations such as ozone (O_3). O_3 and fine particulate matter ($PM_{2.5}$), either emitted directly or formed by chemical transformation, account for the majority of the adverse human health effects; also, controlling these pollutants is the most difficult part of complying with the NAAQS. We found only one report that evaluates secondary pollutants, and regional and local air quality. California's Public Interest Energy Research Program (PIER) used CTMs to model the effect of diesel ICEs on air quality; they found increases in $PM_{2.5}$ and O_3 that exceeded the NAAQS standards in certain areas, noting some health related issues (47).

In this work, we evaluate the private and social costs of operating backup generators with and without emission controls, specifically a catalyzed diesel particulate filter (DPF), to meet peak electricity demand. To decide whether to meet peak load with backup generators or a new peaking generation (a simple cycle natural gas turbine), we compare each options' sum of private (market) costs and the social costs or externalities (or unpriced benefits and costs). The primary social cost is the human health effects from the associated air emissions (11, 12). We use a 'state of science' CTM and Gaussian dispersion plumes to capture the changes in ambient concentrations at the local and regional level from both primary and secondary pollutants.

2.2 Method and data

We compare the generators on the full levelized cost of energy (LCOE). The LCOE represents a technology's average costs per kWh over its life span as defined by Equation 2.1.

$$Full\ Cost\ \left(\frac{\$}{kWh}\right) = \frac{(CC + TD)}{HY} \cdot CRF + \frac{FOM}{HY} + VOM + FC \cdot HR + SC \quad \ldots Eqn\ 2.1$$

Where CC is the capital cost of the generator and emission control technology (in \$/kW);

TD is the T&D cost or generator – grid interconnection costs (in \$/kW);

CRF is the capital recovery factor for depreciation and interest (approximated at 15%/yr);

HY is the hours of operation per year (defined as 200 hours);

FOM is the fixed operating and maintenance (O&M) (in $/kW year);

VOM is the variable O&M (in $/kWh);

FC is the fuel costs (in $/mmBtu);

HR is the heat rate, derived from efficiency (in mmBtu/kWh); and,

SC is the social cost (in $/kWh).

To estimate the social cost, we need to evaluate the air quality effects of our strategy. We use the Comprehensive Air Quality Model with extensions and particulate matter modules ($PMCAM_x$). $PMCAM_x$ is a 'state of science' CTM that simulates the emission, advection (convection), dispersion, gas and aqueous phase chemical reactions, and dry and wet deposition for 35 gaseous species, 12 radical species and 13 aerosol species in 10 size bins on a 3-D Eulerian grid. Additional modules simulate the dynamic behavior (coagulation, condensation, and nucleation) of aerosols species. The gas and aqueous phase chemistry are simulated with the Carbon Bond Mechanism IV (CBM-IV) (19) and the Regional Acid Deposition Model (RADM), respectively (25). The evaporation and condensation processes are modeled using a bulk equilibrium approach (26, 27). Two product adsorptive partitioning models the formation of secondary organic aerosol (SOA) from semi-volatile organic species (28). The inorganic aerosol thermodynamic behavior is modeled using ISORROPIA, an equilibrium method (29). Meteorological inputs are generated with the MM5 meteorological model (29). The baseline emission files are from the Lake Michigan Air Directors Consortium (LADCO) (31). The model domain is discretized into a 36 km by 36 km horizontal grid with 14 vertical layers between the surface and 6 km. The lowest model layer is slightly less than 30 m thick vertically.

Since $PMCAM_x$ has already been evaluated for July 12 to 28 2001, we examined the 2001 hourly load profile for New York City – Long Island (NYC-LI) for a coincident

period of peak electricity. Looking at the top 200 hours of electricity usage per year, we found a match from July 23 to 25, 2001. For each day, we assume 1,000 MW of backup capacity operating from 9 am to 9 pm EST (i.e., 12,000 MWh of electricity generated each day). See Supporting Information (Section 2.6.1) for the derivation of the simulation scenario.

In Table 2.1, we present the mean, minimum and maximum emission factors (EFs) for the different backup options (15, 44, 48). The total emissions are determined by multiplying the maximum EF by the total number of kilowatts (kW) deployed per hour. DPFs have removal efficiencies for $PM_{2.5}$ of > 90% to 99% (49). We scale the $PM_{2.5}$ EF for the diesel ICE by a DPF removal efficiency of 95%. In addition, the DPF requires fuel with a sulfur content of 15 ppm to prevent poisoning of the catalyst. Ultra low sulfur diesel fuel (ULSD) reduces the SO_2 EF. We do not consider reductions of other pollutants, such as hydrocarbons (HC). The raw emission factors are processed for $PMCAM_x$. The NO_x is divided into 85% NO and 15% NO_2. The HCs are speciated with profiles from SPECIATE (18) and grouped into the CBM-IV categories (19, 20) $PM_{2.5}$ is speciated according to Wien et al. (2004) (50), and the mass is divided equally into six size bins.

The emissions are modeled as distributed evenly over the grid cell which contains NYC. A baseline simulation (without any changes to the default emission files) was also run. All runs were conducted from July 19 to 28 with the first four days discarded as model initialization time. Baseline concentrations from $PMCAM_x$ are compared to the concentrations in the Aerometric Information Retrieval System (AIRS) (51) database for NYC in the Supporting Information (Table 2.5).

Table 2.1: Mean, minimum and maximum emission factors for backup generators in g/kWh (15, 44, 48)

Technology	NO_x (g/kWh)	CO (g/kWh)	HC (g/kWh)	$PM_{2.5}$ (g/kWh)	SO_2 (g/kWh)
Diesel ICE	8.1 (2.1 – 18.8)	2.3 (0.08 – 6.4)	0.9 (0.09 – 2.0)	0.5 (0.08 – 1.4)	2.3[a]
Diesel ICE w DPF	8.1 (2.1 – 18.8)	2.3 (0.08 – 6.4)	0.9 (0.09 – 2.0)	0.03 (0.01 – 0.07)	0.01
Natural gas ICE	5.8 (0.2 – 12.9)	1.7 (0.5 – 4.1)	0.8 (0.5 – 1.1)	0.03 (~0 – 0.04)	~ 0
Natural gas microturbine	0.3 (0.1 – 0.6)	0.4 (0.1 – 0.8)	0.1 (0.04 – 0.1)	0.03 (~0 – 0.04)	~ 0

a. The amount of SO_2 is proportional to the amount of sulfur (S) in the fuel. For diesel fuel, we assume a high S content fuel (~ 2500 ppm). Most diesel fuel sold is 350 – 500 ppm. For natural gas, there is a negligible S.

We are also interested in dispersion on a local scale, specifically 'hot spots' near the source. As a first estimate, we model these concentrations using Gaussian dispersion plumes. We assume generators are located on rooftops and ignore highly site-specific behavior such as drawdown from surrounding taller buildings and pollutant trapping in "street canyons". To model more complex behavior, specific building geometry and a computational fluid dynamic (CFD) model would be required. Doing this for each stack and building geometry is beyond the scope of this analysis. Such a tool could be applied to particular cases where the geometry suggests the possibility of high street level concentrations. The Gaussian model is a more generic screening tool. We use urban terrain dispersion parameters from Briggs (1973) (33), and the concentrations predicted at the vertical height of emission to determine the health cost from direct exposure to the exhaust. This generates the most conservative estimate of exposure from this model. Assuming a perfectly reflecting surface as the most conservative boundary condition, the Gaussian equation takes the following form (Equation 2.2).

$$\bar{c}(x,y,z,H) = \frac{Q}{2\pi\bar{u}\sigma_y\sigma_z} \cdot exp\left[-\frac{y^2}{2\sigma_y^2}\right] \cdot \left\{exp\left[-\frac{(z-H)^2}{2\sigma_z^2}\right] + exp\left[-\frac{(z+H)^2}{2\sigma_z^2}\right]\right\} \ldots Eqn\ 2.2$$

Where c is the mean concentration (in g/m^3);

x is the distance from the source in the direction of the wind (in m);

y is the cross wind distance from the source (in m);

z is the vertical height from the ground (in m);

H is the effective height of the release above the ground (in m);

Q is the strength of the emission source (in g/s);

u is the mean wind speed (in m/s);

σ_y is the urban dispersion parameter in the crosswind direction; and,

σ_z is the urban dispersion parameter in the vertical direction.

The strength of the emission source is determined by multiplying the EF by the generator capacity in kW. We make the conservative assumption that all of the NO_x is present as NO_2. We apply the average meteorological conditions for July 23 to 25 assuming a constant wind direction. The wind speed is 5.8 m/s under scattered and partly cloudy conditions (i.e., Pasquill atmospheric stability categories C (slightly unstable) or D (neutral)). We present results for category D, the more conservative condition.

We translate the changes in ambient air quality into morbidity and mortality effects and dollar values using methods and values from the USEPA (1999) benefit-cost analysis of the value of the Clean Air Act (13). First, concentration-response (CR) functions estimate the health endpoints from changes in concentration. The response is then multiplied by the exposed population. For each $PMCAM_x$ cell, we transformed the population from the county level (2000) to the grid resolution using the Geographic Information Systems (GIS) software, ArcMap. For the Gaussian plumes, the area of each concentration isopleth is multiplied by the population density of NYC (10,292 persons/km^2).

To capture the uncertainty in the strength of the relationship between the change in concentration and the response as well as the economic value of the response, we employ the Fast Environmental Regulatory Evaluation Tool (FERET), a Monte Carlo implementation of the USEPA's CR functions and economic cost distributions (35) and present the results with 5% and 95% confidence intervals. We focus our attention on NO_2, O_3, $PM_{2.5}$, and SO_2 as they have been designated as especially harmful to human health. We present a table of important effects for these pollutants and their mean economic values in the Supporting Information (Table 2.6).

2.3 Results and discussion

2.3.1 Private costs

The primary benefit of using installed capacity is that the capital costs of the generator can be fully or partially ascribed to the reliability benefits provided by the backup application. Since the peak power application entails operation for only 200 hours per year, there is a negligible effect on the life span of the generator. Unlike the capital costs, O&M is included in the cost of meeting peak electricity demand, although these costs are small. We show the private costs and characteristics of the technologies in the Supporting Information (Table 2.7) (48). We also consider retrofitting diesel ICEs with a catalyzed DPF to remove $PM_{2.5}$ from the exhaust. The capital cost of the DPF adds up to 40 $/kW (52, 53). Another benefit is that additional T&D is not required. A significant portion of installed backup capacity is located in urban centers, which like NYC are transmission constrained. Difficulties in siting new transmission lines make the installed capacity particularly valuable. Ideally, the T&D costs would be site specific. In the absence of this data, we assume a generic capital cost of $100/kW which likely underestimates the value.

In this operation, the individual owner responds to communication from the grid operator by shifting part of their load to their backup generator. Small generators, however, are commonly installed with an open transition transfer interconnection, creating a physical barrier between the generator and the grid. A closed transition transfer system retrofit is

required to maintain the link, allowing the transfer of load from grid power to the generator without a supply interruption. Meyer et al. (2002) cite costs ranging from $50/kW to $200/kW depending on the size of the generator, the application and utility requirements (43). Interconnection issues are not trivial, but regulatory issues are more significant than technological ones (54). The final element is fuel costs. Our costs are based on prices of $15/Mcf for natural gas and $2.40/gallon of diesel. A DPF requires ULSD with an incremental cost of approximately 10¢/gallon.

Assuming 200 hours per year of operation and a capital recovery factor of 15%, we show the private LCOEs for the backup generators and the peaking plant in Figure 2.1. The most common backup generator is a diesel ICE since it has the lowest capital costs. The capital costs for the natural gas fueled generators are the difference between that generator and the diesel ICE. This comparison shows that the private costs of using backup generators to meet peak demand are about 1/3 of the costs of building a new peaking generator.

Figure 2.1: Levelized private costs of installed backup generators and a peaking plant in ¢/kWh

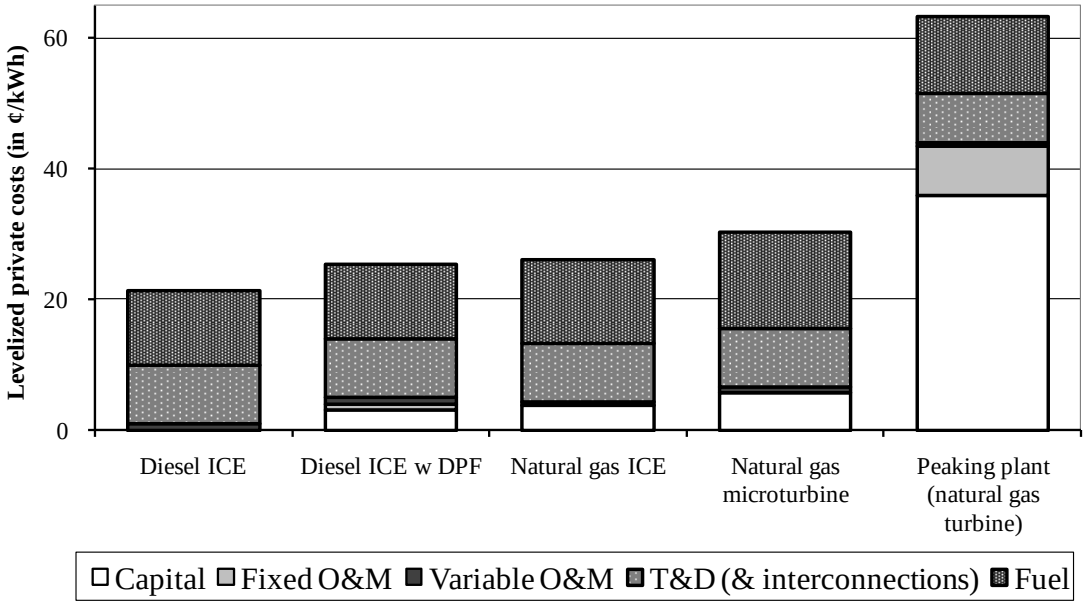

2.3.2 Chemical transport model results

In Table 2.2, we show the daily mean NO_2 (in ppb), the 1-hour peak O_3 (in ppb), the daily mean $PM_{2.5}$ (in $\mu g/m^3$) and the daily mean SO_2 (in ppb) concentrations for the backup generator compared to the baseline concentration in the NYC grid cell for July 25, 2001. For the diesel ICE, the approximately 5 $\mu g/m^3$ $PM_{2.5}$ enhancement is due mostly to increases in primary elemental and organic carbon. The $PM_{2.5}$ enhancements for the natural gas fueled options are less than 1 $\mu g/m^3$ in NYC. In our scenarios, O_3 concentrations decreased in NYC. Previous work has shown that NYC, like many urban centers, is volatile organic compounds (VOC)–limited (55, 56). As more NO_x is emitted, peak O_3 concentrations decrease locally and increase downwind. Negligible increases are observed for SO_2. There is also a negligible residual increase in ambient concentrations after the final day of operation.

In Figure 2.2, the effect on the immediate (and local suburban) and downwind communities is shown for July 25, 2001. For the diesel ICE, enhancements in $PM_{2.5}$ concentrations of 0.01 to 0.1 $\mu g/m^3$ extend over approximately 25,000 km^2 representing 75% of Connecticut, all of Rhode Island and 30% of Massachusetts. The difference in $PM_{2.5}$ for the diesel ICE with a DPF, the natural gas ICE and the microturbine are presented in the Supporting Information (Figure 2.5 and Figure 2.6). The results are similar to the diesel ICE, but the extension of the plume is significantly smaller.

Table 2.2: Simulated daily mean NO_2 in ppb, 1 hour peak daily O_3 in ppb and daily mean $PM_{2.5}$ in µg/m^3 located in the $PMCAM_x$ grid cell corresponding to NYC for the backup generator scenarios compared to the baseline simulation for July 25, 2001

	Baseline	Diesel ICE	Diesel ICE w DPF	Natural gas ICE	Natural gas microturbine
Mean daily NO_2 (in ppb)	75.6	89.9	89.9	85.2	76.2
1-hour peak O_3 (in ppb)	102	75.2	75.2	83.3	101
Mean daily $PM_{2.5}$ (in µg/m^3)	46.4	51.4	46.7	46.6	46.6
Mean daily SO_2 (in ppb)	35.4	37.9	35.4	35.4	35.4

Figure 2.2: Regional difference in daily mean $PM_{2.5}$ concentrations in $\mu g/m^3$ between a diesel ICE with an emission factor of 1.35 g/kWh and basecase for July 25, 2001. The NYC grid cell is indicated as well as CT = Connecticut, MA = Massachusetts, NY = New York State, and RI = Rhode Island. The white areas are concentration enhancements of less than 0.01 $\mu g/m^3$.

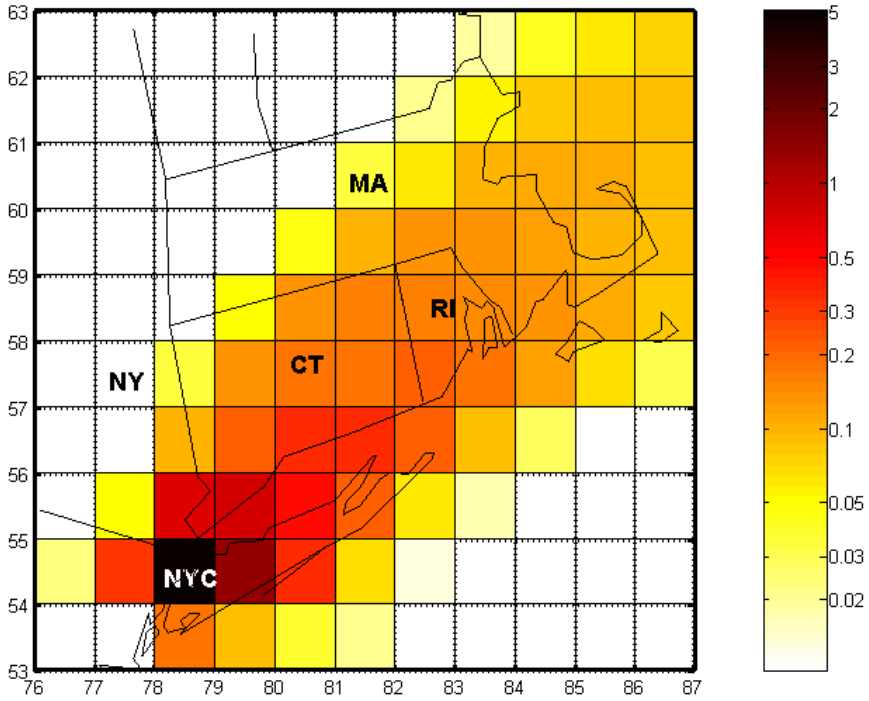

In Figure 2.3, the differences in the 1- hour peak O_3 concentrations and the NO_x/VOC ratios at 9 am EST are displayed for the diesel ICE simulation for July 25, 2001. The difference in peak O_3 is the maximum hourly O_3 concentration in the backup generation simulation minus the maximum hourly O_3 concentration in the baseline simulation. The peak O_3 did not necessarily occur at the same hour. The NYC cell and the adjacent cells see decreases in O_3. There is, however, a large region with increases of approximately 2 ppb in Connecticut and Massachusetts. Defining regions with a NO_x/VOC greater than 8 as NO_x-limited and less than 8 as VOC-limited, the decreases in O_3 correspond to the VOC-limited regions, while increases in O_3 are in NO_x-limited regions. The natural gas ICE has NO_x emissions that are 20x more than the microturbine, resulting in an 18 ppb decrease for the ICE to a 1 ppb decrease for the microturbine. The results for the natural

gas fueled options are presented in the Supporting Information (Figure 2.7 and Figure 2.8).

Figure 2.3: Regional difference in peak 1-hour daily O_3 concentrations in ppb between the diesel ICE simulation and basecase for July 25, 2001. The white areas are concentration enhancements of less than 0.1 ppb. NO_x/VOC ratios at 9 am EST on July 25, 2001 as simulated in $PMCAM_x$. NO_x/VOC ratios are greater than 8 are shown in blue, and NO_x/VOC ratios less than 8 are shown in green. The NYC grid cell is indicated.

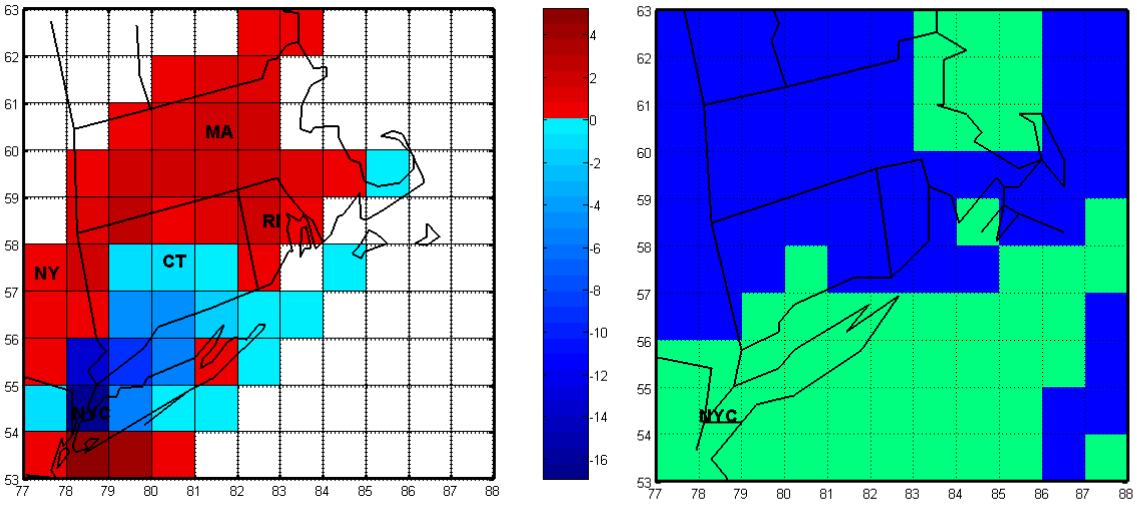

2.3.3 Gaussian dispersion plume result

To investigate the effect of primary pollutants in the immediate vicinity of the exhaust, we develop Gaussian dispersion plumes. Figures of the Gaussian plumes for all pollutants under Pasquill stability class D for an uncontrolled diesel ICE are shown in the Supporting Information (Figures 2.9, 2.10 and 2.11). The plumes for the diesel ICE with a DPF and the natural gas fueled options can be scaled by the EFs from the diesel ICE plumes and are not shown. For stacks located at the tops of multistory buildings, ground level increases in primary pollutants would be small.

2.3.4 Health impacts and economic costs

The mean social costs associated with the concentration increases from $PMCAM_x$ are presented in Table 2.3, along with the Monte Carlo generated 5% and 95% CI. We show the total social cost with and without the benefit from decreased morbidity from O_3. O_3 decreases are observed for both the diesel and natural gas ICEs. While this is an accurate representation of the chemistry, we are uncomfortable counting the addition of substantial amounts of NO_x into NYC as a social positive. Also, most ICEs emit less NO_x than the EFs we modeled with even lower future mandated emission standards.

For all species, the average costs from the $PMCAM_x$ NYC grid cell are greater than the costs generated by the immediate exhaust as estimated by the Gaussian plume. We show a comparison of the values from the dispersion plumes to the NYC grid cell from the $PMCAM_x$ simulations in Table 2.4. We conclude that the immediate effect or 'hot spots' caused by the exhaust do not strongly influence the health costs, and the average costs adequately capture the social costs.

2.4 Conclusions: Full cost comparison

In Figure 2.4, we present the full costs (private and mean social costs) of using different types of installed backup generation with and without emission control technologies compared to a new peaking plant. We present the mean value, although the same conclusions hold at the 5% and 95% CI. In general, the social costs are smaller than the private costs with most of the increase from chronic mortality from $PM_{2.5}$. The exception is the uncontrolled diesel ICE which has full costs larger than the private costs of a new peaking plant. The $PM_{2.5}$ EF for these simulation, however, is higher than those for newer diesel ICEs or those achievable with DPFs. The diesel ICE with the DPF has social costs in the same range as the natural gas fueled options.

This analysis does not address issues of attainment or other emission based standards for stationary sources. The New York Department of Environmental Conservation (DEC) issues exhaust standards for backup generators. In addition, the NY State Implementation

Plan (SIP) to bring the region into compliance with the NAAQS has placed restrictions on new NO_x emission sources. This application would increase NO_x emissions by 3.75 ton/year. Offsets are required only for major sources emitting more than 10 tons/year. Nonetheless, assuming that NO_x offsets were required, the 1.5x offset required for the 3.75 tons adds an incremental cost of less than 0.6 ¢/kWh at $210,000/ton of NO_x, the highest price observed in California in 2004 (57). Thus, the NO_x contribution of these generators does not change the conclusion.

We find that using backup generators to supply electricity during the periods of peak demand has lower private and social costs than a new peaking plant, in addition to making electricity supply more reliable and relieving major problems associated with siting new generation and transmission. We stress that our analysis uses conservative assumptions throughout that tend to overestimate the health costs. While uncontrolled diesel ICEs would harm air quality and health, putting controls on these generators and using ULSD reduce the social costs significantly. We recommend that the relevant regulatory bodies reconsider their ban on using diesel ICEs, taking care that each individual unit maintain appropriate emission standards and be properly sited so as not to cause a nuisance in the immediate area.

Figure 2.4: Total (private and social) costs of operating backup generators compared to the natural gas peaking plant in ¢/kWh

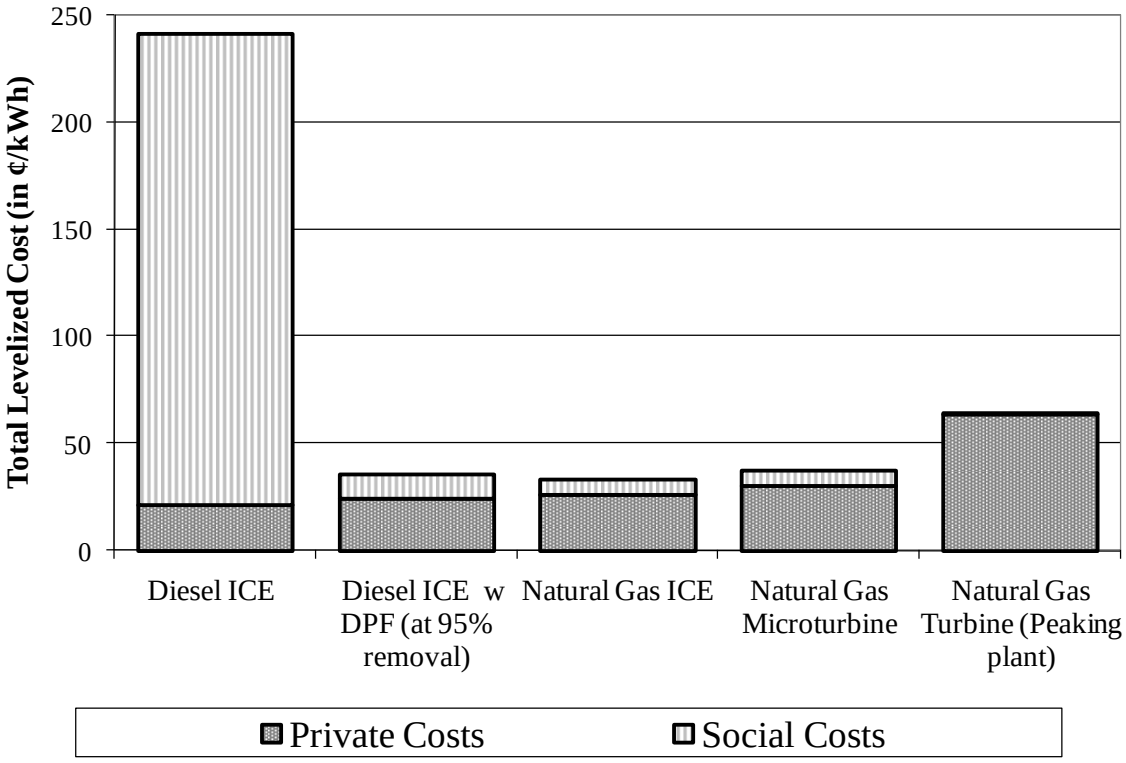

Table 2.3: Mean social costs with 5% and 95% confidence intervals from $PMCAM_x$ simulation in ¢/kWh due to chronic and acute mortality from $PM_{2.5}$ and morbidity from NO_2, O_3, $PM_{2.5}$ and SO_2.

	Diesel ICE	Diesel ICE w DPF	Natural gas ICE	Microturbine
$PM_{2.5}$ chronic mortality	190 (80, 320)	11.2 (4.7, 19)	5.8 (2.4, 9.9)	5.8 (2.4, 9.9)
$PM_{2.5}$ acute mortality	29 (6.4, 63)	1.5 (0.33, 3.3)	0.9 (0.2, 2)	0.9 (0.2, 2)
$PM_{2.5}$ morbidity	0.58 (0.13, 3.6)	0.03 (~0, 0.19)	0.02 (~0, 0.12)	0.02 (~0, 0.12)
NO_2 morbidity	1.3 (0.62, 1.9)	1.3 (0.62, 1.9)	0.94 (0.45, 1.4)	0.05 (0.02, 0.07)
SO_2 morbidity	0.17 (~0, 0.36)	< 0.01	< 0.01	< 0.01
Total social cost without O_3	225 (88, 389)	13.8 (5.7, 24)	7.6 (3, 14)	6.8 (1, 12)
O_3 morbidity	-4.8 (-18, -2)	-4.8 (-18, -2)	-1.9 (-13, -1.5)	-0.1 (-0.8, -0.09)
Total social cost with O_3	220 (69, 390)	9.0 (-12, 22)	5.7 (-10, 12)	6.7 (1.8, 12)

Table 2.4: Mean social costs with 5% and 95% confidence intervals from the dispersion plumes under Pasquill atmospheric stability class D compared to the cost in NYC grid cell from the $PMCAM_x$ simulation in ¢/kWh

Species		Diesel ICE	Diesel ICE w DPF	Natural gas ICE	Microturbine
NO_2 (NO_2 = NO_x)	Gaussian plume	1.07 (0.5, 1.6)	1.07 (0.5, 1.6)	0.67 (0.3, 0.9)	0.06 (0.03, 0.08)
	NYC grid cell	0.84 (0.4, 1.3)	0.84 (0.4, 1.3)	0.63 (0.3, 0.9)	0.04 (0.02, 0.06)
$PM_{2.5}$	Gaussian plume	130 (55, 220)	6.5 (2.8, 11)	3.8 (1.6, 6.5)	3.8 (1.6, 6.5)
	NYC grid cell	180 (77, 310)	10 (4.3, 17)	5.7 (2.4, 9.8)	5.7 (2.4, 9.8)
SO_2	Gaussian plume	0.1 (0, 0.2)	<0.01	< 0.01	< 0.01
	NYC cell	0.14 (0, 0.28)	~0	~0	~0

2.5 Supporting information

2.5.1 Simulation scenario

In 2001, the average peak load in NYC-IL was 971 MW (defining the load as the difference in the load between any of the top 200 hours and the load in 201st hour). We round to 1,000 MW which is consistent with estimates of installed backup capacity in NYC. Peak demand starts mid-morning, lasting from 1 to 13 hours with a mean of 8 hours. Operating for 12 hours/day for three consecutive days allows us to evaluate prolonged generation, creating an upper range for the effect of these generators.

2.5.2 Comparison of $PMCAM_x$ to the AIRS data

Below we provide a comparison between the predicted concentrations in $PMCAM_x$ and those reported in the USEPA Aerometric Information Retrieval System (AIRS) database (51) for NYC in Table 2.5. All modeled species follow the same temporal trend as the measured data. While the modeled mean O_3 concentrations fail to simulate the elevated concentrations on July 25th, the daily maximum O_3 concentrations capture the episode. Both the modeled $PM_{2.5}$ mean and maximum concentrations match well over the course of the simulation, although they are slightly overestimated and failed to tail off as dramatically as the data on the final simulation day.

Table 2.5: Comparison of AIRS and baseline concentrations in New York City

Species		07/23/2001	07/24/2001	07/25/2001	07/26/2001
Mean $PM_{2.5}$ ($\mu g/m^3$)	AIRS	15.7	21.2	38.2	11.9
	Baseline	25.3	23.6	46.4	33.6
	% Difference	61%	12%	21%	183%
Daily max $PM_{2.5}$ ($\mu g/m^3$)	AIRS	27.5	32.4	58.7	28.7
	Baseline	33.1	36.6	87.5	62.7
	% Difference	21%	13%	49%	118%
Mean O_3 (ppb)	AIRS	21.9	29.3	37.8	12.3
	Baseline	23.8	21.5	21.4	13.5
	% Difference	9%	-27%	-44%	10%
Daily 1-h max O_3 (ppb)	AIRS	61.3	67.3	101.0	42.7
	Baseline	67.7	67.6	101.9	33.6
	% Difference	11%	1%	1%	-21%

2.5.3 Selected health effects and average economic values

Table 2.6: Selected health effects and average economic value (in $2005) (13)

Health effect	Change in pollutant	Valuation of outcome	Mean value per event ($)
Chronic and acute mortality	Mean annual $PM_{2.5}$ / Mean daily $PM_{2.5}$	Value of a statistical life	7,200,000
All acute respiratory morbidity	Mean daily NO_2, $PM_{2.5}$, SO_2 / 1-hour peak daily O_3	Hospital admission	9,100
All acute cardiovascular morbidity	Mean daily NO_2, $PM_{2.5}$, SO_2 / 1-hour peak daily O_3	Hospital admission	9,300
Minor illnesses (e.g. restricted activity days)	Mean daily $PM_{2.5}$ / 1-hour peak daily O_3	Value of lost activity or work	90/day

For $PM_{2.5}$ chronic effects, we assume that all 26 days with peak electricity demand in 2001 would see the same changes in concentration as the simulation.

2.5.4 Cost and characteristics for backup generators and peaking plants

Table 2.7: Costs and characteristics for backup generators and peaking plants (48)

Technology	Unit size (MW)	Efficiency (%)	Capital cost ($/kW)	Fixed O&M ($/kW-yr)	Variable O&M (¢/kWh)
Diesel ICE	0.25	35%	600	15	1
Natural gas ICE	0.25	35%	650	15	1
Natural gas microturbine	0.075	25%	700	15	0.6
Simple cycle natural gas turbine (peaking plant)	10	35%	480	15	0.55

2.5.5 Supplemental figures for regional differences in $PM_{2.5}$ and O_3 for backup generators

Figure 2.5: Regional difference in daily mean $PM_{2.5}$ concentrations in $\mu g/m^3$ between a diesel ICE with a DPF for an emission factor of 0.07 g/kWh and basecase for July 25, 2001. The NYC grid cell is indicated as well as CT = Connecticut, MA = Massachusetts, NY = New York State, and Rhode Island (RI). The white areas are concentrated enhancements of less than 0.01 $\mu g/m^3$.

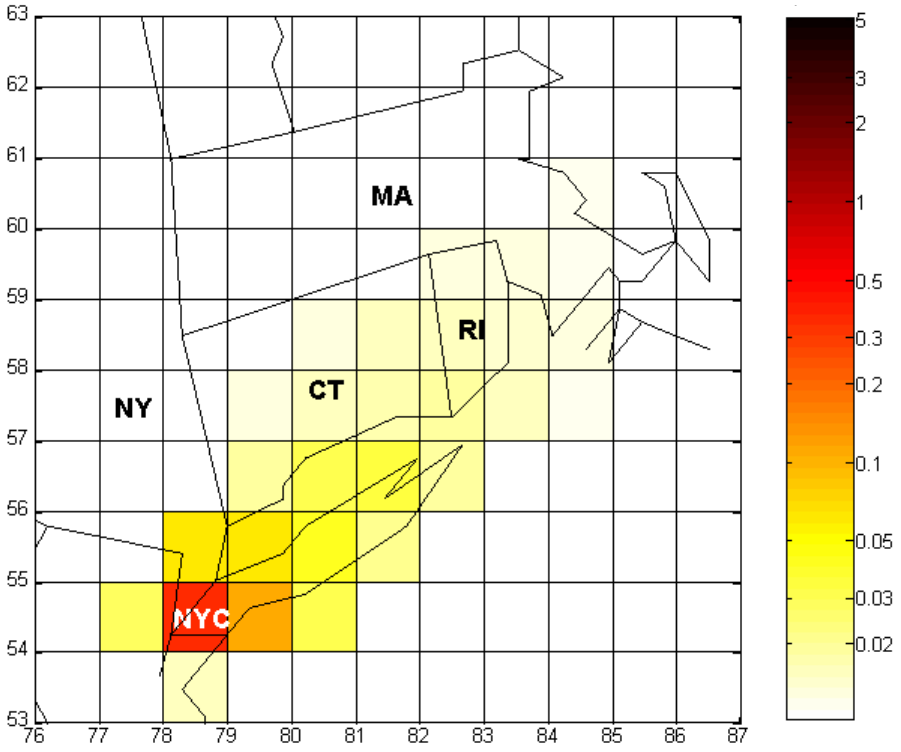

Figure 2.6: Regional difference in daily mean $PM_{2.5}$ concentrations in $\mu g/m^3$ between a natural gas internal combustion engine or a natural gas microturbine for an emission factor of 0.04 g/kWh and basecase for July 25, 2001. The NYC grid cell is indicated as well as CT = Connecticut, MA = Massachusetts, NY = New York State, and Rhode Island (RI). The white areas are concentrated enhancements of less than 0.01 $\mu g/m^3$.

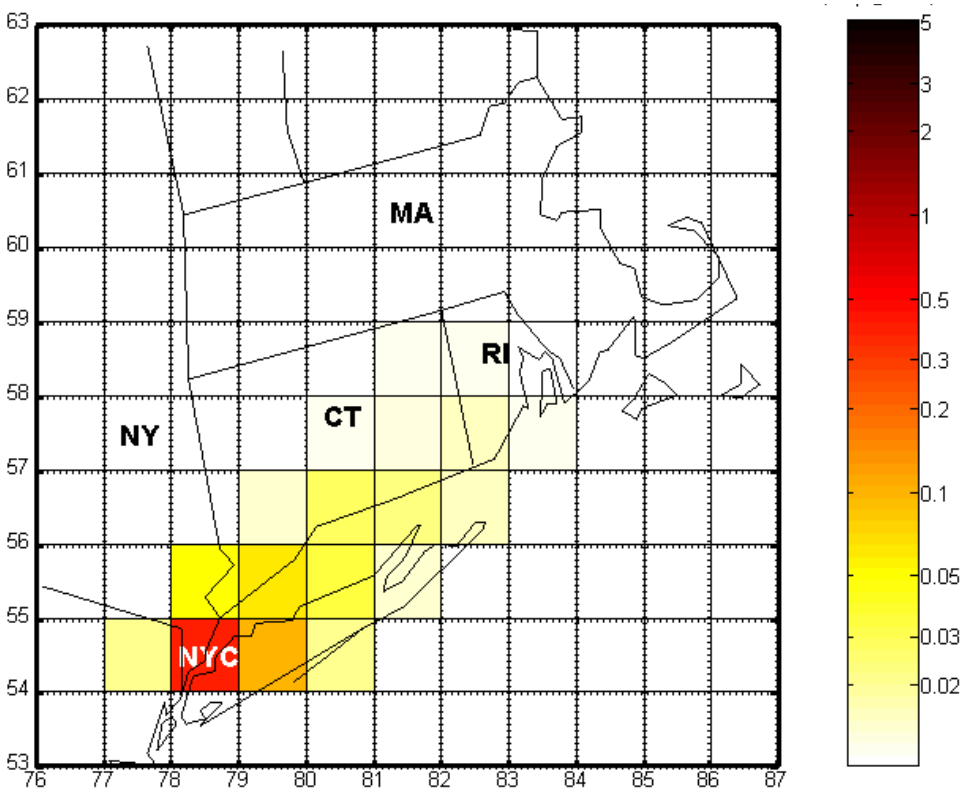

Figure 2.7: Regional difference in peak 1-hour daily O_3 concentrations in ppb between the natural gas ICE simulation and basecase for July 25, 2001. The NYC grid cell is indicated as well as CT = Connecticut, MA = Massachusetts, NY = New York State, and Rhode Island (RI). The white areas are concentrated enhancements of less than 0.1 ppb.

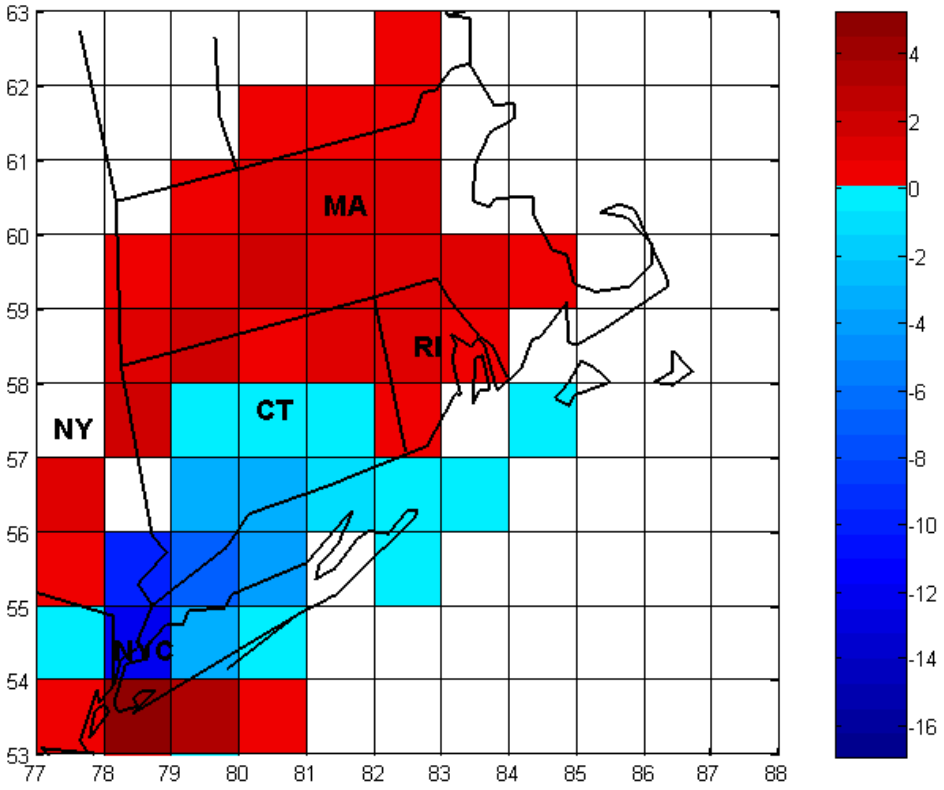

Figure 2.8: Regional difference in peak 1-hour daily O_3 concentrations in ppb between the microturbine simulation and basecase for July 25, 2001. The NYC grid cell is indicated as well as CT = Connecticut, MA = Massachusetts, NY = New York State, and Rhode Island (RI). The white areas are concentrated enhancements of less than 0.1 ppb.

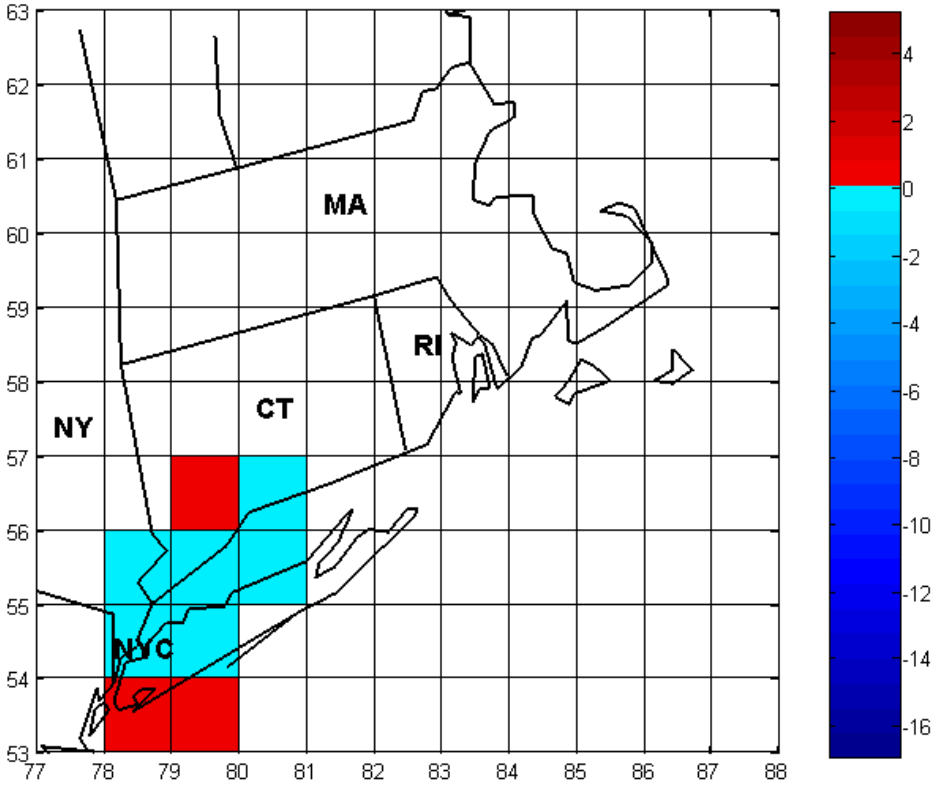

2.5.6 Supplemental figures of Gaussian dispersion plumes

Figure 2.9: Gaussian dispersion plumes for NO_2 in ppb for an emission factor of 2.8 g/kWh for a diesel ICE at a wind speed of u = 5.8 m/s and Briggs correlations for urban terrain with a Pasquill atmospheric stability class D. White areas are concentration increases of less than 0.1 ppb

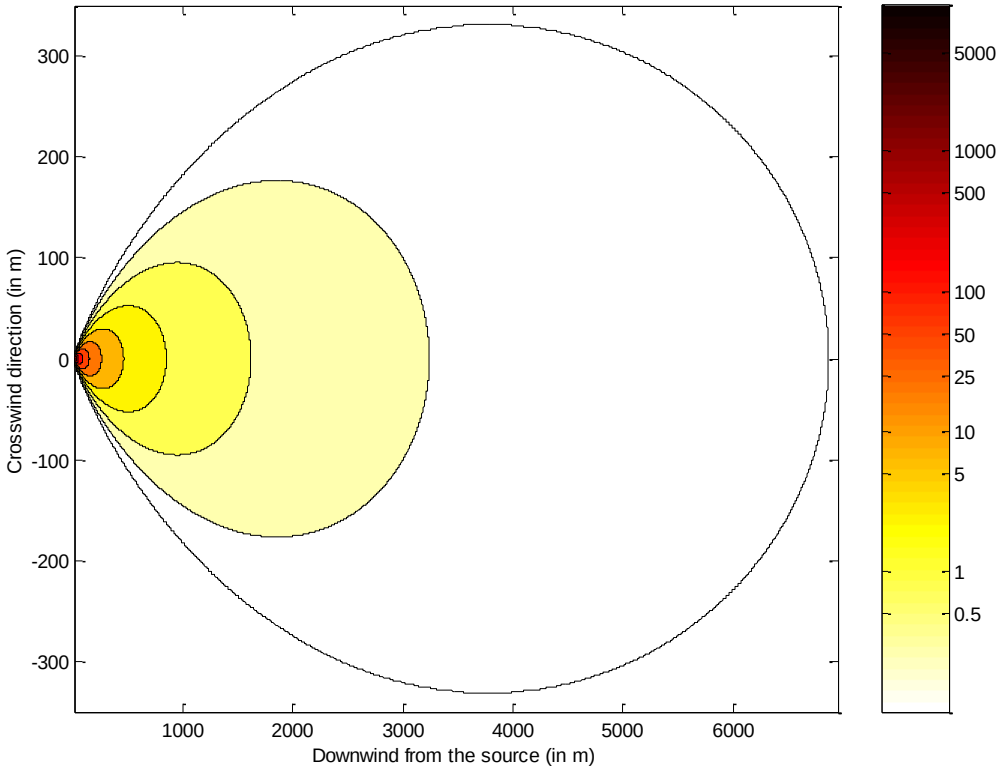

Figure 2.10: Gaussian dispersion plume for $PM_{2.5}$ in $\mu g/m^3$ for an emission factor of 1.35 g/kWh for a diesel ICE at a wind speed of u = 5.8 m/s and Briggs correlations for urban terrain with a Pasquill atmospheric stability class D. White areas are concentration increases of less than 0.1 $\mu g/m^3$ for $PM_{2.5}$

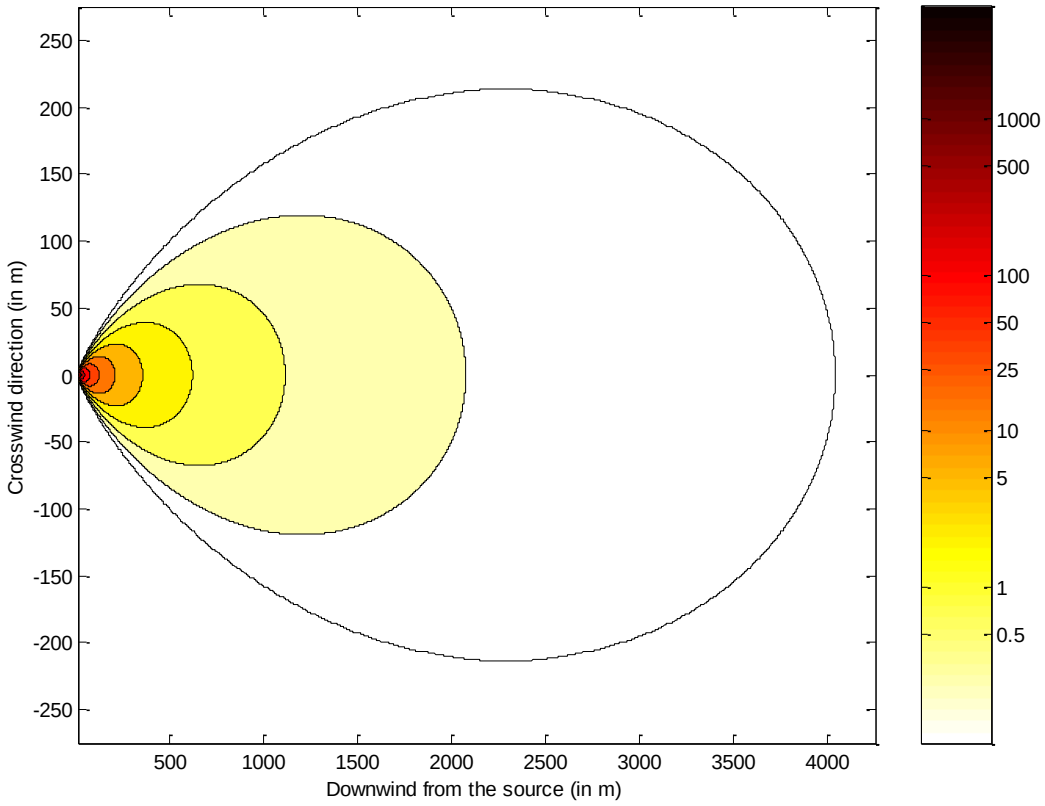

Figure 2.11: Gaussian dispersion plumes for SO_2 in ppb for an emission factor = 2.3 g/kWh for a diesel ICE at a wind speed of u = 5.8 m/s and Briggs correlations for urban terrain for Pasquill atmospheric stability class D. White areas are concentration increases of less than 0.1 ppb

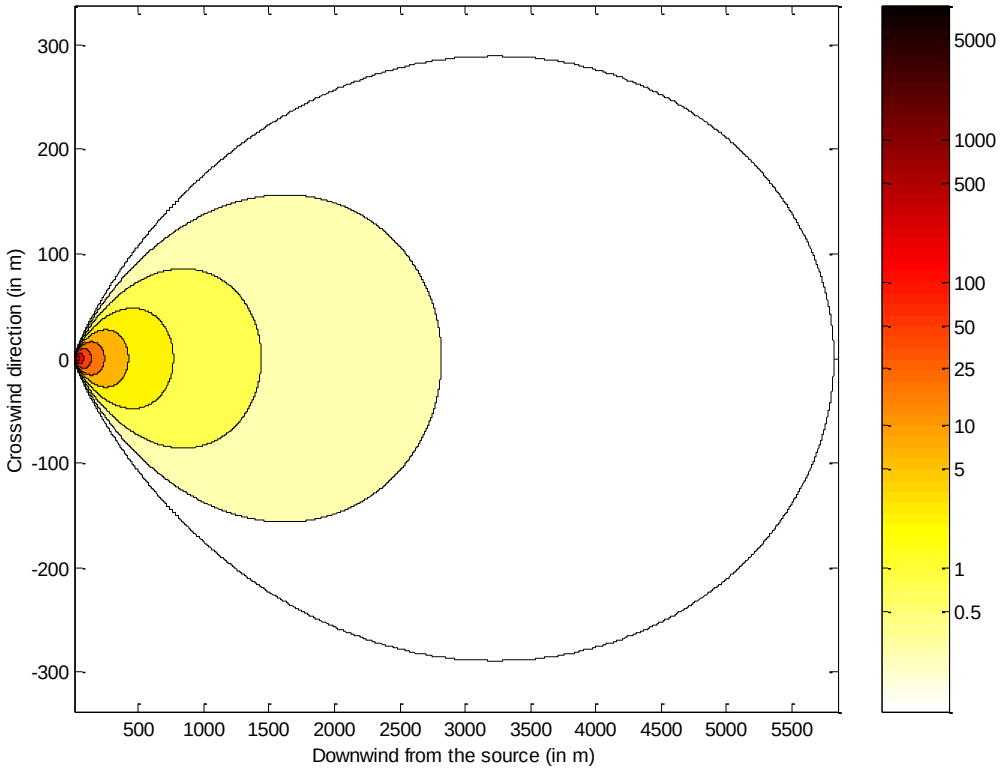

3. Using backup generators for meeting peak electricity demand: a sensitivity analysis on emission controls, location and health endpoints

Abstract

Existing generators installed for backup power during blackouts could operate during periods of high electricity demand. Many are diesel generators, however, with non-negligible air emissions that could damage air quality and human health. In this paper, we investigate the full (private and social) cost of using diesel generators without and with controls for fine particulate matter ($PM_{2.5}$) and nitrogen oxides (NO_x) compared to a new peaking plant (a natural gas turbine) in four Eastern US cities (Atlanta, Chicago, Dallas and New York). To calculate the social costs from air quality degradation, we model the ambient concentration enhancements in ozone (O_3) and $PM_{2.5}$ from operating 1,000 MW of backup generation for 12 hours in each city for six days using the chemical transport model, $PMCAM_x$. These enhancements are translated to their equivalent human health effects using concentration-response functions and a social cost using estimates of "willingness-to-pay" to avoid ill health. In all cities, $PM_{2.5}$ concentrations increase (up to 5 $\mu g/m^3$) due mainly to primary emissions. Smaller increases and decreases are observed for secondary $PM_{2.5}$ with more variation between cities. Increases in NO_x emissions result in significant nitrate formation (up to 1 $\mu g/m^3$) in Atlanta and Chicago. In New York City, nitrate is limited by higher temperatures. The NO_x emissions also cause O_3 decreases in the urban center and increases in the surrounding area. While the magnitude of the relationship between O_3 and premature mortality is uncertain, these decreases could produce a significant social benefit. Limiting our analysis to $PM_{2.5}$, we calculate a social cost of approximately 2 \$/kWh for uncontrolled diesel generators in highly populated centers and < 10 ¢/kWh with $PM_{2.5}$ and NO_x controls. On a full cost basis, we find that properly controlled diesel generators are cost-effective for meeting peak electricity demand. To limit the potential for secondary $PM_{2.5}$ formation, NO_x controls should be employed in addition to controls for $PM_{2.5}$.

3.1 Introduction

For a few number of hours per year, electricity demand is much higher than during the remainder of the year. Due to congested transmission lines and insufficient generation capacity, these peak hours are associated with wholesale electricity prices that are 10 times or more than in off peak periods. This effect is especially acute in urban centers, which are constrained by available transmission and distribution (T&D) and electricity generation capacity. In extreme cases, electricity supply and demand cannot be balanced, leading to brownouts and blackouts. To help improve the reliability of the electricity grid, end users with on-site generation capacity, specifically backup generators installed to provide electricity during blackouts, could generate electricity during periods of peak demand (e.g. (43, 58)). These generators represent a significant source of under-utilized capacity; for example, it is estimated that there is at least 1,000 MW of installed backup generation in New York City (42). Several independent system operators (ISOs) have developed reliability programs that harness these generators. For example, the New York ISO (NYISO) allows backup generators to participate in emergency electricity and special capacity markets (59). Despite the potential benefits, many backup generators are excluded from these programs because they are diesel internal combustion engines (ICEs). There is concern about adverse human health effects from exposure to the non-negligible air emissions from a backup diesel ICE without advanced emission controls for nitrogen oxides (NO_x) and fine particulate matter ($PM_{2.5}$).

In a previous paper (Chapter 2), we evaluated the private (market) and social (air quality costs) of using installed backup diesel and natural gas fueled ICEs for meeting peak electricity demand in New York City compared to a conventional peaking plant (a simple cycle natural gas turbine) (60). To quantify the social costs from air quality, we converted the emissions from these generators to ambient concentrations using a 'state of science' air quality chemical transport model (CTM), the Particulate Matter Comprehensive Air Quality Model with extensions ($PMCAM_x$) (7). We found that a diesel ICE retrofitted with a catalyzed diesel particulate filter (DPF) could operate less expensively than a new peaking plant and without causing severe damage to human health. Since that work, the United States National Research Council concluded that there is sufficient evidence to

support a causal relationship between exposure to ozone (O_3) and pre-mature mortality (38). Thus, there is an increased emphasis on reducing the emissions of O_3 precursors from diesel ICEs, specifically by reducing NO_x. Retrofit emissions control options for NO_x that can be combined with a DPF on stationary diesel ICEs include low NO_x catalyst (LNC) and exhaust gas recirculation (EGR) (61). There is also the possibility of retrofitting to a dual fuel, also known as bifuel, ICE. With this retrofit, the engine uses mostly natural gas with a smaller amount of diesel used to ignite the mixture, reducing $PM_{2.5}$ and NO_x emissions (62). The natural gas is supplied by the existing natural gas infrastructure.

In this piece, we extend our previous analysis of backup generators for meeting peak electricity demand to include emission controls for NO_x. We also conduct a sensitivity analysis on our previous case study air quality modeling results from New York City by adding three additional cities: Atlanta, Chicago, and Dallas. Finally, we evaluate the robustness of our full cost results (private and social) with respect to uncertainties in the mechanisms for the formation of secondary $PM_{2.5}$ in the CTM and health endpoints.

3.2 Methods and data

We use a levelized approach to compare the full cost of using diesel backup generators with and without emission controls for $PM_{2.5}$ and NO_x to a simple cycle natural gas turbine. We include both the private (or market) prices and the social (or unpriced externalities) as defined by Equation 3.1 and Equation 3.2.

$$Levelized\ Full\ Cost = Private\ Cost\ (PC) + \ Social\ Cost\ (SC) \ldots Eqn\ 3.1$$

$$Levelized\ Full\ Cost = \frac{(CC + TD + RF)}{HR} \cdot CRF + \frac{FOM}{HY} + VOM + FC + SC \ldots Eqn\ 3.2$$

Where CC is the capital cost of the generator attributable to the peak electricity generation (in $/kW);

CRF is the capital recovery factor to convert cost into equal annual payments at a specified discount rate (estimated at 15%);

FC is the fuel cost (in $/kWh);

FOM is the fixed operating and maintenance (in $/kW-yr);

HR is the number of hours per year of operation (estimated at 200 hours);

RF is the capital cost of an emission control retrofit (in $/kW);

TD is the capital cost of T&D or grid-generator interconnections (in $/kW);

VOM is the variable operating and maintenance (in $/kWh); and

SC is the social cost (in $/kWh)

The fuel cost (FC) is calculated as the heat rate (in Btu/kWh) of the generator multiplied by the price of fuel for the relevant consumer class (in $/Btu). Fuel costs are obtained from Energy Information Agency (EIA) and are updated from our previous work (Chapter 2) (63). We use the mean, minimum and maximum values from 2005 to 2008. We use a diesel fuel price of $2.50/gallon with a 10 ¢ premium for ultra low sulfur diesel (ULSD) fuel with a range of $1.50/gallon to $4.00/gallon. For natural gas, we use a price of $9.00/Mcf with a range of $5.50/Mcf to $12.50/Mcf for electricity production and $14.50/Mcf with a range of $10.80/Mcf to $20.30/Mcf for commercial deliveries.

We present the capital costs and operating and maintenance (O&M) for the emission controls in Table 3.1. The retrofit costs were obtained from the Manufacturer of Emissions Control Association (2000) (64) and the Western Regional Air Partnership, WRAP (2005) (65). Following the guidance of WRAP (2005), we assume that the fixed maintenance cost for all retrofits is dominated by the cost of maintaining the diesel particulate filter (DPF). We estimate an annual fixed cost of $1.90/kW, based on California Air Resources Board (CARB) annual maintenance costs of $156 to $312. For the dual fuel retrofit, we estimate costs from $35/kW (approximately the value at which the retrofitted dual fuel ICE would have the same levelized cost as an uncontrolled diesel ICE at the mean fuel prices for diesel and natural gas) to $100/kW (62, 66). We assume a cost of $125/kW for interconnections required for the generators to operate in parallel with the electricity grid (43). Finally, we assume a variable O&M cost of 0.01$/kWh for

all backup generators. We compare this to a natural gas turbine with a capital cost of $500/kW and a fixed O&M of $15/kW-yr (48). We estimate $100/kW for T&D to transport the electricity from the turbine to the urban center.

We quantify the social cost of air quality using a bottom-up impact pathway technique. The first step is modeling the enhanced ambient concentrations from operating the generators. Second, we transform these concentrations into their equivalent health endpoints and economic values. To model the ambient concentration changes, we start by collecting emission factors (EF) for all generator/retrofit combinations. In Table 3.1, we show the baseline EFs corresponding to an uncontrolled diesel ICE and the reductions from baseline for retrofitting with a catalyzed DPF, a DPF-LNC, a DPF with a low pressure EGR, and dual fuel operation. The EFs and fuel economy penalties for the generator/retrofit combinations are derived from the California Air Resources Board (2008) (67), the Environmental Defense Fund (2004) (61), and the Natural Resources Defense Council (2004) (68). For all retrofit options, we employ an ULSD fuel, which reduces the sulfur dioxide (SO_2) by approximately 95%. The reductions for the dual fuel option are highly dependent on the percent of diesel which is replaced by natural gas. We present a range of 70% to 95% natural gas. For $PM_{2.5}$ from the retrofit, we assume that the EF is a linear combination of the EFs for an uncontrolled diesel and natural gas ICE multiplied by the fraction of the two fuels. For NO_x, the emissions are a function of combustion characteristics with most retrofits reporting reductions of approximately 50%. There is also evidence that the carbon monoxide (CO) and hydrocarbons (HC) can be higher than the diesel ICE (69).

To construct a scenario for operating these generators, we isolate the top 200 hours with hourly load data from the Federal Energy Regulatory Commission (FERC) Form 714 (21). For New York City and Chicago, we used electricity load data specific to the city control area. For Dallas and Atlanta, we assume that these cities follow the same trend as the lower resolution state level data. For detailed air quality simulations, we identify two peak periods of three days each from July 17 – 19, 2001 and July 23 – 25, 2001, a time period for which our basecase $PMCAM_x$ simulations have been evaluated extensively

(32). While not all cities experienced peak electricity demand on all days, we run all six days for all cities to capture additional variability in the meteorological conditions. To investigate a scenario with substantial use of backup power, we assume that 1,000 MW of capacity operates from 9 am – 9 pm local time per city per day. In NYC, 1,000 MW is approximately the average peak load (defining the load as the difference in the electricity demand between any of the top 200 hours and the load in the 201st hour) and is consistent with estimates of available backup generation capacity in the area. While 1,000 MW exceeds the average peak electricity demand in Atlanta, Chicago and Dallas, we model 1,000 MW in each city to produce a conservative estimate of the costs from air quality. We calculate the total hourly emissions by multiplying the emission factors in Table 3.1 by 1,000 MW for each hour of operation.

We transform the emissions into their equivalent ambient concentrations using the Comprehensive Air Quality Model with extensions and particulate matter modules ($PMCAM_x$). $PMCAM_x$ is a 'state of the science' CTM that simulates the emission, advection (convection), dispersion, gas and aqueous phase chemical reactions, and dry and wet deposition for 35 gaseous species, 12 radical species and 13 aerosol species in 10 size bins on a 3-D Eulerian grid. The gaseous chemistry is simulated using the Carbon Bond Mechanism (CBM) IV (19). Additional modules simulate the dynamic behavior (coagulation, condensation, and nucleation) of aerosols species. The model domain is discretized into a horizontal grid of 36 by 36 km with 14 vertical layers from the surface to 6 km. The lowest model layer is slightly less than 30 m thick vertically. Details and evaluation of the model can be found in Gaydos et al. (2007) (7) with evaluation in Karydis et al. (2007) (32).

We conduct separate model runs for each city to capture all the air quality effects from operating the generators in that city; these results are used to calculate the social costs. We also conduct one model run with generators operating in all cities at once and one run with no changes to the basecase emission fields. We show the difference between these two runs in the plots in this manuscript. The emissions are modeled as an evenly distributed area source over the coarse grid cell that contains the majority of the urban

area. The baseline concentrations are generated with emission files from the Lake Michigan Air Directors Consortium (LADCO) (31).

Table 3.1: Retrofit options, heat rate in Btu/kWh and fuel efficiency penalties in % from baseline, baseline emission factors in g/kWh and reductions in % from baseline

Emission Control Retrofit	Capital Cost ($/kW)	O&M ($/kW - yr)	Heat rate (Btu/kWh) or Penalty (%)	NOx (g/kWh) or (%)	$PM_{2.5}$ (g/kWh) or (%)	CO (g/kWh) or (%)	HC (g/kWh) or (%)	SO_2 (g/kWh) or (%)
Baseline	-	-	9,750	18.8	1.40	6.40	2.0	1.25
DPF	25 - 40	1.90	0 - 4%	NA	85- 99%	90 %	90 %	95 %
DPF - LNC	40 - 60	1.90	0 - 7%	10-25 %	85- 99%	90 %	90 %	95 %
DPF - EGR	40 - 55	1.90	0 – 5%	25-60 %	85-99%	90 %	90 %	95 %
Dual fuel (70% - 95% natural gas)	35 -100	-	0 – 8%	~ 50%	68 -92%	-	-	95-99 %

The changes in ambient air quality are translated into mortality and morbidity effects and dollar values, using concentration-response (CR) functions, economic valuations and population distribution from the Environmental Benefits Mapping and Analysis Program (BenMap), version 2.4.85 (34). Focusing on the relationship between long-term (annual) exposure to $PM_{2.5}$ and premature mortality, we use a fixed pooling of CR relationships from Laden et al. (2006) (70) and Pope et al. (2002) (71). We model the value of a statistical life (VSL) as a Weibull distribution with a mean of $7.5 million (in 2005 dollars) (Weibell scale parameter: 8,300,000; Weibull shape parameter: 1.5096). We also report 5% and 95% confidence intervals. In addition to the relationships for long-term mortality from $PM_{2.5}$, we evaluate short-term (daily) mortality from $PM_{2.5}$ based on Klemm and Mason (2003) (72) and Schwartz (2003) (73). We also examine a range of estimates for carcinogenic effects from diesel particulate matter (DPM). The US Environmental Protection Agency (EPA) estimated a range of 1×10^{-3} to 1×10^{-5} cancer cases for each $\mu g/m^3$ of DPM of continuous exposure over a 70 year lifetime, but concluded that the existing data is insufficient to derive quantitative risk factors (36). The California Office of Environmental Health Hazard Assessment (OEHHA) and the Air Resources Board (CARB) established a "reasonable estimate" of 3.0×10^{-4} $\mu g/m^3$ (37). To calculate the increase in cases, we multiply the annual average concentration enhancements by the cancer risk estimate and divide by 70 years to estimate the number of cases on an annual basis. We cost all cancer outcomes at the VSL since most cases are lung cancer which has a poor prognosis. We assume that the average of our six modeled days is representative of the change in ambient concentrations that would be observed on any peak electricity day, and that there are thirty days of operation over the year.

3.3 Results and discussion

3.3.1 Private costs

In Figure 3.1, we show the private costs of operating diesel ICEs with and without emission control retrofits compared to constructing a new natural gas simple cycle turbine. All backup options are less expensive for meeting peak electricity demand than the turbine. The capital costs of the backup generators do not need to be included when using the generator for peak power. The capital cost as well as the fixed operating and maintenance (O&M) is already attributed to the increased reliability (e.g. protection from a blackout) provided by the generator to its owner. Since the additional number of hours of operation for peak power is small (e.g. less than 200 hours per year), there is only minimal additional wear on the ICE. By contrast, the owner of a new peaking plant would need to recover the capital costs and the fixed O&M as well as the marginal cost of producing electricity. Using the costs in Table 3.1, the emissions control retrofits have a levelized cost of 2 to 4 ¢/kWh. As with the DPF, there is a small fuel efficiency penalty associated with the NO_x controls and the dual fuel retrofit which we include in Figure 3.1. We also include the small premium associated with ULSD. We do not include selective catalytic reduction (SCR) as a NO_x emission control option as it is impractical for an emergency generator to have urea available for operation. As the full cost of all control options is similar, quantifying the effectiveness of these options at reducing the air quality and adverse human health effects is necessary to make a recommendation on the type of retrofit.

Figure 3.1: Private costs for installed backup generators with and without emission controls and a peaking plant in ¢/kWh. The costs shown are the average of the range presented in Table 3.1. The bars represent the low and high fuel prices. The fuel cost for the dual fuel option is calculated for 80% natural gas and 20% diesel.

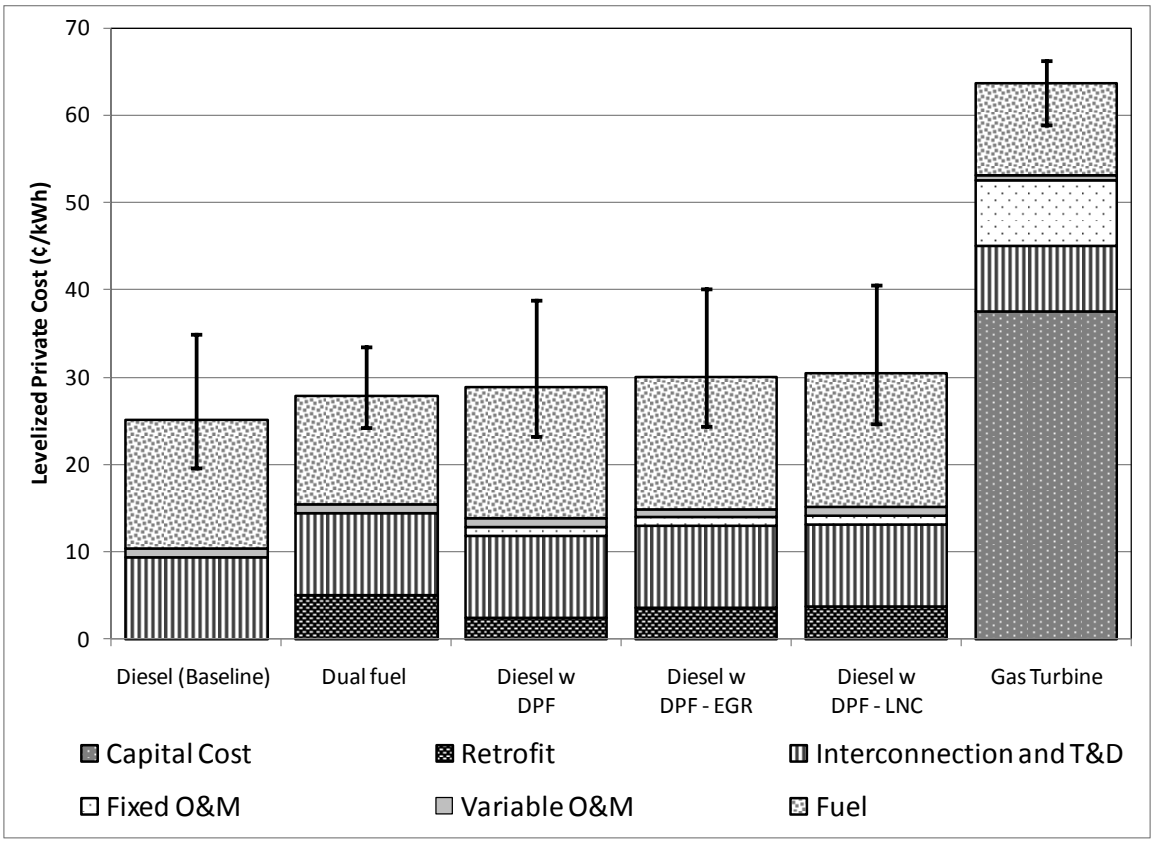

3.3.2 Air quality effects

In Figure 3.2, we show the average of the difference in 1-hour peak O_3 concentrations (in ppb) over the six days for an uncontrolled diesel ICE and a diesel ICE with DPF-EGR emission controls. In Figure 3.3, we show the average change in the daily mean O_3 concentrations (in ppb) over the six days for an uncontrolled diesel ICE and a diesel ICE with DPF-EGR emission controls. The diesel ICE with a DPF has the same changes in O_3 as an uncontrolled diesel ICE. The dual fuel option has approximately the same O_3 changes as a diesel ICE with DPF-EGR controls. For the DPF-LNC option (not shown), the changes in O_3 are in-between an uncontrolled diesel ICE and a diesel ICE with DPF-EGR controls. At the high NO_x emissions from the uncontrolled diesel ICE, the decreases in O_3 are pronounced in the urban centers with smaller increases downwind. This effect is reduced as the NO_x emissions decrease with the emission control retrofits or by shifting to dual fuel. These O_3 concentrations are consistent with the representation of the VOC to NO_x ratios in the model. When the initial ratio of NO_x to VOC is high (i.e., VOC-limited), adding more NO_x will decrease the formation of O_3. At lower ratios (i.e., NO_x-limited), the additional NO_x increases the formation of O_3. Urban centers tend to have high NO_x to VOC ratios, and hence, adding more NO_x results in the observed decreases (55). Outside of the urban centers, there are small increases in O_3. These increases are more pronounced around Atlanta and Dallas which are more strongly NO_x-limited in our model than around Chicago and New York City. These results are broadly consistent with the sensitivities of O_3 with respect to NO_x for these cities found in a modeling study by Liao et al. (2008) (74). The pattern of increases and decreases in O_3 can be observed for both the maximum difference in 1-hour and daily mean averaging periods, although the increases are more pronounced for the maximum 1-hour O_3 concentrations. We explore the implications of the choice of averaging period on health effects and social costs in the next section.

Figure 3.2: Average change in 1-hour O_3 concentrations in ppb for an uncontrolled diesel ICE [top] and a diesel controlled with a DPF-EGR [bottom] over the six days of modeling. The EGR reduces the NO_x emissions by 50%.

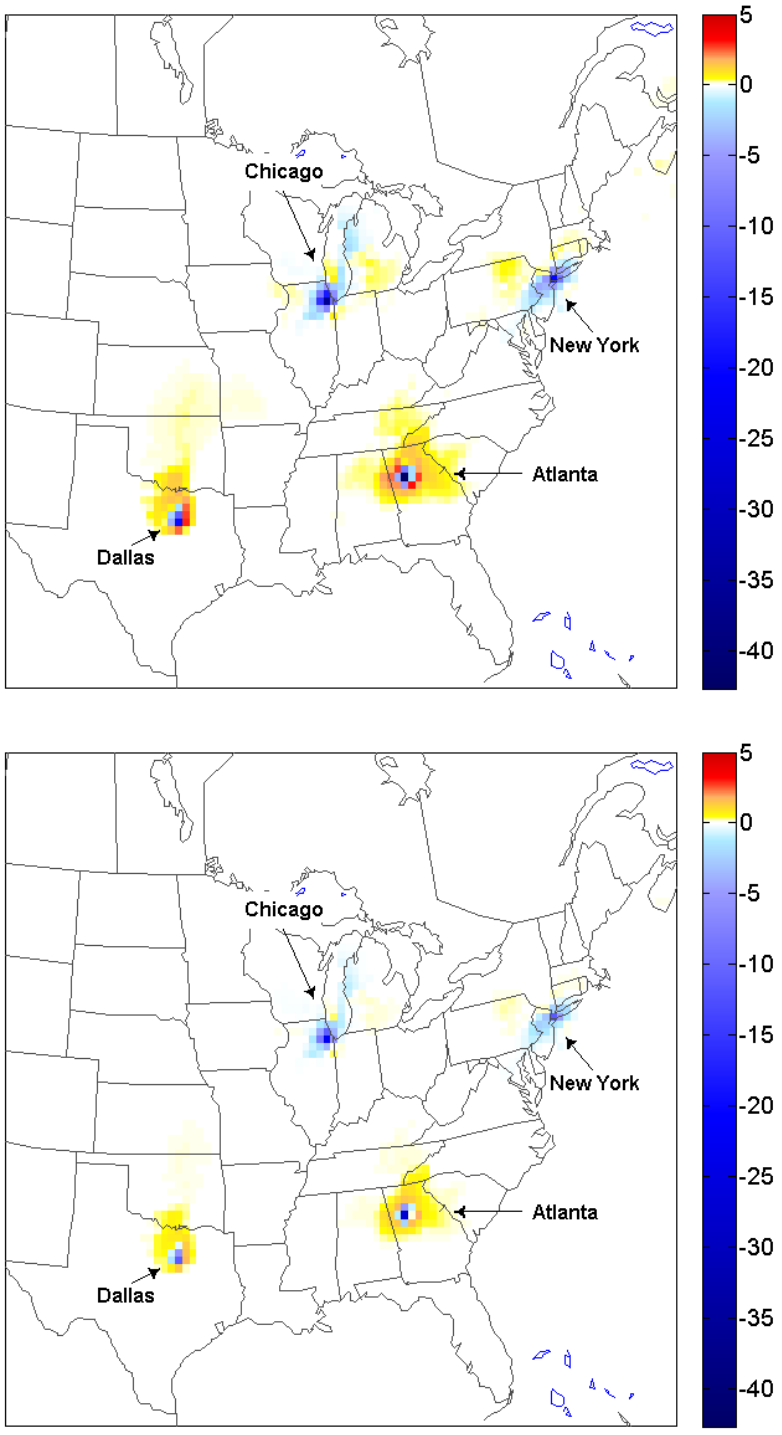

Figure 3.3: Average change in daily mean O_3 concentrations in ppb for an uncontrolled diesel ICE [top] and a diesel controlled with a DPF-EGR [bottom] over the six days of modeling. The EGR reduces the NOx emissions by 50%.

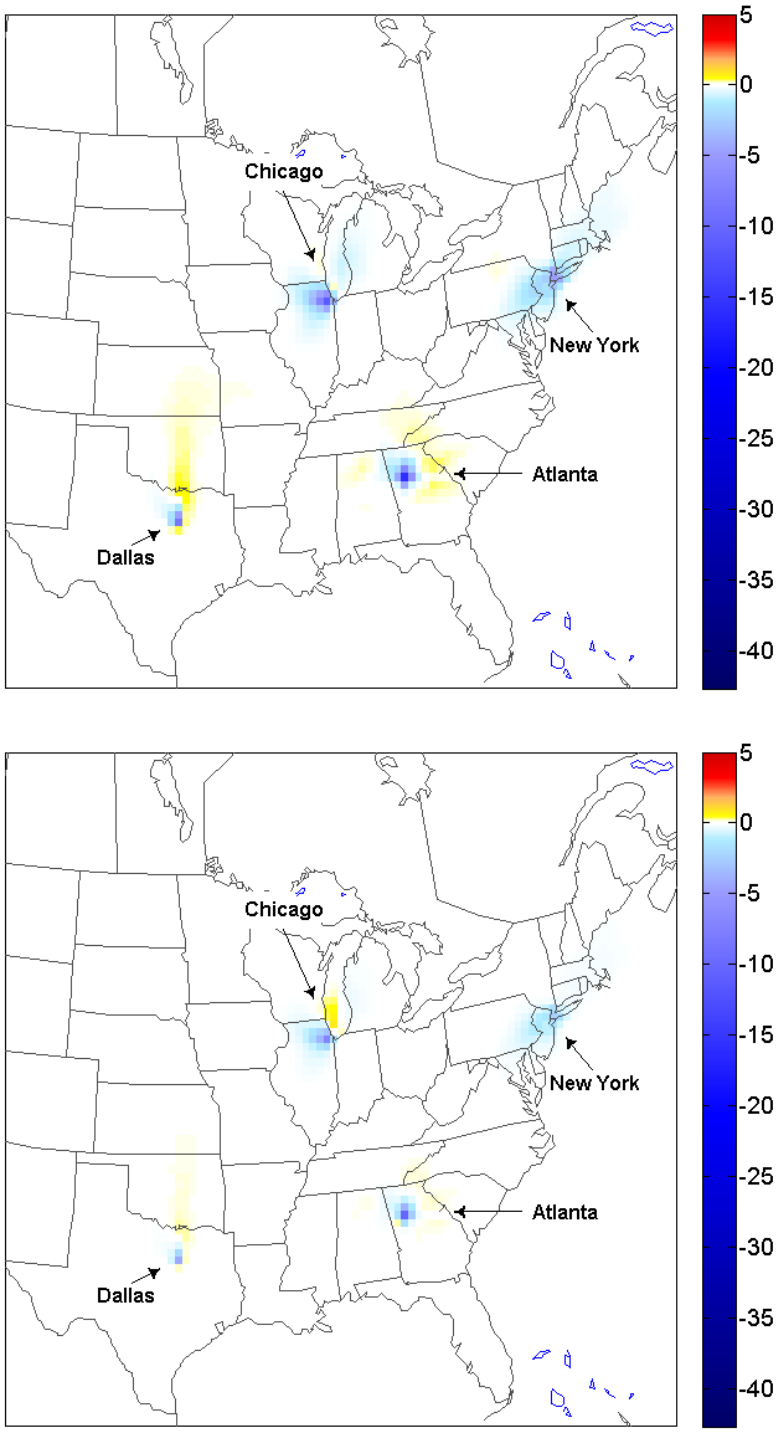

In Figure 3.4, we show the daily mean $PM_{2.5}$ enhancement (in $\mu g/m^3$) averaged over all six days of operation for an uncontrolled diesel ICE and a diesel ICE retrofitted with a DPF-EGR for all cities. The increase in $PM_{2.5}$ is due mainly to increases in primary elemental (PEC) and organic carbon (POC). Since much of the $PM_{2.5}$ is primary, adding a DPF reduces ambient concentrations. We also observe small increases and decreases of approximately 0.5 to 1 $\mu g/m^3$ in secondary $PM_{2.5}$ which is formed by chemical reactions of NO_x, SO_2 and VOCs. In VOC-limited urban centers, an increase in NO_x emissions results in a decrease of oxidant concentrations (e.g. O_3 and the hydroxyl radical, OH) which are necessary to oxidize the precursor gases to their aerosol form (75). As a result, despite the increases in SO_2 and VOC emissions, particulate matter sulfate (PSO_4) and secondary organic aerosol (SOA) decrease slightly (76). Further, although there is a decrease in oxidants, we still observe increases in secondary nitrate (PNO_3) due to the substantial increases in NO_x emissions. In order for PNO_3 to form, there must also be sufficient ammonia (NH_3) to neutralize the nitric acid (HNO_3). The decrease in PSO_4 releases NH_3 to react with the HNO_3, making PNO_3 increases more likely. Predicting the amount of "free" NH_3 is challenging because it typically depends on small differences between NH_3 and PSO_4 concentrations and, therefore, tends to magnify errors in model predictions of both quantities (77). Evaluating whether the modeled PNO_3 increases are plausible is further compounded by uncertainties in NH_3 emission inventories and a lack of suitable measurements for gaseous or total NH_3 (78). However, the largest increase in PNO_3 is found in Atlanta where previously measurements campaigns have found that the formation of PNO_3 is not limited by the available NH_3 (79, 80). The magnitude of the increases and decreases also vary with the meteorology, especially for PNO_3. Days with higher PNO_3 formation have colder temperatures and higher relative humidity which favors the partition of nitrate to the particulate phase (81). However, $PMCAM_x$ has known problems representing PNO_3 due to difficulties simulating the heterogeneous nighttime formation rate of HNO_3 (32). In addition, the current representation of SOA formation in $PMCAM_x$ does not reflect the present state of knowledge (82). We discuss the implications and conduct a sensitivity analysis on the formation of secondary $PM_{2.5}$ with respect to health costs. See the Supporting Information (Figures 3.6 – 3.13) for complete speciation of $PM_{2.5}$ for each emission control combination.

Figure 3.4: Change in daily mean $PM_{2.5}$ in $\mu g/m^3$ as an average of all six days of operation for an uncontrolled diesel ICE [top] and for a diesel ICE with a DPF-EGR [bottom].

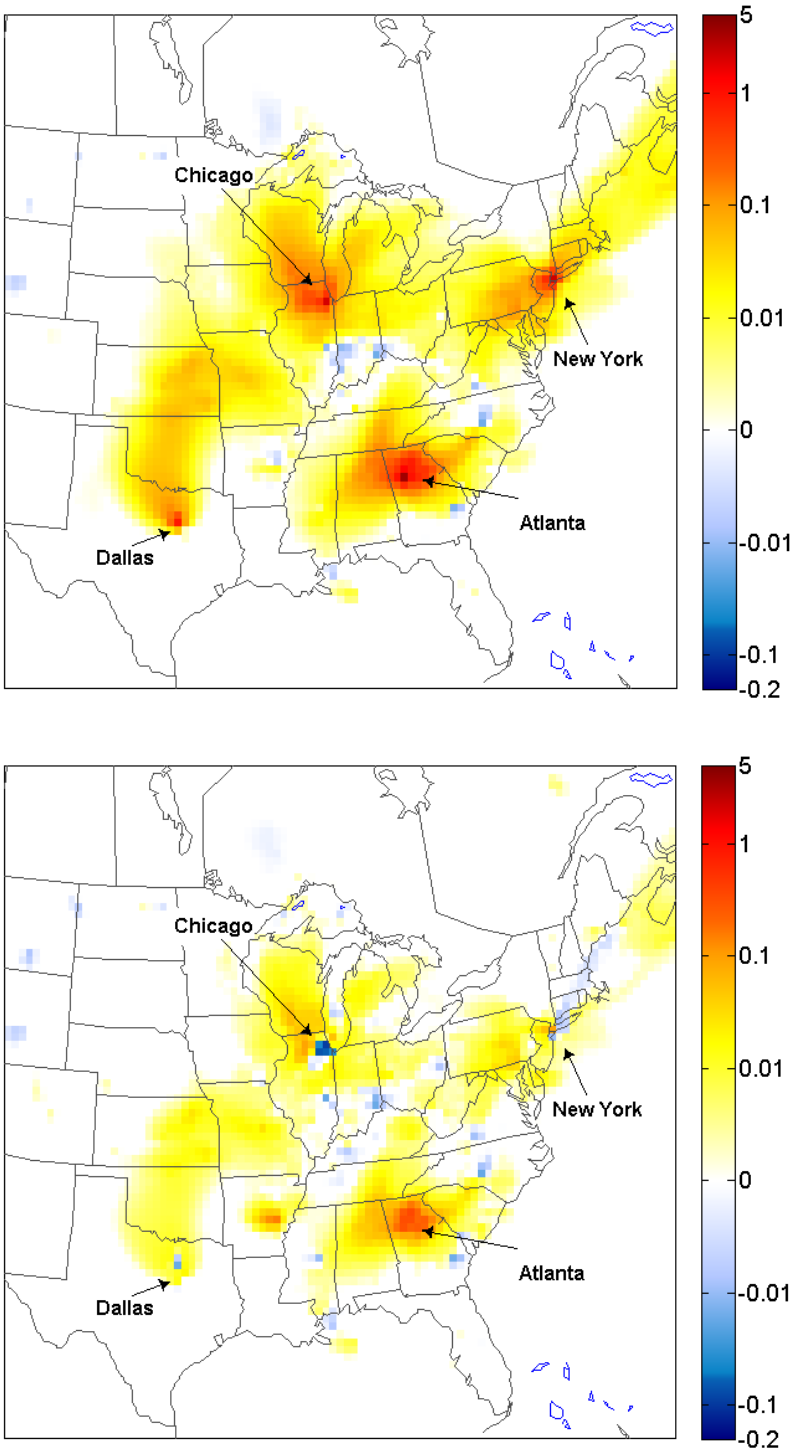

3.3.3 Human health effects and social costs

In Table 3.2, we present the social costs for operating the backup generator by city for long-term mortality from exposure to $PM_{2.5}$ for the following specifications: 1) sum of positive changes in $PM_{2.5}$ species only, 2) primary $PM_{2.5}$ species only, and 3) sum of all changes in all species. We look at these three measures of social cost to explore the uncertainty on the representation of the formation of secondary $PM_{2.5}$ in $PMCAM_x$. We assume that the mortality relationship for each species is the same as for the total $PM_{2.5}$ mass. Changes in long-term mortality from $PM_{2.5}$ comprise the majority of the costs. Morbidity effects are approximately 10% of the long-term mortality cost.

Looking at the individual $PM_{2.5}$ species, the primary (directly emitted) components comprise the majority (> 70 %) of the cost for the uncontrolled diesel. Depending on the city, however, we find that the secondary $PM_{2.5}$ can have a significant influence on the total cost once the primary $PM_{2.5}$ is controlled with a DPF. In Chicago, changes in secondary $PM_{2.5}$ results in an overall negative social cost. This "all species" approach may be considered a best estimate of the current model configuration, but known problems and uncertainties in predicting different secondary $PM_{2.5}$ species limits our confidence in these results. Since the errors in predicting the different secondary $PM_{2.5}$ species are largely uncorrelated, it is possible that backup power could lead to the increases predicted for some species but not the decreases predicted for others. Therefore, the "positive changes" results reflect this worst case scenario.

We find that there is an order of magnitude difference in social costs from city to city which is driven mainly by the population density in and around the urban center. The large populations in New York City and Chicago result in higher social costs than in Atlanta and Dallas. Local chemistry, however, also plays an important role. This effect is more pronounced in Atlanta and Chicago. In Atlanta, increases in secondary $PM_{2.5}$ species account for approximately 30% of the total health costs for an uncontrolled diesel ICE. This limits the effectiveness of the DPF in reducing the social cost. When considering only increases in secondary $PM_{2.5}$, we find a similar effect in Chicago. In

Dallas, the social costs are small due to a smaller population in the surrounding area and less formation of secondary $PM_{2.5}$.

By using the CR functions for all $PM_{2.5}$, we assume that the $PM_{2.5}$ observed from operating diesel and dual fuel ICEs is similar to the $PM_{2.5}$ observed in the epidemiological studies. This is not strictly true as the composition of diesel particulate matter (DPM) differs from average ambient compositions. Of specific concern is the relationship between DPM and lung cancer. Using the highest estimate of the relationship from the USEPA, we calculate a social cost at approximately 10% of the costs from the long-term $PM_{2.5}$ CR functions. The California OEHHA relationship yields a cost of approximately 3% of cost from long-term mortality from $PM_{2.5}$. The USEPA, however, also finds that a zero cancer risk cannot at present be dismissed. In addition, Pope et al. (2002) (71) and Laden et al. (2006) (70) include lung cancer as an endpoint in their studies linking ambient $PM_{2.5}$ to mortality. To the extent that ambient DPM contributed to this outcome, there is the potential for double counting if we include both long-term mortality and carcinogenic effects. Nevertheless, at 3% to 10% of the total social cost, these factors do not represent a significant source of uncertainty in our assessment. The long-term CR function and the carcinogenic DPM relationship are both based on constant changes in daily exposure (i.e., every day of the year); in this scenario, the generators would operate for only the top 200 hours a year. Thus, we also evaluate the social cost from the short term mortality CR function for $PM_{2.5}$. We find that the short-term costs are approximately 15% of the costs from using the long-term mortality relationships. Short-term mortality from $PM_{2.5}$, however, is not included in the 2006 regulatory impact analysis for the revised National Ambient Air Quality Standard (NAAQS) for $PM_{2.5}$ since there is concern that including both the long and short-term effects may result in double counting (83).

Table 3.2: Mean social cost in ¢/kWh with 5% and 95% confidence intervals from generator/retrofit options using the long-term (annual) relationship between exposure to $PM_{2.5}$ and mortality for the sum of positive changes in concentrations, primary species, and the sum of all changes in concentrations by city

		Uncontrolled diesel ICE	Diesel w DPF	Diesel w DPF - LNC	Diesel w DPF - EGR	Dual fuel retrofit
Atlanta	Positive changes	62.7 (14.0 – 150)	18.8 (4.20 – 45.0)	18.4 (4.10 – 44.0)	12.2 (2.72 – 29.2)	14.3 (3.20 – 34.2)
	Primary species	42.3 (9.45 – 101)	2.12 (0.47 – 5.07)	2.12 (0.47 – 5.07)	2.12 (0.47 – 5.07)	4.23 (0.94 – 10.1)
	All species	60.8 (13.6 – 146)	16.1 (3.58 – 38.4)	16.5 (3.70 – 39.6)	10.5 (2.35 – 25.2)	12.6 (2.82 – 30.2)
Chicago	Positive changes	101 (22.6 – 242)	27.1 (6.05 – 65.0)	22.8 (5.10 – 54.7)	16.6 (3.72 – 39.9)	20.5 (4.59 – 49.2)
	Primary species	78.2 (17.5 – 187)	3.91 (0.87 – 9.36)	3.91 (0.87 – 9.36)	3.91 (0.87 – 9.36)	7.82 (1.75 – 18.7)
	All species	80.2 (17.9 – 192)	-2.01 (-4.81 - -0.45)	3.32 (0.74 – 7.96)	-0.67 (-1.59 - -0.15)	3.24 (0.72 – 7.76)
Dallas	Positive changes	15.9 (3.55 – 38.1)	1.55 (0.35 – 3.71)	2.89 (0.64 – 6.91)	1.58 (0.35 – 3.79)	2.22 (0.50 – 5.32)
	Primary species	12.8 (2.86 – 30.7)	0.64 (0.14 – 1.53)	0.64 (0.14 – 1.53)	0.64 (0.14 – 1.53)	1.28 (0.29 – 3.07)
	All species	15.6 (3.47 – 37.3)	1.13 (0.25 – 2.71)	2.56 (0.57 – 6.13)	1.31 (0.29 – 3.14)	1.95 (0.44 – 4.67)
New York	Positive changes	186 (41.4 – 445)	28.1 (6.28 – 67.3)	27.0 (6.04 – 64.7)	19.3 (4.31 – 46.2)	26.5 (5.92 – 63.5)
	Primary species	161 (35.9 – 385)	8.04 (1.80 – 19.3)	8.04 (1.80 – 19.3)	8.04 (1.80 – 19.3)	16.1 (3.60 – 38.5)
	All species	173 (38.6 – 413)	10.7 (2.39 – 25.6)	15.3 (3.41 – 36.6)	8.46 (1.89 – 20.3)	16.5 (2.69 – 39.5)

In addition to the health effects from $PM_{2.5}$, the US National Research Council (2008) concluded that short term exposure to O_3 is associated with premature mortality based on new evidence from recent studies (38). In Table 3.3, we compare the social value of the health effects from changes in O_3 using a 24-hour (daily mean) metric from Bell et al. (2004), (2005) and (2006) (84-86) and the peak 1-hour metric from Levy et al. (2005) (87). With either metric, we calculate a social benefit from decreased mortality due to the decreases in O_3 concentrations in the highly populated urban centers. Using the CR function from Levy et al. (2005), however, generates benefits 2 to 3 times that of the daily mean CR functions. Presently, it is not known which averaging period is a better predictor of mortality.

While the formation of $PM_{2.5}$ is subject to error and uncertainties, the chemistry that drives the formation of O_3 is well understood, and our results are robust in all modeled cities. By contrast, the magnitude of relationship between mortality and O_3 is subject to greater uncertainty. In addition, while we show a social benefit from the reduced O_3 due to the large populations in the urban centers, parts of the surrounding region experience small social costs. Also, while the benefit from the decreases in O_3 from adding the additional NO_x to the urban centers exceeds the cost from the increases in PNO_3, the suburban/rural areas experience up to a 10x greater social cost from PNO_3 than the urban center. Recognizing these uncertainties and possible equity issues, we suggest a conservative strategy of controlling NO_x emissions which decreases both the benefit from O_3 reductions as well as the costs from increased secondary $PM_{2.5}$. For all $PM_{2.5}$ species and O_3, we show the distribution of the costs for each city between the urban center and the surrounding region in the Supporting Information (Tables 3.4 – 3.13).

Table 3.3: Comparison of the costs of mortality from O_3 in ¢/kWh with 5% and 95% confidence intervals for the daily 24-hour mean and peak 1-hour concentration-response functions by city. Note that a negative value is a social benefit from reduced mortality.

	O_3 metric	Uncontrolled diesel	Diesel with DPF	DPF-LNC	DPF-EGR	Dual Fuel
Atlanta	Daily mean	-17.7 (-4.52 – -37.8)	-17.7 (-4.52 – -37.8)	-15.0 (-3.84 – -32.0)	-11.3 (-2.88 – -24.1)	-11.3 (-2.88 – -24.1)
	Max 1-h	-37.9 (-12.1 – -68.0)	-37.9 (-12.1 – -68.0)	-32.8 (-10.5 – -58.7)	-24.2 (-7.74 – -43.3)	-24.2 (-7.74 – -43.3)
Chicago	Daily mean	-41.6 (-10.6 – -88.6)	-41.6 (-10.6 – -88.6)	-34.9 (-8.90 – -74.4)	-25.4 (-6.47 – -54.1)	-25.4 (-6.47 – -54.1)
	Max 1-h	-138 (-44.2 – -248)	-138 (-44.2 – -248)	-116 (-37.1 – -208)	-84.1 (-26.9 – -151)	-84.1 (-26.9 – -151)
Dallas	Daily mean	-9.62 (-2.45 – -20.5)	-9.62 (-2.45 – -20.5)	-7.78 (-1.98 – -16.6)	-5.25 (-1.34 – -11.2)	-5.25 (-1.34 – -11.2)
	Max 1-h	-25.6 (-8.20 – -45.9)	-25.6 (-8.20 – -45.9)	-21.1 (-6.74 – -37.8)	-13.6 (-4.36 – -24.4)	-13.6 (-4.36 – -24.4)
New York City	Daily mean	-55.4 (-14.1 – -118)	-55.4 (-14.1 – -118)	-44.7 (-11.4 – -95.2)	-31.4 (-8.01 – -66.9)	-31.4 (-8.01 – -66.9)
	Max 1-h	-155 (-49.7 – -278)	-155 (-49.7 – -278)	-124 (-39.6 – -222)	-84.9 (-27.2 – -152)	-84.9 (-27.2 – -152)

3.4 Conclusions: Full costs

The decision to operate backup generators for peak electricity demand rather than construct a new peaking plant is based on the sum of the private costs and the social costs from changes in air quality. In Figure 3.5, we show the full cost by city for each generator/emission control technology combination with the social costs for the sum of positive changes in concentrations, primary species, and the sum of all changes in concentrations. We show only the costs for pre-mature mortality from the long-term CR relationship for $PM_{2.5}$. We focus on the long-term CR relationship because of the comparatively small costs from the short-term CR mortality relationship and the potential carcinogenic effects from DPM as well as the potential for double counting mortality effects.

For the three different estimates at the mean social cost, the full cost of all emission control options is less than a new peaking plant. Although the differences in small, we find minimum full costs for a DPF without any NO_x controls or a DPF with 50% reductions in NO_x achieved with EGR controls for changes in all species. If we consider only positive enhancements in $PM_{2.5}$, however, the lowest full cost is achieved with DPF–EGR controls. In the more densely populated cities of New York City and Chicago, however, the worst case of costing only increases in $PM_{2.5}$ species results in a full cost that is approaching the peaking plant cost. As a result, it is important that the emission controls achieve their expected performance. While adding the social benefit from the reductions in O_3 would decrease the full costs, we do not include this effect because of the importance of reducing the formation of PNO_3. In areas where PNO_3 increases are projected to occur, however, we could have greater confidence in projecting $PM_{2.5}$ impacts of using distributed backup power if a network of total NH_3 measurements were established (78). To date, the National Atmospheric Deposition Program (NADP) has established a monitoring network, and Clean Air Status and Trends Network (CASTNET) is planning to measure NH_3 (88). Given the low cost of NO_x controls, we recommend retrofitting the generators with these controls.

This sensitivity analysis confirms the results from the case study in Gilmore et al. (2006) for New York City (60) and shows that this strategy could also work in Atlanta, Chicago and Dallas. Based on these results, we renew our recommendation that the relevant regulatory bodies reconsider their ban on using diesel ICEs for meeting peak electricity demand, taking care that taking care individual generators maintain appropriate emission standards for both $PM_{2.5}$ and NO_x and are properly sited so as not to cause a nuisance in the immediate area.

Figure 3.5: Total (private and social) cost by city and control technology in ¢/kWh. The white bars are the private costs. The patterned bars are the social costs from long term mortality from $PM_{2.5}$ for the all species approach. The high error bars represent the cost associated with positive changes in $PM_{2.5}$ species only. The low error bar represents the cost associated with primary species only. The black line is the levelized cost of constructing and operating a simple cycle natural gas turbine for the peak electricity application (approx 60 ¢/kWh).

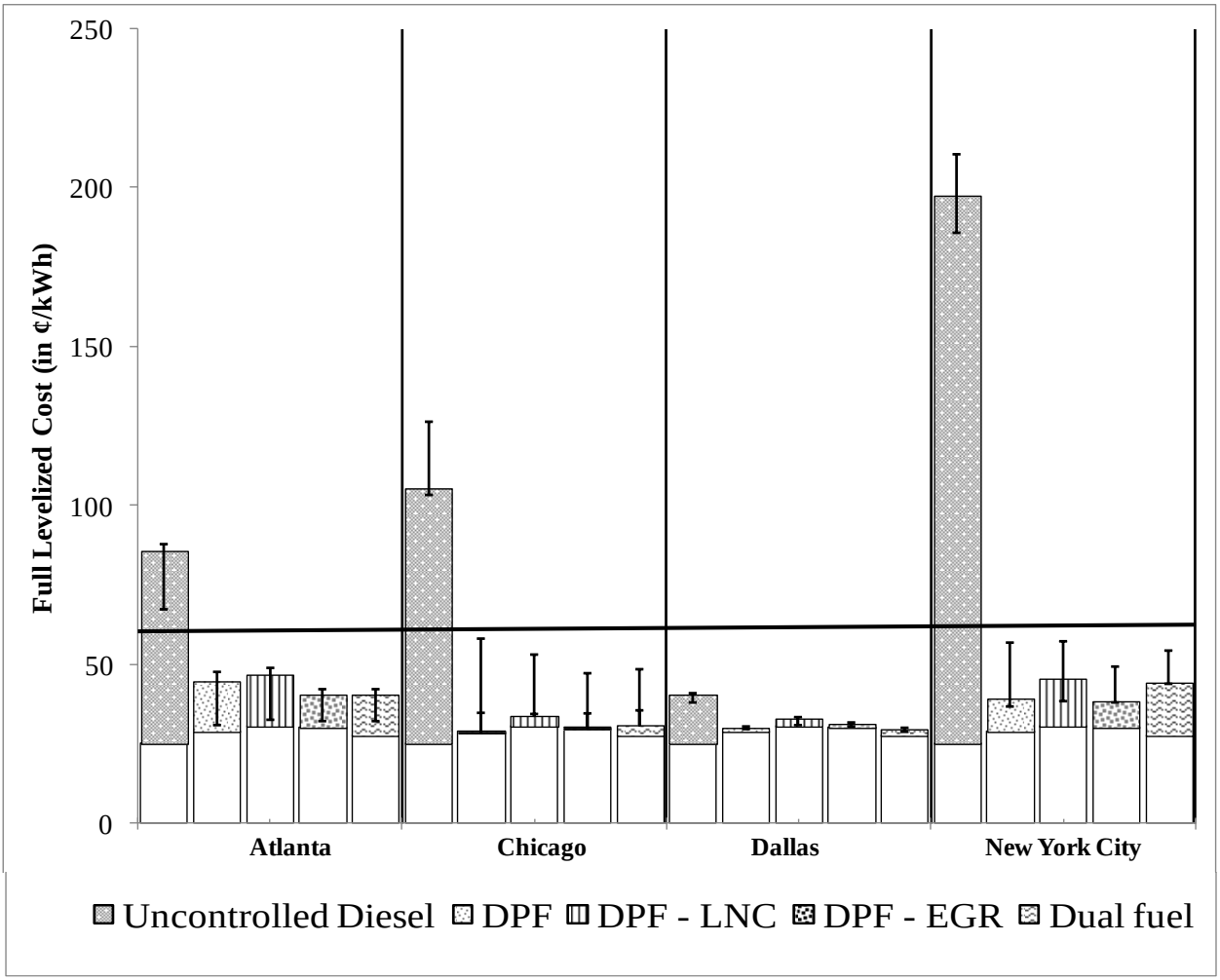

3.5 Supporting information

3.5.1 Supplemental figures for the speciation of $PM_{2.5}$ for the emission control options

Figure 3.6: Change in daily mean primary $PM_{2.5}$ in µg/m^3 as an average of all six days of operation for an uncontrolled diesel ICE

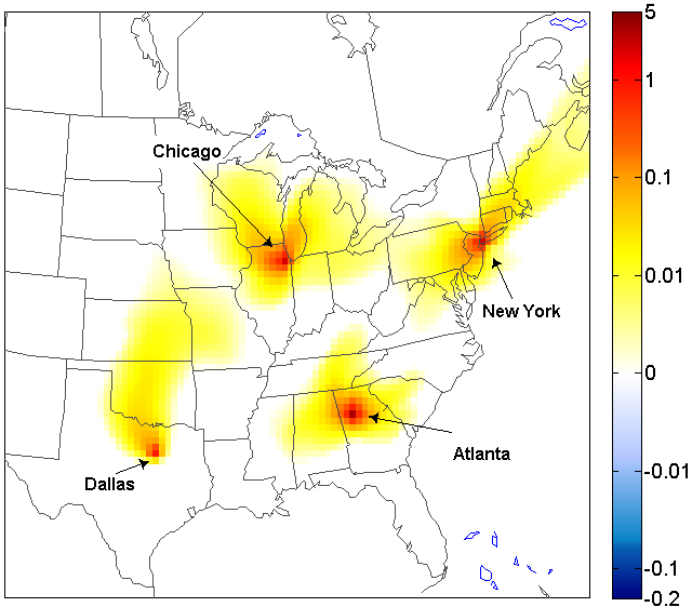

Figure 3.7: Change in daily mean primary $PM_{2.5}$ in µg/m^3 as an average of all six days of operation for an uncontrolled diesel ICE with a DPF. The same result is observed for a DPF-LNC and a DPF-EGR. Since the EGR retrofit decreases the temperature of the exhaust to reduce NO_x, there is the potential for slight increases in the $PM_{2.5}$ EF above the EF for the uncontrolled diesel ICE. By coupling an EGR with a DPF, there is a little appreciable effect on $PM_{2.5}$ emissions (89).

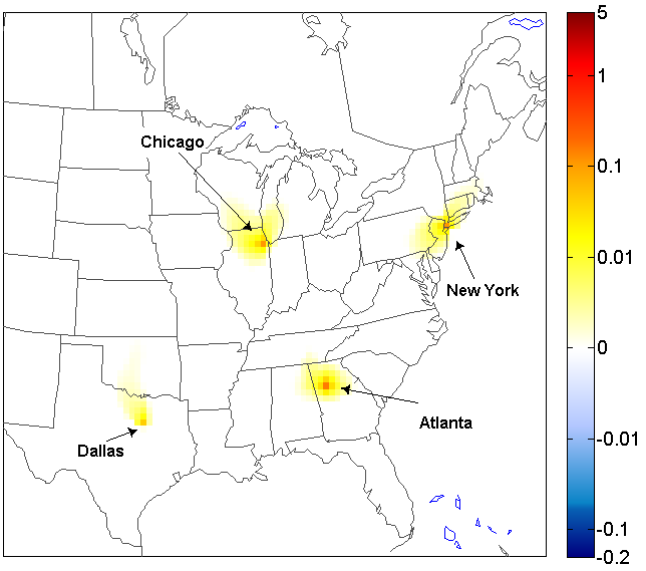

Figure 3.8: Change in daily mean primary $PM_{2.5}$ in µg/m^3 as an average of all six days of operation for a dual fuel generator

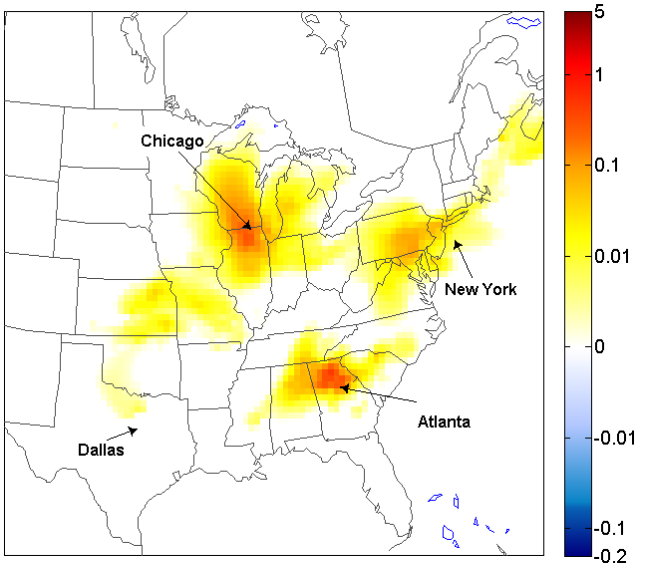

Figure 3.9: Change in daily mean secondary $PM_{2.5}$ (PSO_4, PNO_3 and SOA) in $\mu g/m^3$ as an average of all six days of operation for an uncontrolled diesel ICE

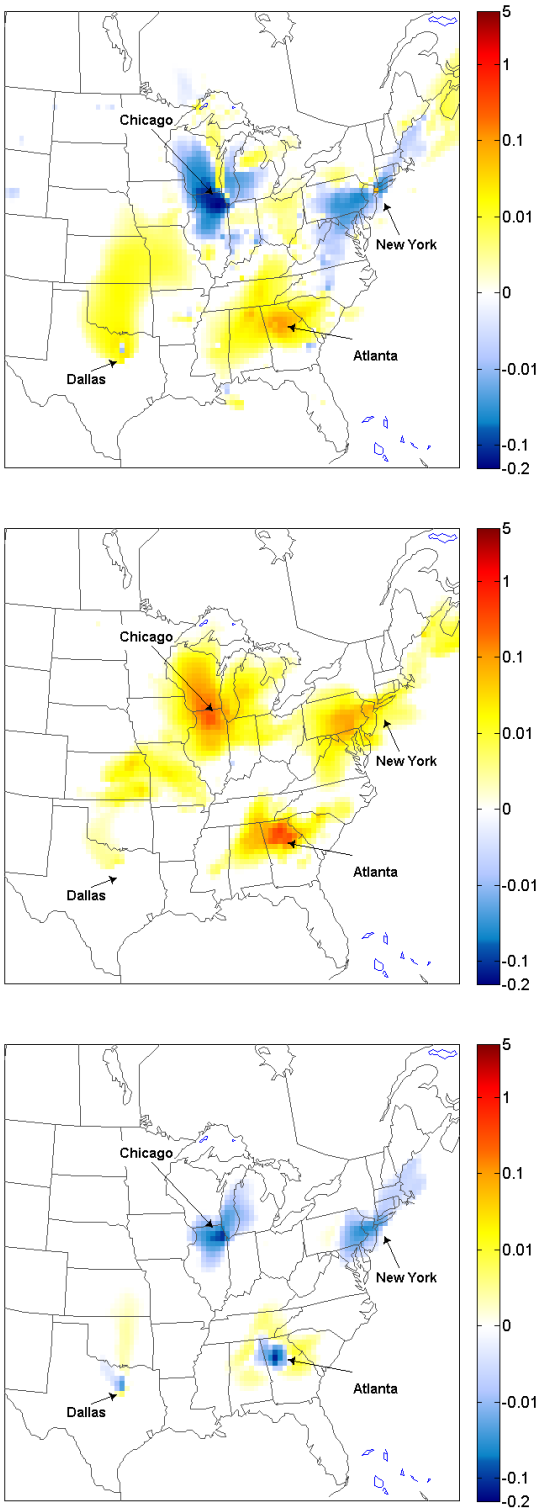

Figure 3.10: Change in daily mean secondary $PM_{2.5}$ (PSO_4, PNO_3 and SOA) in $\mu g/m^3$ as an average of all six days of operation for a diesel ICE with a DPF

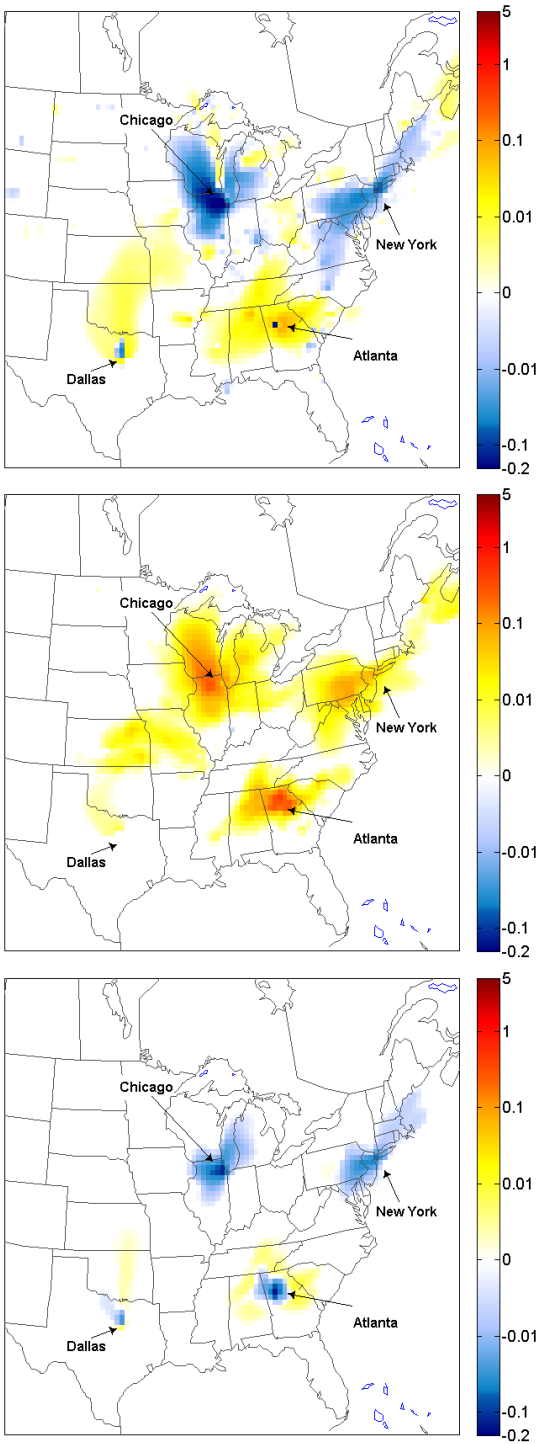

Figure 3.11: Change in daily mean secondary $PM_{2.5}$ (PSO_4, PNO_3 and SOA) in $\mu g/m^3$ as an average of all six days of operation for a diesel ICE with a DPF-LNC

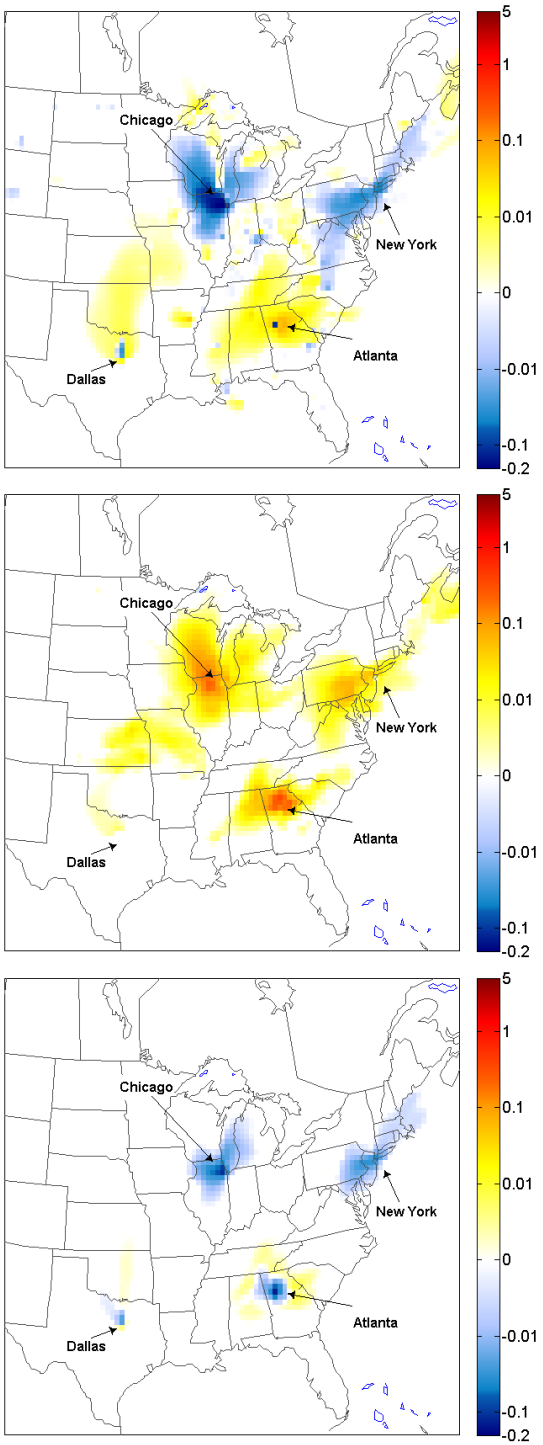

Figure 3.12: Change in daily mean secondary $PM_{2.5}$ (PSO_4, PNO_3 and SOA) in $\mu g/m^3$ as an average of all six days of operation for a diesel ICE with a DPF-EGR

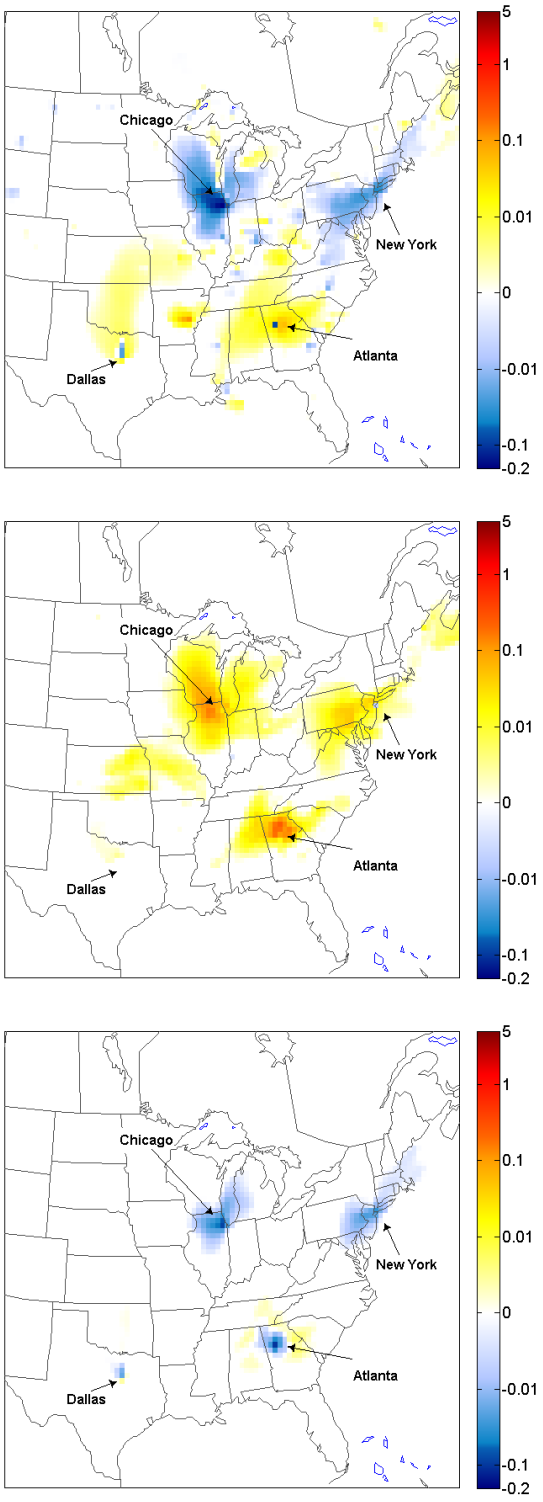

Figure 3.13: Change in daily mean secondary $PM_{2.5}$ (PSO_4, PNO_3 and SOA) in $\mu g/m^3$ as an average of all six days of operation for a diesel retrofit to a dual fuel

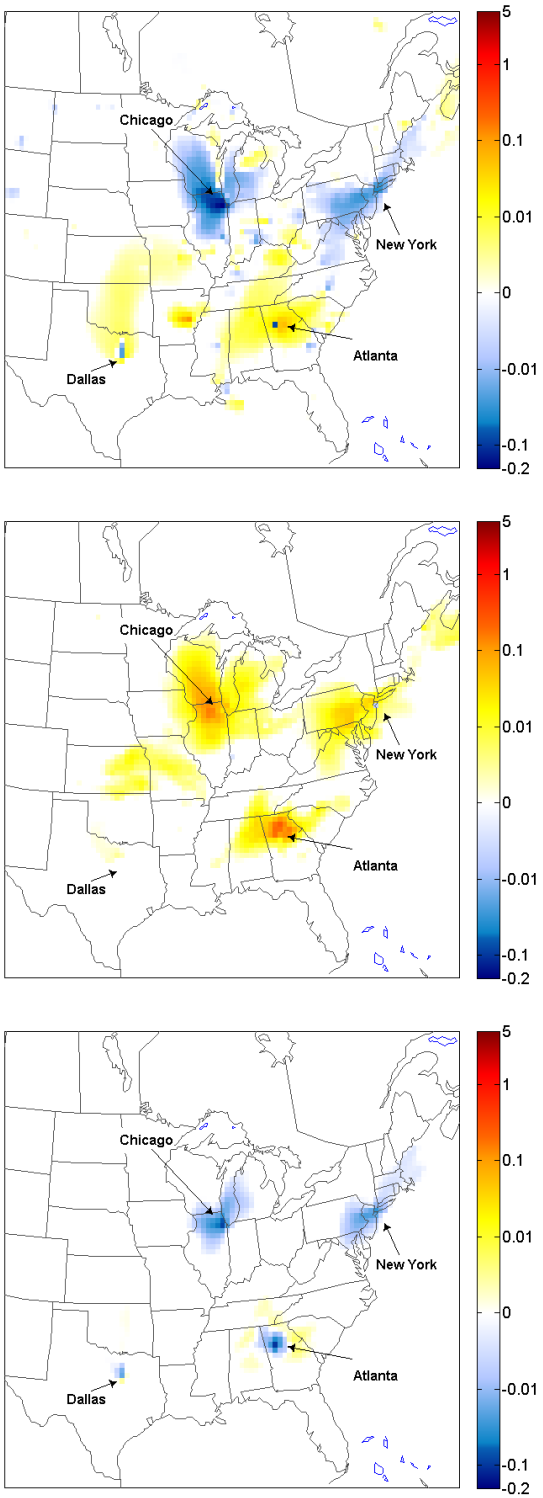

3.5.2 Distribution of social cost for $PM_{2.5}$ and O_3 between the urban center and surrounding region

Table 3.4: Costs in urban center and surrounding region for long-term mortality from primary $PM_{2.5}$, PNO_3, PSO_4, SOA and total $PM_{2.5}$ mass in ¢/kWh for an uncontrolled diesel ICE. The urban area is defined as the grid cell that contains the urban center. The surrounding region is all other cells.

Species	City	Urban	Surrounding
Primary	Atlanta	30.9	11.4
	Chicago	52.0	26.2
	Dallas	6.82	5.98
	New York City	106	53.1
PNO_3	Atlanta	2.70	7.03
	Chicago	2.00	14.0
	Dallas	0.00	0.61
	New York City	1.89	13.0
PSO_4	Atlanta	0.49	4.00
	Chicago	-3.70	-10.6
	Dallas	0.20	1.22
	New York City	2.00	-5.10
SOA	Atlanta	-1.33	-0.58
	Chicago	-2.54	-4.10
	Dallas	-0.18	-0.19
	New York City	-1.15	-5.37
Total $PM_{2.5}$	Atlanta	34.9	26.0
	Chicago	50.2	30.1
	Dallas	7.05	8.51
	New York City	112	63.0

Table 3.5: Distribution of costs in urban center and surrounding region for long-term mortality from primary $PM_{2.5}$, PNO_3, PSO_4, SOA and total $PM_{2.5}$ mass in ¢/kWh for a diesel ICE with a DPF. The urban area is defined as the grid cell that contains the urban center. The surrounding region is all other cells.

Species	City	Urban	Surrounding
Primary	Atlanta	1.58	0.57
	Chicago	2.69	1.32
	Dallas	0.34	0.29
	New York City	5.45	2.60
PNO_3	Atlanta	2.64	7.00
	Chicago	2.22	14.3
	Dallas	0.00	0.61
	New York City	2.11	13.1
PSO_4	Atlanta	-1.68	2.60
	Chicago	-7.40	-14.1
	Dallas	-0.31	0.03
	New York City	-3.60	-8.99
SOA	Atlanta	-1.61	-0.69
	Chicago	-3.16	-4.52
	Dallas	-0.20	-0.22
	New York City	-2.66	-6.28
Total $PM_{2.5}$	Atlanta	9.22	6.87
	Chicago	-2.50	0.49
	Dallas	0.51	0.62
	New York City	6.85	3.85

Table 3.6: Distribution of costs in urban center and surrounding region for long-term mortality from primary $PM_{2.5}$, PNO_3, PSO_4, SOA and total $PM_{2.5}$ mass in ¢/kWh for a diesel ICE with a DPF and LNC. The urban area is defined as the grid cell that contains the urban center. The surrounding region is all other cells.

Species	City	Urban	Surrounding
Primary	Atlanta	1.58	0.57
	Chicago	2.69	1.32
	Dallas	0.34	0.29
	New York City	5.45	2.60
PNO_3	Atlanta	2.29	5.31
	Chicago	1.63	10.8
	Dallas	0.00	0.46
	New York City	1.56	9.70
PSO_4	Atlanta	-1.25	2.14
	Chicago	-6.07	-11.0
	Dallas	-0.25	0.18
	New York City	-2.80	-7.02
SOA	Atlanta	-1.32	-0.53
	Chicago	-2.62	-3.56
	Dallas	-0.18	-0.17
	New York City	-2.12	-4.89
Total $PM_{2.5}$	Atlanta	7.09	9.41
	Chicago	2.41	0.91
	Dallas	0.68	1.88
	New York City	8.79	6.51

Table 3.7: Distribution of costs in urban center and surrounding region for long-term mortality from primary $PM_{2.5}$, PNO_3, PSO_4, SOA and total $PM_{2.5}$ mass in ¢/kWh for a diesel ICE with a DPF and EGR. The urban area is defined as the grid cell that contains the urban center. The surrounding region is all other cells.

Species	City	Urban	Surrounding
Primary	Atlanta	1.58	0.57
	Chicago	2.69	1.32
	Dallas	0.34	0.29
	New York City	5.45	2.60
PNO_3	Atlanta	1.87	3.58
	Chicago	1.25	7.56
	Dallas	0.00	0.31
	New York City	1.23	6.40
PSO_4	Atlanta	-0.81	1.68
	Chicago	-4.73	-7.91
	Dallas	-0.19	0.33
	New York City	-2.00	-5.04
SOA	Atlanta	-1.03	-0.37
	Chicago	-2.07	-2.60
	Dallas	-0.15	-0.12
	New York City	-1.58	-3.49
Total $PM_{2.5}$	Atlanta	3.01	7.51
	Chicago	-1.47	0.81
	Dallas	0.10	1.21
	New York City	4.31	4.16

Table 3.8: Distribution of costs in urban center and surrounding region for long-term mortality from primary $PM_{2.5}$, PNO_3, PSO_4, SOA and total $PM_{2.5}$ mass in ¢/kWh for a diesel ICE with a dual fuel retrofit. The urban area is defined as the grid cell that contains the urban center. The surrounding region is all other cells.

Species	City	Urban	Surrounding
Primary	Atlanta	1.58	0.57
	Chicago	2.69	1.32
	Dallas	0.34	0.29
	New York City	5.45	2.60
PNO_3	Atlanta	1.52	2.45
	Chicago	0.86	5.37
	Dallas	0.00	0.21
	New York City	1.21	5.16
PSO_4	Atlanta	-0.29	1.11
	Chicago	-2.93	-5.00
	Dallas	-0.07	0.18
	New York City	-0.83	-2.93
SOA	Atlanta	-0.69	-0.21
	Chicago	-1.36	-1.63
	Dallas	-0.10	-0.06
	New York City	-0.86	-2.11
Total $PM_{2.5}$	Atlanta	5.41	7.19
	Chicago	2.35	0.89
	Dallas	0.52	1.43
	New York City	9.48	7.02

Table 3.9: Distribution of costs in urban center and surrounding region for mortality from O_3 in ¢/kWh for an uncontrolled diesel ICE for daily 24 hour mean and 1-hour maximum CR - functions. The urban area is defined as the grid cell that contains the urban center. The surrounding region is all other cells.

		Urban	Surrounding	Total
Atlanta	Daily Mean	-12.8	-4.90	-17.7
	1-Hour Max	-38.3	0.40	-37.9
Chicago	Daily Mean	-21.1	-20.5	-41.6
	1-Hour Max	-84.5	-53.5	-138
Dallas	Daily Mean	-5.66	-3.96	-9.62
	1-Hour Max	-15.6	-9.96	-25.6
New York City	Daily Mean	-18.1	-37.3	-55.4
	1-Hour Max	-93.6	-61.4	-155

Table 3.10: Distribution of costs in urban center and surrounding region for mortality from O_3 in ¢/kWh for a diesel ICE with a DPF for daily 24 hour mean and 1-hour maximum CR - functions. The urban area is defined as the grid cell that contains the urban center. The surrounding region is all other cells.

		Urban	Surrounding	Total
Atlanta	Daily Mean	-12.8	-4.89	-17.7
	1-Hour Max	-38.8	0.92	-37.9
Chicago	Daily Mean	-21.1	-20.5	-41.6
	1-Hour Max	-84.5	-53.5	-138
Dallas	Daily Mean	-5.66	-3.96	-9.62
	1-Hour Max	-15.6	-9.96	-25.6
New York City	Daily Mean	-18.2	-37.3	-55.4
	1-Hour Max	-93.6	-61.4	-155

Table 3.11: Distribution of costs in urban center and surrounding region for mortality from O_3 in ¢/kWh for a diesel ICE with a DPF and LNC for daily 24 hour mean and 1-hour maximum CR - functions. The urban area is defined as the grid cell that contains the urban center. The surrounding region is all other cells.

		Urban	Surrounding	Total
Atlanta	Daily Mean	-11.3	-3.72	-15.0
	1-Hour Max	-33.2	0.41	-32.8
Chicago	Daily Mean	-18.3	-16.6	-34.9
	1-Hour Max	-72.3	-43.7	-116
Dallas	Daily Mean	-4.64	-3.14	-7.78
	1-Hour Max	-13.0	-8.07	-21.1
New York City	Daily Mean	-14.8	-29.9	-44.7
	1-Hour Max	-76.9	-47.1	-124

Table 3.12: Distribution of costs in urban center and surrounding region for mortality from O_3 (in ¢/kWh) for a diesel ICE with a DPF and EGR for daily 24 hour mean and 1-hour maximum CR - functions. The urban area is defined as the grid cell that contains the urban center. The surrounding region is all other cells.

		Urban	Surrounding	Total
Atlanta	Daily Mean	-11.3	-3.72	-11.3
	1-Hour Max	-33.2	0.41	-24.2
Chicago	Daily Mean	-18.3	-16.6	-25.4
	1-Hour Max	-72.3	-43.7	-84.1
Dallas	Daily Mean	-4.64	-3.14	-5.25
	1-Hour Max	-13.0	-8.07	-13.6
New York City	Daily Mean	-14.8	-29.9	-31.4
	1-Hour Max	-76.9	-47.1	-84.9

Table 3.13: Distribution of costs in urban center and surrounding region for mortality from O_3 in ¢/kWh for a diesel ICE with a dual fuel retrofit for daily 24 hour mean and 1-hour maximum CR - functions. The urban area is defined as the grid cell that contains the urban center. The surrounding region is all other cells.

		Urban	Surrounding	Total
Atlanta	Daily Mean	-10.0	-1.29	-11.3
	1-Hour Max	-24.6	0.43	-24.2
Chicago	Daily Mean	-15.5	-9.94	-25.4
	1-Hour Max	-55.0	-29.1	-84.1
Dallas	Daily Mean	-4.24	-1.01	-5.25
	1-Hour Max	-9.50	-4.10	-13.6
New York City	Daily Mean	-9.74	-21.7	-31.4
	1-Hour Max	-58.2	-26.7	-84.9

4. The air quality and human health effects of integrating utility scale batteries into the New York State electricity grid

Abstract

In a restructured electricity market, utility-scale batteries can generate revenue by discharging when electricity prices are high and charging when prices are low. This strategy, however, also changes the magnitude and distribution of air quality emissions, ambient concentrations, human health effects and social costs and benefits. We evaluate these effects with a case study of a 500 MW sodium sulfur battery displacing peak electricity generators in New York City from 1 – 5 pm and charging using off-peak generation in the New York Independent System Operator (NYISO) electricity grid from 1 – 6 am. First, we map displaced and charging plant types to generators in the NYISO. Second, we convert the changes in emissions into ambient concentrations with a chemical transport model, the Particulate Matter Comprehensive Air Quality Model with extensions ($PMCAM_x$). Finally, we transform the concentrations into their equivalent human health effects and social benefits and costs. Focusing on the relationship between premature mortality and fine particulate matter ($PM_{2.5}$), we calculate a benefit of 4.5 ¢/kWh and 17 ¢/kWh from displacing a natural gas (NG) and distillate fuel oil (DFO) fueled peaking plant, respectively, in New York City. By contrast, ozone (O_3) concentrations increase due to the decrease in nitrogen oxide (NO_x) emissions, although the magnitude of the social cost is less certain. For most charging plants, there is a net social benefit when a DFO peaker is displaced. By contrast, we find a net social cost if a NG peaker is displaced. By using the present base-load capacity for charging, the upstate population will experience an increase in adverse health effects. Newer wind generation, however, which could charge the battery, would ensure benefits to the upstate charging location and in New York City.

4.1 Introduction

Electric energy storage (EES) decouples the generation of electricity from its consumption, by storing electricity or energy to produce electricity during one period and releasing the electricity during another (90). This can provide a range of benefits including reducing the need for new electricity generation capacity to meet peak electricity demand, relieving strain on transmission and distribution (T&D) infrastructure and supporting variable renewable sources such as wind (91). Another benefit of EES installations is that they can be easier to site than conventional power plants, allowing them to be located where electricity and capacity is most valuable. For example, Walawalkar et al. (2007) found that a sodium sulfur (NaS) battery located in New York City could operate profitably by selling electricity at peak prices and charging at off peak prices and by participating in the installed capacity markets (92). One of the reasons these facilities may experience fewer barriers to siting is that there are no emissions that affect air quality at the point of use. This could be especially beneficial in highly populated urban load centers where the battery could displace dirtier capacity installed for peak electricity demand (93). Depending on the location and type of generation used to charge the battery and the generation displaced by the battery, however, there may be net positive or negative social costs in terms of air quality, exposure and human health. In addition, there are also equity concerns about shifting emissions from one location to another.

There have been limited studies which have investigated how EES facilities would interact with existing generation capacity and influence air quality. Restricting their analysis to the change in total emissions, Denholm and Holloway (2005) investigated a system composed of a new compressed air energy storage (CAES) charged with existing older coal-fired generators. They found that this system would exceed the maximum emission rates for new generation (e.g. New Source Performance Standards) established by the United States Environmental Protection Agency (USEPA) (94). Total emissions, however, do not provide information about ambient concentrations, exposure or allow for the quantification of the human health effects. Using total emissions also neglects the

effect of the changes in spatial and temporal distribution of the emissions on ambient concentrations. Finally, emissions cannot capture the formation of ozone (O_3) and a portion of fine particulate matter ($PM_{2.5}$), which are formed as a result of chemical reactions of the directly emitted chemical species. O_3 and $PM_{2.5}$ are important as they are linked to premature mortality.

The most comprehensive tool for converting emissions to ambient concentrations is a chemical transport model (CTM). CTMs have been widely employed to predict changes in air quality from small-scale distributed generation (DG) such as utility-scale batteries. For example, Gilmore et al. (2006) evaluated the air quality effects of using diesel generators with and without emission controls for meeting peak electricity demand in New York City (60). Similarly, Rodriguez et al. (2006) employed a CTM to evaluate the change in ambient air quality from introducing varying amounts of different forms of DG into California. Depending on the magnitude, location and type of DG, they found decreases and increases in ambient concentrations of O_3 and $PM_{2.5}$ (95). Carreras-Sospedra et al. (2008) ran similar scenarios in the Northeast United States, but retired older base load generation such as pulverized coal plants (96). By contrast to Rodriquez et al. (2006), O_3 and $PM_{2.5}$ decreased in these scenarios. To the best of our knowledge, there has been no study which has used CTMs to evaluate the air quality effects of integrating EES into electricity grids.

In this paper, we isolate the changes in air quality and human health effects by modeling a single NaS battery located in New York City, New York, charging with off peak base-load resources in the New York Independent System Operator (NYISO) region. First, we evaluate the benefits and costs of changes in human health effects for individual charging plants that exist in the NYISO as well as new generation such as wind capacity. Second, we estimate the overall benefits or costs to the system by investigating the frequency that plants would be used for charging. Finally, we investigate the distribution of the benefits and costs from the charging and displaced plant. We consider the social cost from changes in health effects only and do not include other potential social costs and benefits such as reducing peak electricity prices. We conduct the air quality modeling with a ‘state

of science' chemical transport model, the Particulate Matter Comprehensive Air Quality Model with extensions ($PMCAM_x$).

4.2 Methods and data

For our case study, we site a 500 MW NaS battery facility in New York City, New York. Consistent with the market analysis of Walawalkar et al. (2007), we assume that the battery is operated to maximize revenue, discharging from 1 – 5 pm and charging from 1 – 6 am (Eastern Standard Time). The additional hour of charging time is required to account for battery round-trip charging efficiency. This scenario results in 2,000 MWh (500 MW x 4 hours) of electricity generated per day by the battery. This configuration is a good case study as New York City is highly populated, and there is a wide range of generators in the NYISO region.

4.2.1 Charging and displaced plants

First, we develop a list the potential power plants types used for charging and plants displaced by the battery. While the NYISO has information on the actual charging and displaced plants, it does not release this data publicly. Since we cannot restrict the types of charging plants, we investigate the effect of coupling the battery with a range of different fuel-generator types available in NYISO as listed in the US Environmental Protection Agency's Emissions & Generation Resource Integrated Database, 2006 (eGRID) (22). We identify a pulverized coal plant, natural gas (NG) fueled combined cycle turbine, a residual fuel oil (RFO) fueled boiler-steam turbine, and a NG fueled boiler-steam turbine. For the coal plant, we model a plant without any emission controls as well as a plant with modern emission controls. In New York, coal plants have modern emission controls as a result of legal settlements to a New York State lawsuit against dirtier coal plants in 2005 (97). In addition to the fuel types, we model different locations for the charging plants including co-locating the plant with the battery in New York City. This charging plant may be either a NG or RFO boiler-steam turbine. We do not consider nuclear or hydro-electric facilities as they are not the marginal plants in the NYISO system at night during the summer. These plants are classified as must-run plants, and the

minimum load during the summer months in New York State exceeds their combined capacity.

In addition to the existing plant types, we evaluate two long run possibilities for the charging plant. First, we model a coal plant as an integrated gas combined cycle (IGCC) facility. This facility would reduce emissions in a manner consistent with an emission-based air quality rule such as the USEPA Clean Air Interstate Rule (CAIR) (98). Under this type of regulation, the total emissions of a given pollutant are capped, and each generator must procure sufficient permits to cover its emissions (99). Facing a shortfall of permits, a generator can purchase credits from another generator which has reduced its emissions or it can reduce its own emissions by adding additional emission controls or making other modifications to the facility. Under some circumstances, it may become uneconomical to operate the generator. We limit our modeling to a generator which chooses to reduce its emissions. Second, we model base-load wind as the marginal plant. The New York Renewable Portfolio Standard (RPS) mandates that renewable sources provide 25% of electricity in 2013 (100). It is expected that 4.7% will be met by new generation and that substantial amounts of wind generation will be installed (101).

We assume that the battery would displace a simple cycle turbine (peaking plant) located in New York City. In New York, many of these peaking plants are subject to the Minimum Oil Burn reliability rule which requires that they operate on a minimum level of a fuel other than NG during periods of high demand (102). As a result, for each possible charging plant, we model two options for the displaced plant: a NG fueled simple cycle turbine and a distillate fuel oil (DFO) simple cycle turbine. We do not evaluate the potential that upstate generators could also be displaced by the battery, and as such, we do not model potential benefits from avoided thermal transmission loss.

For all of these facility types, we map these plant types to indicative facilities in the NYISO as shown in Figure 4.1. Coordinates for these facilities are obtained from the Facility Registry Service (FRS) managed by the USEPA (103).

Figure 4.1: Location of charging and displaced generators

The coal plants are modeled at the outlined black square in Western New York State. The NG fueled combined cycle turbine is modeled at the dashed square. The RFO or NG boiler-steam turbine is located at the black circle. The battery displacing the NG or DFO peaking turbine is located in New York City, shown at the outlined white square. A charging plant, either a RFO or NG boiler-steam turbine, may also be located in New York City. Population per 12 km by 12 km grid cell is shown. CT = Connecticut, MA = Massachusetts, NH = New Hampshire, NJ = New Jersey, NY = New York, PA = Pennsylvania and VT = Vermont.

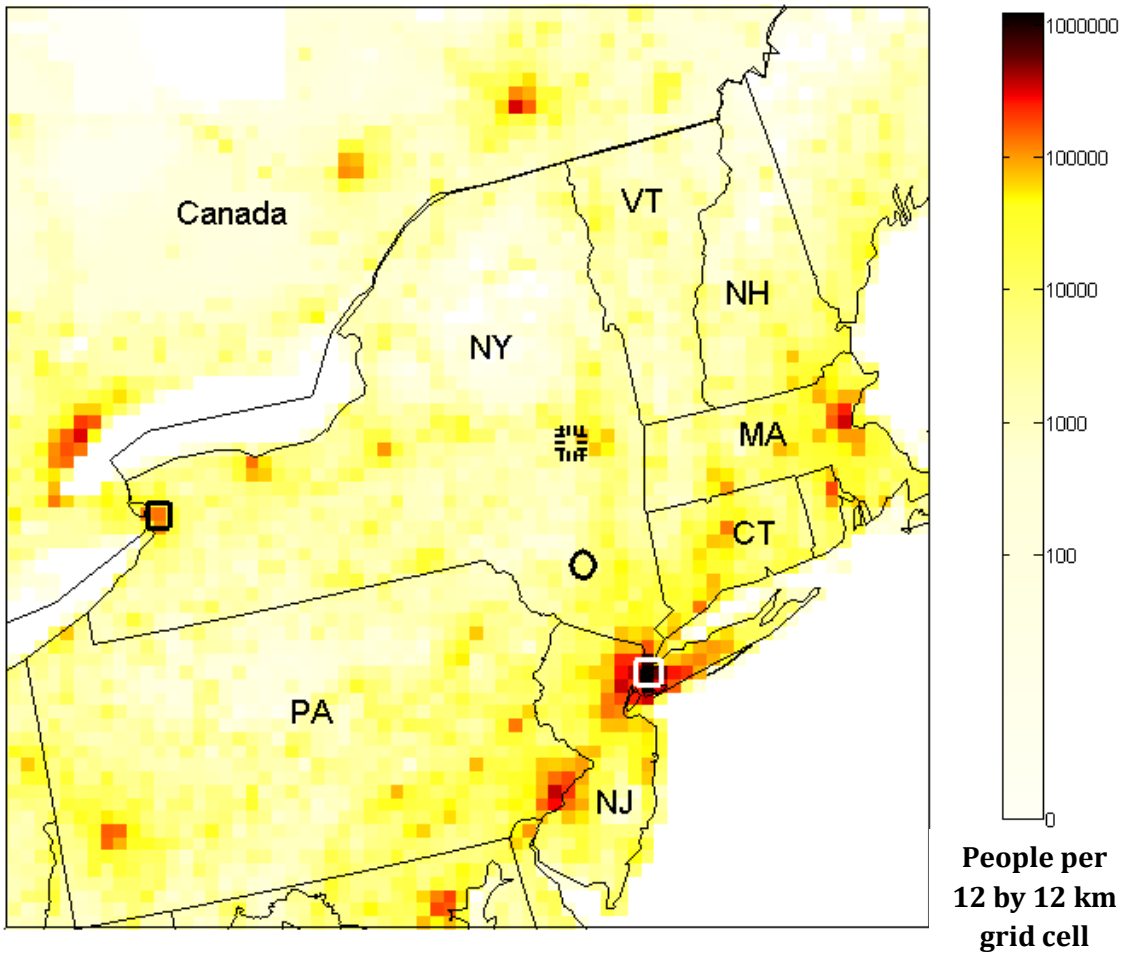

4.2.2 Air quality modeling and emission factors

To model the air quality effects, we develop emission profiles for each fuel-generator type. Emissions from these plants are characterized by emission factors (EFs) which measure the amount of a pollutant released (in grams) per unit of electricity generated (in kilowatt-hours, kWh). These EFs can vary significantly for any given fuel type, depending on plant configuration, operating conditions, and emission control technologies. In Table 4.1, we present the EFs used in this work. For the NG and oil fueled generation, the EFs are derived from the USEPA AP-42 compilation (15). For the coal plants, we model three different configurations with the Integrated Environmental Control Model (IECM) (16, 104): a coal plant without emission controls, a plant with modern emission controls, and an IGCC. For all coal plants, we specify a bituminous coal consistent with the quality of coal delivered for electricity generation in New York State with 8.1 % ash and 2.2 % sulfur (105). For the plant with emission controls, we add an electrostatic precipitator (ESP) to reduce $PM_{2.5}$, flue gas desulfurization (FGD) to reduce SO_2 and selective catalytic reduction (SCR) to reduce NO_x. With the possibility of regulations restricting carbon dioxide (CO_2) emissions, some new coal plants may be constructed with carbon capture and storage CO_2 emission controls. We do not model CO_2 emission controls on any plants.

The EFs from Table 4.1 are split into species consistent with the representation in $PMCAM_x$. The NO_x emissions are split into 85% nitrogen oxide (NO) and 15% nitrogen dioxide (NO_2). The $PM_{2.5}$ is split equally into elemental and organic carbon and into six size bins. These emissions are calculated by multiplying these speciated EF by the amount of electricity generated (i.e., 2,000 MWh per day for the displaced plant and 2,500 MWh per day for the charging plant). We allocate these emissions to the appropriate hours and plant location. Since the emissions are based on literature values rather than emissions specific to that plant, the results should not be interpreted as the actual effect of altering emissions at the actual plant. Rather, these results are broadly indicative of the emissions from each plant type. We consider only emissions associated with electricity generation.

Table 4.1: Emission factors in g/kWh and the heat rate in Btu/kWh for plant types (15, 22, 104, 106)

Plant Type	Nitrogen Oxides (NO_x) (g/kWh)	Sulfur Dioxide (SO_2) (g/kWh)	Fine particulate matter ($PM_{2.5}$) (g/kWh)	Heat Rate (Btu/kWh)
Uncontrolled pulverized coal	2.20	2.66	0.582	10,400
Controlled pulverized coal	0.70	1.10	0.058	10,200
IGCC coal	0.45	0.23	0.038	9,900
RFO boiler	1.00	2.35	0.139	11,700
NG boiler	0.67	~0	0.037	11,700
DFO turbine	1.53	0.093	0.158	12,500
NG turbine (simple cycle)	1.31	~0	0.036	12,500
NG turbine (combined cycle - NGCC)	0.186	~0	0.023	6,900

To transform the total emissions to ambient concentrations, we employ $PMCAM_x$. $PMCAM_x$ is a 'state of science' CTM that simulates the emission, advection (convection), dispersion, gas and aqueous phase chemical reactions, and dry and wet deposition for 35 gaseous species, 12 radical species and 13 aerosol species in 10 size bins on a 3-D Eulerian grid. Additional modules simulate the dynamic behavior (coagulation, condensation, and nucleation) of aerosols species. Details and evaluation of the model can be found in Gaydos et al. (2007) (7) and Karydis et al. (2008) (32). We model the ambient air quality concentrations for each charge-displace combination for a period of two weeks in July 2001 (July 12 – 28), corresponding to a period when $PMCAM_x$ has been extensively evaluated. We interpolate the available meteorological fields produced by the mesoscale model, known as MM5 (30), and the baseline emission files from the Lake Michigan Air Directors Consortium (LADCO) (107) from a 36 km horizontal grid resolution to a 12 km grid to better resolve the change in emissions and the resulting concentrations. The vertical grid is discretized to 14 layers from the surface to 6 km. The lowest model layer is slightly less than 30 m thick vertically. For the coal plant, the emissions are modeled as emitted into the second layer from the ground. Emissions from all other plants are modeled as emitted into the first layer. This is consistent with the stack height of these facilities.

4.2.3 Human health effects and social costs

We evaluate the human health effects for each separate charging plant and displaced plant, for each potential charge-displace combination, and for the entire system (i.e. accounting for the frequency that each plant is used for charging). The social value is then generated by translating the changes in ambient air quality into morbidity and mortality effects and then to a dollar value associated with these effects using concentration-response (CR) functions (as shown in Equation 4.1). We express the resulting social cost or benefit as a value normalized by the electricity provided by the battery (e.g. 2,000 MWh per day).

$$SC = \sum_{i=1}^{n} [1 - exp(\beta_i \cdot \Delta conc)] \cdot pop \cdot y_o \cdot WTP_i \quad \ldots Eqn\ 4.1$$

Where i is each different health endpoints;

n is the total number of different health endpoints;

β is the strength of the relationship between the change in ambient concentration of a given pollutant and the endpoint (in cases per 24-hour average ppb or cases per 24-hour average $\mu g/m^3$);

Δconc is the change in ambient concentration of a given pollutant (in 24-hour average ppb or 24-hour average $\mu g/m^3$);

pop is the population exposed to the change in concentration;

SC is the social cost (in $);

WTP is the "willingness to pay" to avoid the adverse health effect (in $); and,

y_o is the baseline incidence of the adverse health effect in the absence of the pollutant.

We use βs, WTPs, y_o, and population distribution from the Environmental Benefits Mapping and Analysis Program (BenMap), version 2.4.85 (34). We also extend the BenMap population and incidence values to include Canada with population from the Gridded Population of the World dataset (108). We focus on changes to in premature mortality from O_3 and $PM_{2.5}$. To evaluate mortality due to changes in O_3, we use a 24-hour averaging metric from Bell et al. (2004), (2005) and (2006) (84-86). To evaluate the long term (annual) effects of $PM_{2.5}$ and mortality, we use a fixed pooling of CR relationships from Laden et al. (2006) (70) and Pope et al. (2002) (71). We assume that the average of our 14 modeled days is representative of the change in ambient concentrations that would be observed over any given summer time day. We restrict our analysis to the summer as previous analysis found that the NaS facility will derive most of its revenue in the NYISO summer capability period from May 1st – October 31st (92). To convert premature mortality into dollars, we model the value of a statistical life (VSL)

as a Weibull distribution with a mean of $7.5 million (in 2005 dollars) (Weibell scale parameter: 8,300,000; Weibull shape parameter: 1.5096). We also show 5% and 95% confidence intervals to capture the uncertainty in the health endpoints and WTP estimates.

In addition to calculating the cost of the change in human health effects for the separate charging and displaced plants and for the charge-displace combinations, we are also interested in evaluating the overall social cost of operation. This requires multiplying the social value of each possible charge plant and the each possible displaced plant by the frequency with which that plant type is employed as shown in Equation 4.2.

$$Overall\ Efficiency = \sum_{1}^{j} SC_j \cdot XMP_j + \sum_{1}^{k} SC_k \cdot XMP_k \quad \ldots Eqn\ 4.2$$

Where j is the number of possible charging plants;

k is the number of possible displaced plants;

SC is the social cost for each plant used for charging or displaced (in $); and

XMP is the fraction that each plant type is used for charging or displaced.

As mentioned in section 4.2.1, the NYISO does not release information about the fuel or plant type on the margin. We review the available data for making independent estimates in the Supporting Information (section 4.5). While we cannot derive conclusive frequencies, we find that eGRID can be used for preliminary estimates. Details on the development of these estimates can be found in the Supporting Information (Section 4.5.2).

4.3 Results and discussion

4.3.1 Ambient air quality concentrations

In Figure 4.2, we show the average change in concentration for $PM_{2.5}$ in μg/m^3 over the two week simulation for displacing a DFO peaking turbine in New York City. Small decreases in $PM_{2.5}$ are observed due to a reduction in primary emissions with very small

changes in the portion of $PM_{2.5}$ (secondary) that is formed by reactions of gases. In Figure 4.3, we show the average change in concentrations of O_3 in ppb over the two simulation weeks. Small increases in O_3 are observed. These O_3 increases are consistent with the VOC to NO_x ratios predicted by $PMCAM_x$. When the initial ratio of NO_x to VOC is high (i.e., VOC-limited), adding more NO_x will decrease the formation of O_3. At lower ratios (i.e., NO_x-limited), the additional NO_x increases the formation of O_3. Urban centers tend to have high NO_x to VOC ratios, and hence, adding more NO_x results in the observed decreases (55). Differences in wind patterns over the two-week modeling period account for the cloud of ambient concentrations. For displacing a NG turbine, the spatial patterns for both O_3 and $PM_{2.5}$ are the same with the change in ambient concentrations reflecting the difference in the EFs.

In Figure 4.4, we show the average change in the concentration for $PM_{2.5}$ in $\mu g/m^3$ for an uncontrolled coal plant and for RFO boiler-steam turbine plant. For $PM_{2.5}$, we observe small increases. In Figure 4.5, we show the average change in concentrations of O_3 in ppb over the two simulation week for an uncontrolled coal plant and for a RFO boiler-steam turbine plant. We observe both increases and decreases consistent with VOC/NO_x ratios. For a coal plant with emission controls and the IGCC, we observe the same spatial patterns for both O_3 and $PM_{2.5}$ as the uncontrolled coal plant. Similarly, we observe the same spatial patterns for a NG boiler-steam turbine plant as the RFO boiler. The concentrations for the NG combined cycle plant are not shown since only very small changes in ambient concentrations are observed.

Figure 4.2: Change in daily mean $PM_{2.5}$ in $\mu g/m^3$ concentrations as an average of two weeks for displacing a DFO peaking turbine in New York City. The white box shows the location of New York City. CT = Connecticut, NJ = New Jersey, NY = New York, and PA = Pennsylvania.

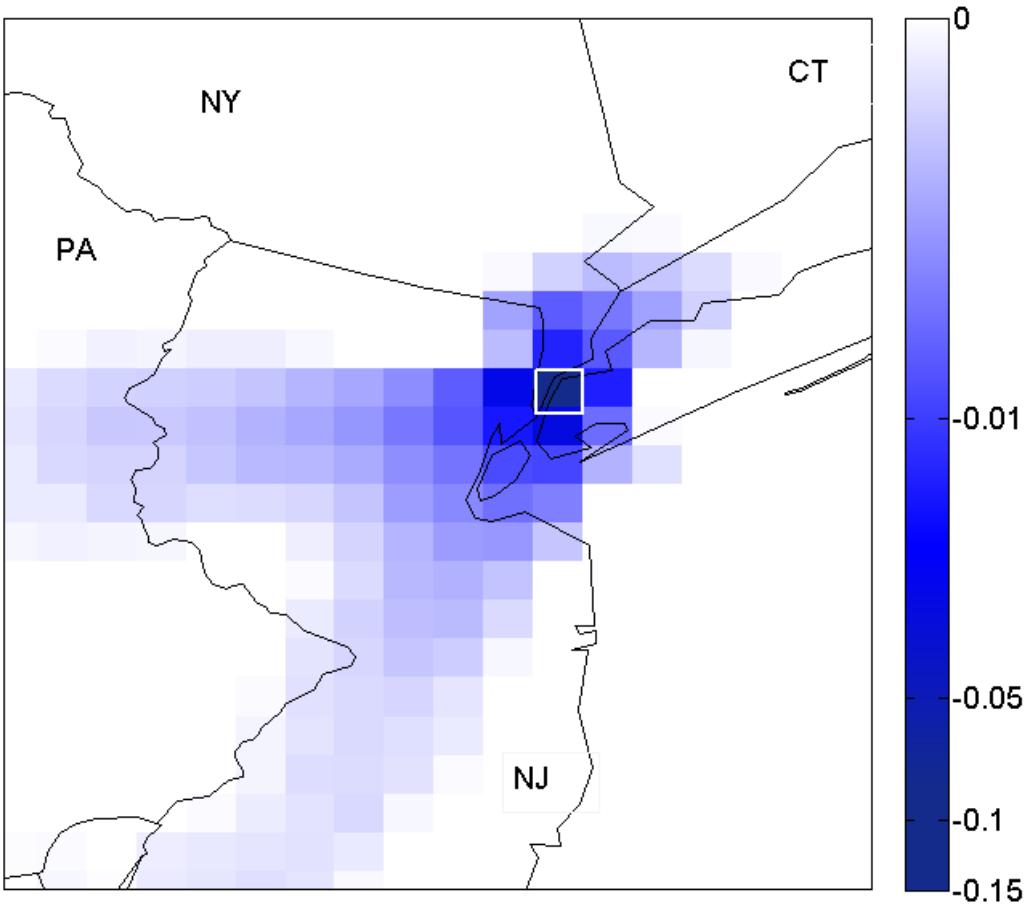

Figure 4.3: Change in daily mean O_3 in ppb concentrations as an average of two weeks for displacing a DFO peaking turbine in New York City. The white box shows the location of New York City. CT = Connecticut, MA = Massachusetts, NJ = New Jersey, NY = New York, and PA = Pennsylvania.

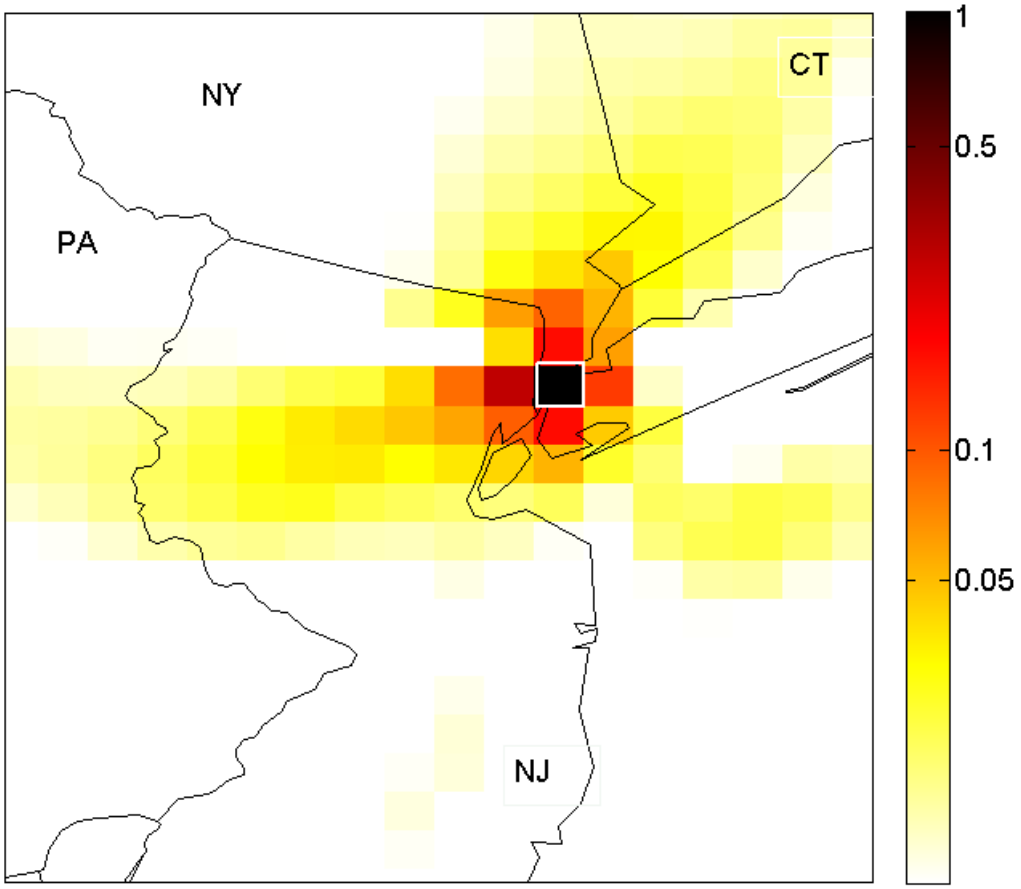

Figure 4.4: Average change in concentration for $PM_{2.5}$ in µg/m^3 for an uncontrolled coal plant [top] and for RFO boiler-steam turbine plant [bottom]

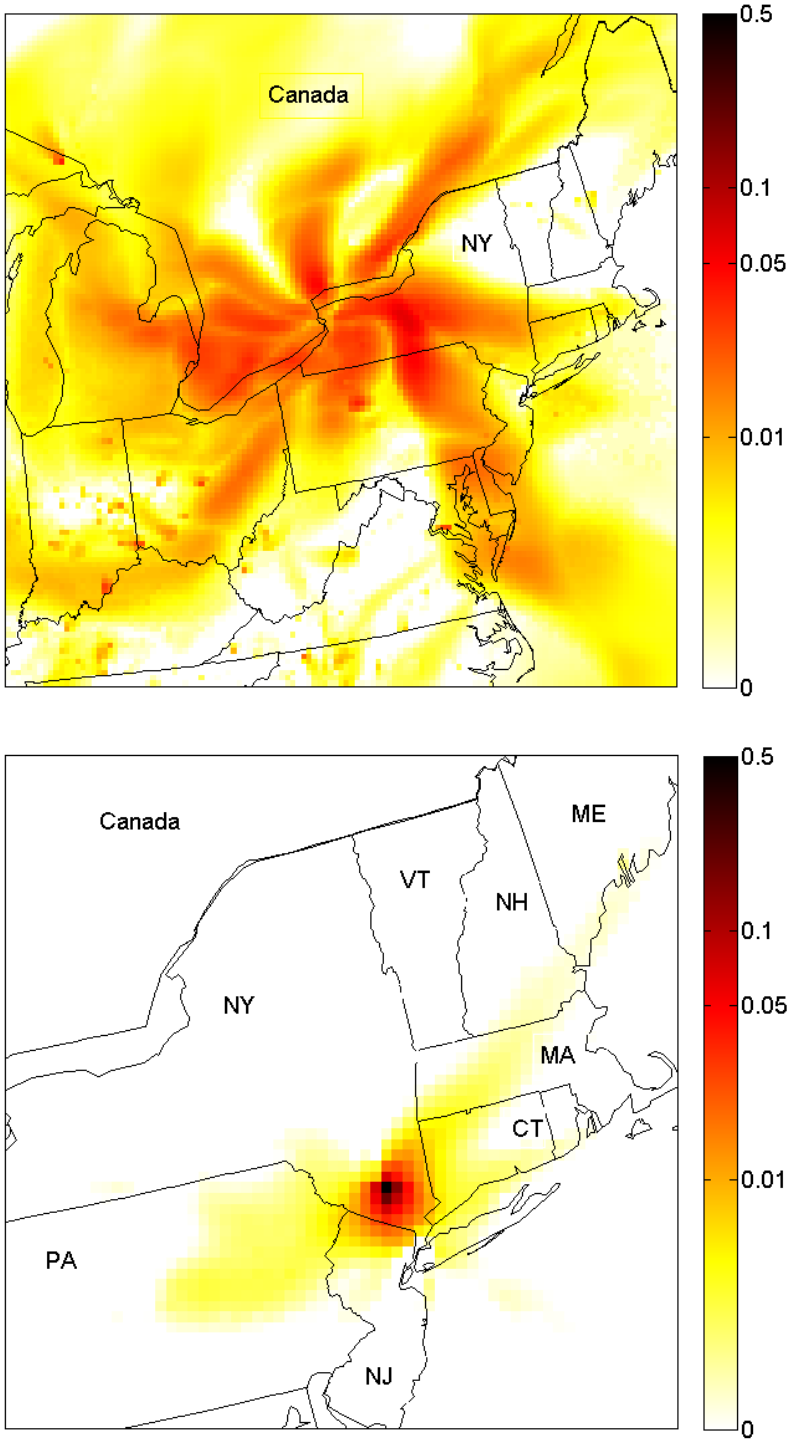

Figure 4.5: Average change in concentrations of O_3 in ppb for an uncontrolled coal plant [top] and for a RFO boiler-steam turbine plant [bottom]

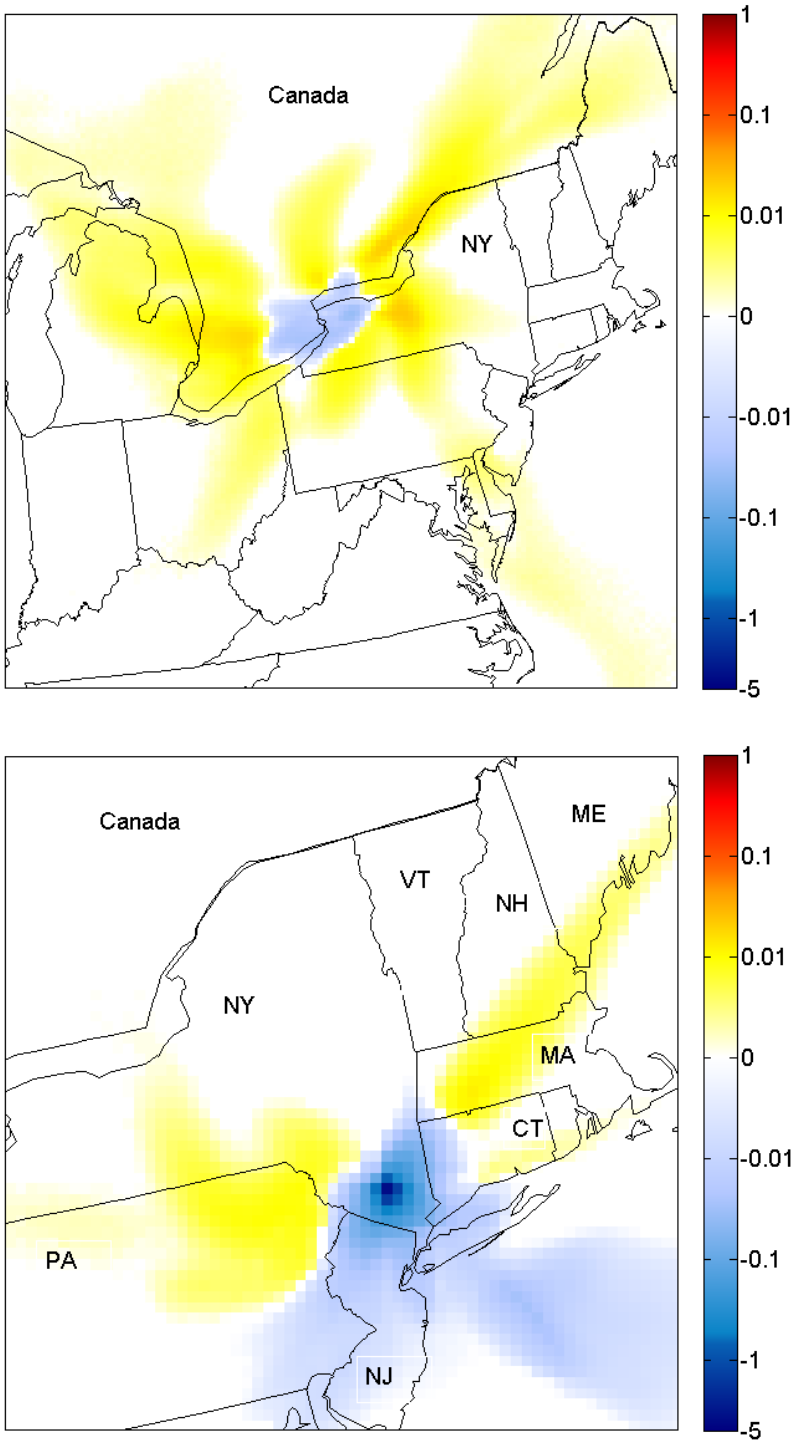

4.3.2 Human health effects and social costs

In Figure 4.6 and Figure 4.7, we show the social costs from mortality from $PM_{2.5}$ and O_3 for each charge-displace plant combination for displacing a DFO and NG peaking turbine, respectively. These values with the 5% and 95% confidence intervals are also tabulated in Table 4.2 in the Supporting Information. The values calculated in this work are slightly higher than other CR type studies (9), but are within the range of values from the European ExternE project (10, 109). The higher values in ExternE are the result of denser populations in parts of Europe. These population densities are consistent with the population in the New York City region. Our values are also slightly higher as we are levelizing the social values over the amount of electricity discharged by the battery rather than the amount of electricity used for charging.

The health benefits from reducing $PM_{2.5}$ are well established. For the New York City region, we observe a social benefit from reducing $PM_{2.5}$. Adding the costs from increases in $PM_{2.5}$ associated with the charging plant, we still observe social benefits for displacing a DFO unless an uncontrolled coal plant or a RFO boiler located in New York City is used for charging. For displacing a NG peaking plant, a social cost is observed for an uncontrolled coal plant, a RFO boiler either located upstate or in New York City or a NG boiler in New York City. We also note that charging with the coal plant with emission controls yields only a very small social benefit when displacing a NG peaking plant.
We also evaluate the changes in mortality from O_3. The increases in O_3 from displacing a peaking plant in New York City leads to a social cost from increased mortality. These social costs decrease the benefit from reducing $PM_{2.5}$. For displacing a NG peaking plant, summing the social value from changes in mortality for $PM_{2.5}$ and O_3 results in a net social cost for all possible charging plants. While the relationship between exposure to $PM_{2.5}$ and premature mortality is relatively well understood, the magnitude of relationship between mortality and O_3 is subject to greater uncertainty (38). As a result, we caution against a simplistic summing of O_3 and $PM_{2.5}$ social costs. Since we have more confidence in the magnitude of the health effect from $PM_{2.5}$, we will focus on these results but will evaluate how adding O_3 influences the outcome.

Figure 4.6: Net social cost for $PM_{2.5}$ [top] and the sum of $PM_{2.5}$ and O_3 [bottom] for displacing a DFO peaking plant in ¢/kWh. The blue bars are the separate charge-displace combinations. The orange bars are for different system-level charging plant combinations. DF indicates which types of fuel (either natural gas, NG, or residual fuel oil, RFO) a dual fuel charging plant is using. NYC indicates that the charging plant is located in New York City.

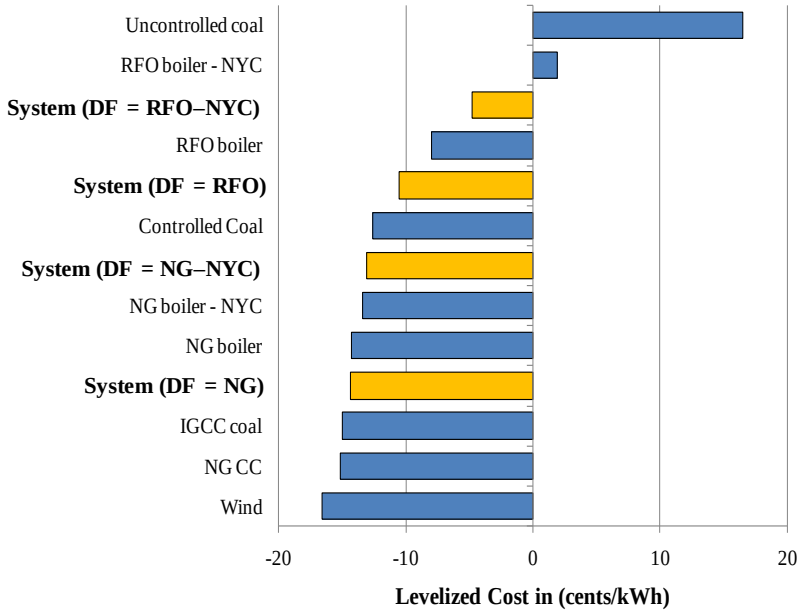

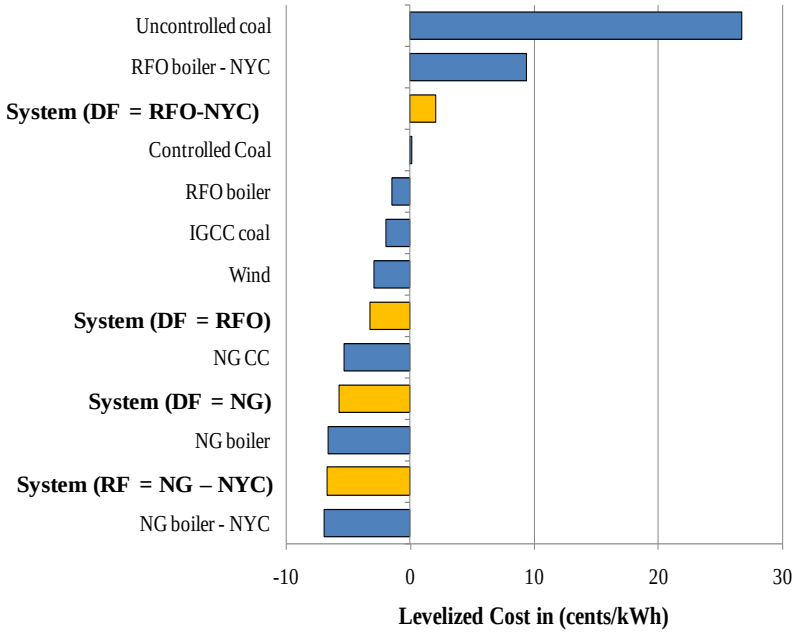

Figure 4.7: Net social cost for $PM_{2.5}$ [top] and the sum of $PM_{2.5}$ and O_3 [bottom] for displacing a NG peaking plant in ¢/kWh. The blue bars are the separate charge-displace combinations. The orange bars are for different system-level charging plant combinations. DF indicates which types of fuel (either natural gas, NG, or residual fuel oil, RFO) a dual fuel charging plant is using. NYC indicates that the charging plant is located in New York City.

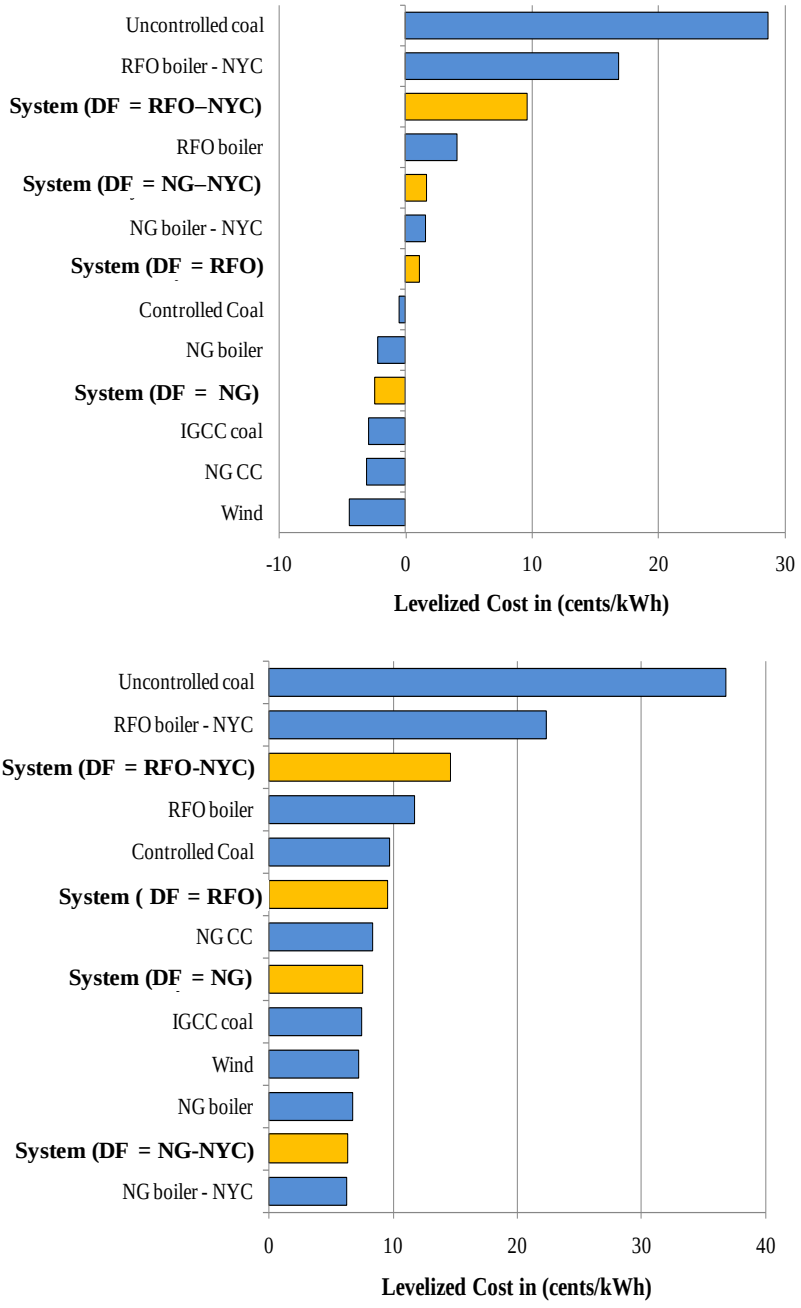

In addition to the social costs and benefits for each charge-displace combination, we would also like to calculate the total system social cost for the battery. In the Supporting Information (Section 4.5.2), we evaluate the existing publicly available data for dispatch frequencies and deem it insufficient to allow us to perform more than a rough estimate which we show in Table 4.4. Using these frequency estimates, we find an overall social benefit when a DFO peaking plant is displaced for mortality from $PM_{2.5}$ only and the sum of mortality from $PM_{2.5}$ and O_3. If a cleaner NG peaking plant is displaced, however, a system social cost is observed in almost all cases. We show the social values for all combinations with our estimated frequencies in the Supporting Information Table 4.5 and Table 4.6.

In this analysis, we use average values for heat rate and full-load emissions factors. Some generators, however, would be operating at partial load during off peak periods (94). Since most generators operate more efficiently at full-load conditions (e.g. lower average heat rate), the additional demand for charging the battery could potentially decrease the air quality emissions per kWh generated from these plants. Thus, this analysis may lead to an overestimation of the cost of integrating a battery in NYISO. Again, better information about the dispatch order of the plants would be necessary to identify a plant operating at partial load.

We also separate the social cost into the charging and displaced portions to evaluate the distribution of the benefits and costs. We show the results in Figure 4.8. To isolate the cost imposed by the charging, the social benefit from displacing the peaking plant in New York City is subtracted from the value of each charge-displace combination. The social benefit from displacing a peaking plant is equivalent to using wind as a charging plant. In all cases except wind, a population located in the upstate portion of New York state experiences deterioration of ambient air quality and adverse human health effects. For charging plants located upstate, New York City may also experience a change in ambient concentrations. We find that this effect is small except in the case of the charging plant co-located with the battery. As a result, we do not separate the charging and discharging components for a co-located charging plant. In the case of the charging plant being co-

located in NYC, however, the cost is imposed on the same population that observes the benefit from displacing peaking generation, reducing equity concerns.

If we consider only short term effects, therefore, there are important distributional effects. The battery, however, will also interact with existing generation capacity and regulations affecting the electricity sector. Under a rule similar to CAIR, operating any of the charging plants may require the purchase of additional emission credits. If emissions allowances are purchased (assuming that no party is using banked allowances), then a reduction in emissions must be observed in another location. Since the premise of emission trading is that each generator in the trading group has emissions with approximately equal marginal damages (99), these trades should result in a net zero change in social cost. These benefits, however, may or may not accrue to the New York State populace depending on the location of the generator that sells the credits. It is outside the scope of this paper to evaluate potential trades. We do, however, investigate shifting the coal plant to an IGCC as a response to CAIR. We find that the IGCC has a significant benefit, reducing the social costs from charging to values in the same range as NG fueled options. The battery installation can also interact and support intermittent renewable resources. At the end of 2008, there was approximately 1.15 GW of installed wind capacity in New York State with a doubling expected in the next several years as a result of the RPS (110, 111). If wind is the charging plant, there could be no effect on the population at the charging location. In addition to cleaner charging plants, the IGCC and the wind turbines have the additional benefit of reducing the social cost for all electricity that is generated from that plant.

Figure 4.8: Social cost distribution for $PM_{2.5}$ for the charging and displaced source in ¢/kWh. The red bars are the social costs from charging the battery. The blue bars are the social benefit from displacing the peaking plant in New York City.

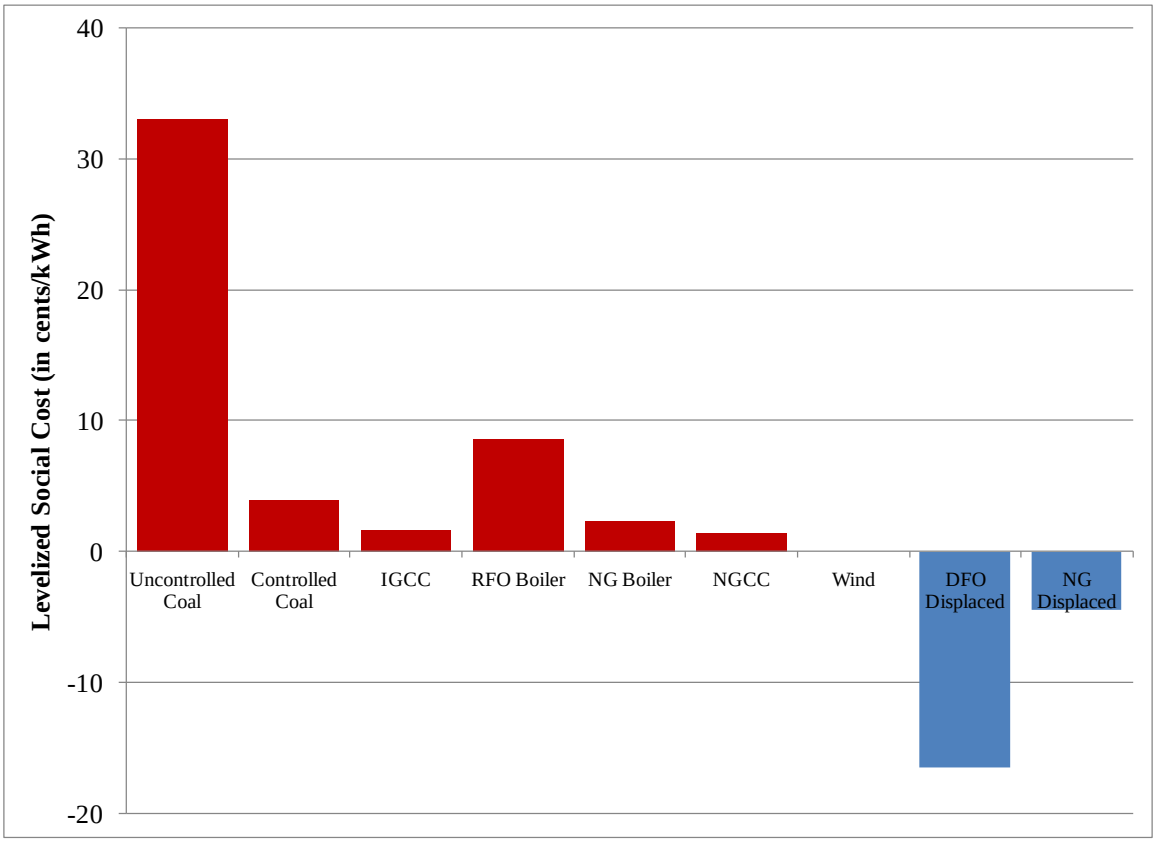

4.4 Conclusions

Depending on the charging plant and the displaced plant, there is a potential for a social cost or benefit from integrating battery storage into the NYISO. If dirtier in-city peaking plants are displaced by the battery and cleaner upstate facilities such as NG combined cycle plants are used for charging, a social benefit results. However, if NG peaking plants are displaced in New York City, there may be a social cost from charging with existing base load generation with higher emissions in the NYISO such as a RFO fueled boiler. Regardless of the overall value for a charge-displace combination, there may be an equity concern for the upstate population, although emission trading under a rule such as CAIR might alleviate some of these issues. In the long term, the battery could support cleaner generation, specifically base load wind, improving both the overall efficiency and equity of the system.

Evaluating whether there will be a net benefit or cost to the NYISO system, however, requires detailed information about the dispatch order of the generators and the frequency that each plant type is on the margin in NYISO. Given the complexities of determining the dispatch order, we are unable to make an adequate estimate using public data. As a result, we recommend that the Federal Energy Regulatory Commission (FERC) task NYISO to provide this data to allow for a comprehensive analysis of the changes in air quality and human health before siting new battery facilities.

4.5 Supporting Information

4.5.1 Tabulated social costs for charge-displace plant combinations

Table 4.2: Social costs for charge-displace plant combinations in ¢/kWh with 5% and 95% confidence intervals for changes in $PM_{2.5}$ and O_3. Positive values represent a social cost and negative values represent a social benefit.

Charging Plant \ Displaced Plant	**DFO turbine**	**NG turbine**
Uncontrolled coal	$PM_{2.5}$: 16.5 (4.14 – 35.3) O_3: 10.2 (2.36 – 19.1)	$PM_{2.5}$: 28.6 (7.17 – 61.1) O_3: 8.20 (1.89 –15.3)
Controlled coal	$PM_{2.5}$: -12.6 (-26.9 – -3.15) O_3: 12.7 (2.93 – 23.7)	$PM_{2.5}$: -0.52 (-1.11 – -0.13) O_3: 10.2 (2.36 – 19.1)
IGCC coal	$PM_{2.5}$: -15.0 (-32.0 - -3.75) O_3: 13.0 (3.00 – 24.3)	$PM_{2.5}$: -2.90 (-6.21 – -0.73) O_3: 10.4 (2.41 – 19.1)
RFO boiler	$PM_{2.5}$: -8.00 (-17.1 – -2.00) O_3: 6.55 (1.51 – 12.2)	$PM_{2.5}$: 4.06 (1.02 – 8.68) O_3: 7.66 (1.77 – 14.3)
NG boiler	$PM_{2.5}$: -14.3 (-30.5 – - 3.58) O_3: 7.65 (1.77 – 18.2)	$PM_{2.5}$: -2.22 (-4.74 – -0.55) O_3: 8.95 (2.07 – 21.9)
NG combined cycle	$PM_{2.5}$: -15.1 (-32.4 – -4.15) O_3: 9.74 (2.25 – 18.2)	$PM_{2.5}$: -3.08 (-6.58 – -0.77) O_3: 11.4 (2.63 – 21.3)
Wind	$PM_{2.5}$: -16.6 (-35.4 – -4.15) O_3: 13.7 (3.17 – 25.6)	$PM_{2.5}$: -4.49 (-9.60 – -1.13) O_3: 11.7 (2.70 – 21.9)
RFO boiler – New York	$PM_{2.5}$: 1.88 (0.47 – 4.01) O_3: 7.51 (1.74 – 14.0)	$PM_{2.5}$: 16.8 (4.21 – 35.9) O_3: 5.51 (1.27 – 10.3)
NG boiler – New York	$PM_{2.5}$: -13.4 (-28.5 – -3.34) O_3: 6.43 (1.48 – 12.0)	$PM_{2.5}$: 1.59 (0.40 – 3.39) O_3: 4.71 (1.10 – 8.81)

4.5.2 Comparison of datasets and frequency estimates

To calculate the overall efficiency of integrating a battery with the NYISO system, it is necessary to know the frequency that each fuel-plant type will be used for charging the battery. This frequency is a function of the demand for electricity, the efficiency of the generator, the cost of fuel, the availability of generators (e.g. minimum run times, outages, etc…) and constraints in the transmission infrastructure. While NYISO has access to this information, it does not release these data to the public.

In this section, we describe our attempt to develop estimates of the dispatch frequencies, using an approach described in Newcomer et al. (2008) (112). In this approach, the cost of using a given generator is estimated as the heat rate (e.g. the amount of heat required, and hence fuel, to produce a unit of electricity) multiplied by the cost of the fuel with an adder for variable maintenance and operating (VOM) as shown in equation 4.3.

$$MC = HeatRate \cdot FC + VOM \ldots . Eqn\ 4.3$$

Where MC is the marginal cost of generating electricity (in $/kWh);

HeatRate is the efficiency of the generator (in Btu/kWh);

FC is the cost of fuel (in $/Btu); and

VOM is the operating and maintenance that occurs from generating (in $/kWh).

The generators are sorted from lowest to highest MC, plotting the MC versus the available capacity for that generator. This curve is an approximation of the order that these plants would be dispatched. We then intersect this curve with the amount of electricity demanded in each hour to approximate the frequency that a plant or fuel type is used.

To construct this curve, first, we evaluate and compare three available datasets to estimate the frequency which with a given fuel-plant type is dispatched: 1) USEPA's Emissions & Generation Resource Integrated Database 2006 (eGRID2006) (22), 2)

USEPA's National Electric Energy Data System (NEEDS) (23), and 3) the Ventyx Velocity Suite, a private dataset (24). We find that none of these datasets can produce estimates of the dispatch frequencies suitable for calculating the overall efficiency as defined by Equation 4.2. We conclude, however, that eGRID can be used to make preliminary estimates. Second, we show the calculations and assumptions used to construct this MC curve. Finally, we show the dispatch frequency estimates from this curve in Table 4.4.

4.5.2.1 Comparison and evaluation of datasets

While the three datasets are based on similar data from the Energy Information Administration (EIA) (113), each of the datasets has a different amount of detail about the facilities and generators in the system and make different assumptions about generators that can operate on two different fuels (e.g. dual fuel generators that can operate on natural gas or fuel oil) and the amount of available generation. In this section, we describe the available datasets. Unfortunately, differences in generator names and other features between the three datasets, however, make a direct comparison infeasible.

The eGRID dataset is compiled by the USEPA and is a comprehensive inventory of the environmental attributes of electric power plants. eGRID 2006 is based on data from 2004. It contains the heat rate for each facility. Any given facility, however, may include several units which have different heat rates and operate on different fuel types. Aggregating this heat rate and fuel types over several units could misallocate generation to either a lower or higher MC. Despite these shortcomings, Newcomer et al. (2008) (112) used this dataset for their MC curves as it is publicly available and easy to manipulate.

The Ventyx Velocity Suite dataset is a private dataset. It has the most up-to-date information regarding the available generators in the NYISO and reflects the retirement of several large coal plants in 2007 and the addition of newer, cleaner generation. It has also disaggregated the facilities into the unit level heat rates and fuel types. This disaggregation makes this dataset more appealing for constructing the MC curve.

However, this dataset is harder to manipulate as there are several build-in assumptions about the available generation capacity and it does not contain the nameplate capacity.

The NEEDS dataset is used to project air quality emissions for the USEPA's regulatory air quality modeling efforts (e.g. for the regulatory impact assessment of the CAIR regulations). It contains information on the heat rate and the fuel types for each unit in the system. It includes both current as well as some units which are expected to come online in the near future. While this dataset is appealing because it has information by unit, it cannot be used for this analysis since the heat rates are gross rather than net and the amount of electricity generated by fuel type is not presented.

The main problem with all these datasets is that they are static in time. In reality, the available capacity at any given generator and in the NYISO system varies by hour and by season due to maintenance, forced outages, transmission constraints and other factors. In addition, no datasets provides information on when the dual fuel capable plants are operating on which fuel. Without information on the time dependency of the available capacity and fuel usage, we cannot produce adequate estimates.

4.5.2.2 Constructing the dispatch curve

To construct dispatch curves to make a rough estimate of the dispatch frequencies, we use eGRID2006 since it is publicly available. We show the curves in Figure 4.9. First, we calculate the MC by multiplying the heat rates with fuel prices consistent with the costs for electricity generation in New York State, obtained from the Energy Information Agency (EIA) (112, 114). We assume that there are no net imports from outside the NYISO. The fuel costs and VOMs are shown in Table 4.3. Second, for each generator with a MC, we need to assign an amount of available generating capacity. As discussed above, the available capacity for any given generator is a function of the hour of the day and the day of the year, and this information is not available. To attempt to capture the availability of the generation, we investigate the overall availability of generation in the NYISO. We find that generation in the NYISO system has an availability of

approximately 87%. Thus, we multiply the nameplate capacity of the generator by the system availability to account for forced outages, maintenance schedules and reserve margins. Whether this average captures enough of the variation in the available generation is unknown. In addition, several plants can operate on more than one fuel type. In NYISO, there are numerous turbines and boiler - steam turbine plants that can operate on natural gas (NG) and DFO as a result of the Minimum Oil Burn rule (102). It is unclear, however, how to account for these plants in an average dispatch curve. With the eGRID data, we assign the entire plant to natural gas or fuel oil, and then compare the dispatch frequencies from these two curves as a bounding analysis.

We also show the dispatch curve provided by Ventyx in Figure 4.9. In general, we find good agreement with the curves from eGRID. We observe differences due to the assumptions about the cost of fuel and the type of fuel employed, specifically at plants that can operate on more than one fuel, as well as assumptions about the amount of available capacity. One of the main differences in the curve occurs between 25,000 MW to 32,000 MW where the higher fuel prices for distillate fuel oil (DFO) and residual fuel oil (RFO) have a significant effect on the marginal cost. The fuel prices and VOM costs from Ventyx are also shown in Table 4.3. Also, Ventyx calculates the cost of dispatching a generator as a weighted average of the cost for a given fuel and the fraction of the electricity produced by the fuel. We judge this approach unsatisfactory as it does not tell us which fuel is actually being used.

Table 4.3: Comparison of costs for fuel (in $/mmBTU) and variable O&M ($/MWh) between Ventyx and this work (110, 112, 114)

Fuel/Plant type	eGRID fuel cost	Ventyx fuel cost	Our VOM	Ventyx VOM
Coal	2.40	2.58 (avg) 1.90 – 16.00[a] (range)	0	1.36 (avg) 1.02 – 1.75 (range)
Natural gas	7.60	7.53 (avg) 7.23 – 7.73 (range)	0	1.84 (avg) 0.45 – 5.32 (range)
Light oil/Distillate fuel oil	15.20	19.02	0	2.44 (avg) 0.49 – 4.76 (range)
Heavy oil/Residual fuel oil	9.40	15.10	0	1.33 (avg) 0.81 – 1.79 (range)
Nuclear	0	0.44	18.00	2.95 (avg) 2.77 – 3.50 (range)
Wind	0	0	20.00	0
Hydro	0	0	10.00	0.95 (avg) 0.43 – 2.77 (range)
Hydro - Pumped storage	0	0	50.00	1.2
Landfill gas	0	11.23	50.00	4.49 (avg) 4.19 – 4.69 (range)
Solid waste	0	3.04	50.00	1.58 (avg) 1.01 – 3.20 (range)
Wood (wood waste solids)	0	3.09	50.00	1.12

a. The high value of 16.00 $/mmBTU is associated with a small amount of coal purchased by a plant which generates mostly on gas and oil. The average value excludes this outlier.

Figure 4.9: Dispatch Curves for NYISO for eGRID and Ventyx (22, 110)

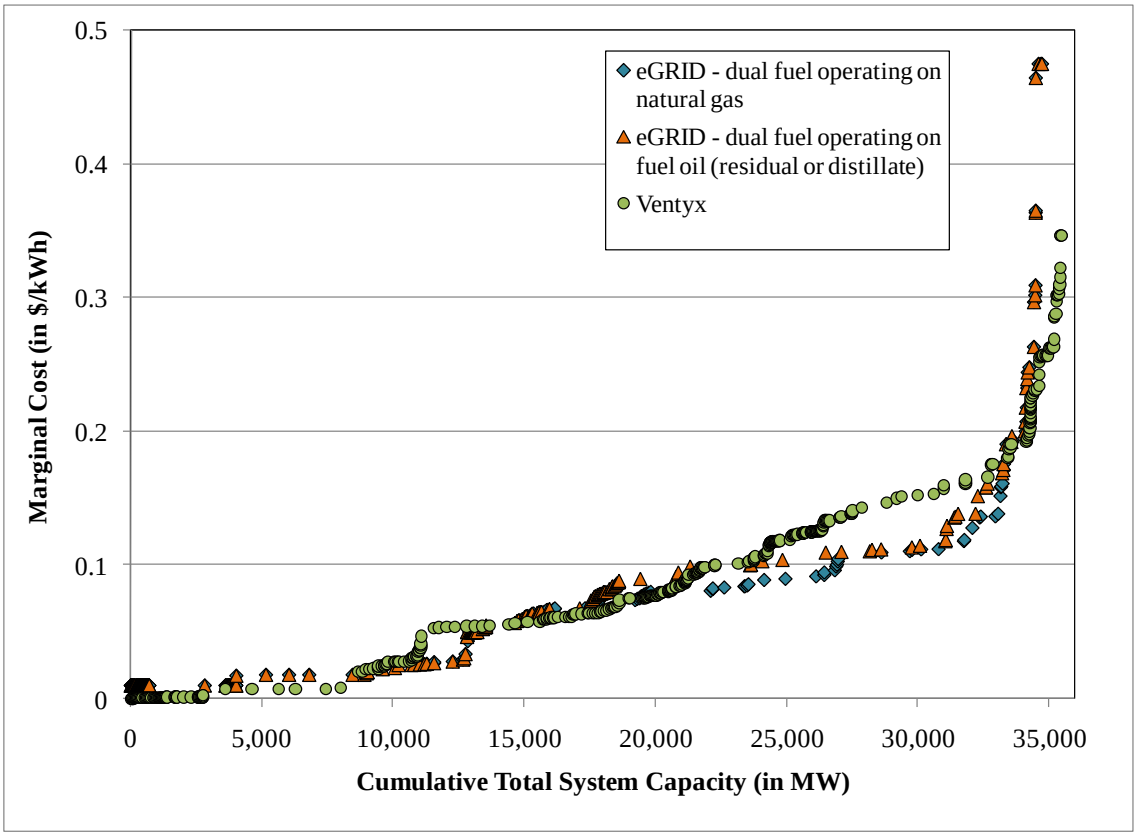

4.5.2.3 Dispatch frequency estimates

To develop estimates of the dispatch frequencies, we intersect the eGRID curves shown in Figure 4.7 with actual system loads by hour for the NYISO area (115). We show the resulting frequencies in Table 4.4. First, we present the frequencies if all plants that can operate dual fuel are using natural gas (NG). Second, we present the frequencies if all plants that can operate on dual fuel are using fuel oil (DFO or RFO). We use these values in section 4.3.2 to estimate the net social value to the system of installing the battery. More information on calculating the frequency can be found in Walawalkar (2008) (116). In Table 4.5 we show the net social benefits and costs for the system for dual fuel plants operating on natural gas for displacing a DFO and a NG peaking plant, respectively. In Table 4.6, we show the net social benefits and costs for the system for dual fuel plants operating on fuel oil for displacing a DFO and a NG peaking plant, respectively. The values in the table are the average of all plants with a given fuel type.

Table 4.4: Estimated frequency NYISO plant types are used for charging the battery. To obtain the frequency estimates, the dispatch curve for either all dual fuel plants operating on natural gas or on fuel oil is intersected with observed hourly loads in the NYISO. Summing the number of hours that the load intersects a given fuel type and dividing by the number of hours a year yields the following frequencies.

Fuel Type	Dual Fuel Plants Operating as Natural Gas	Dual Fuel Plants Operating as Fuel Oil
Coal plant	1.3%	1.3 %
Natural gas plant	97.4 %	42.6%
Fuel oil (residual or distillate)	-	52.6%
Other	1.3%	3.5 %

Table 4.5: Net social values for the system in ¢/kWh with 5% and 95% confidence intervals if dual fuel plants are using natural gas

Displaced Plant / Charging Combination	DFO turbine	NG turbine
Coal – NG	$PM_{2.5}$: -14.4 (-30.9 - -3.60) O_3: 8.62 (2.00 - 16.1) Total: -5.74 (-14.6 - -1.61)	$PM_{2.5}$: -2.47 (-5.32 - -0.62) O_3: 10.0 (2.32 - 18.8) Total: 7.56 (1.70 - 13.5)
Coal – NG (in NYC)	$PM_{2.5}$: -13.1 (-28.2 - -3.29) O_3: 6.42 (1.49 - 12.0) Total: -6.68 (-16.2 - -1.80)	$PM_{2.5}$: 1.66 (0.42 - 3.57) O_3: 4.71 (1.09 - 8.82) Total: 6.37 (1.51 - 12.4)

Table 4.6: Net social values for the system in ¢/kWh with 5% and 95% confidence intervals if dual fuel plants are using fuel oil

Charging Combination \ Displaced Plant	**DFO turbine**	**NG turbine**
Coal – RFO – NG	$PM_{2.5}$: -10.5 (-22.6 - -2.64) O_3: 7.30 (1.69 - 13.7) Total: -3.21 (-8.95 - -0.95)	$PM_{2.5}$: 1.12 (0.28 - 2.40) O_3: 8.49 (1.96 - 15.9) Total: 9.60 (2.24 - 18.3)
Coal – RFO – NG (in NYC)	$PM_{2.5}$: -9.96 (-21.4 - -2.50) O_3: 6.34 (1.47 - 11.9) Total: -3.21 (-9.57 - -1.03)	$PM_{2.5}$: 2.92 (0.73 - 6.29) O_3: 6.16 (1.43 - 11.5) Total: 9.60 (2.16 - 17.8)
Coal – RFO (in NYC) – NG (in NYC)	$PM_{2.5}$: -4.77 (-10.3 - -1.20) O_3: 6.85 (1.58 - 12.8) Total: 2.08 (0.39 - 2.56)	$PM_{2.5}$: 9.62 (2.41 - 20.7) O_3: 5.03 (1.16 - 9.42) Total: 14.7 (3.58 - 30.1)

5. Conclusions and policy recommendations

In this work, I investigate the air quality, human health effects and costs associated with two applications for distributed electricity generation (DG): 1) using installed backup generators for meeting peak electricity demand in Atlanta, Chicago, Dallas and New York City, and 2) integrating utility scale battery storage located in New York City into the New York Independent System Operator (NYISO) grid. For both applications, I use an impact pathway approach that couples comprehensive air quality modeling, specifically chemical transport models (CTMs), with policy analysis tools. This technique captures changes in ambient air quality as well as the resulting human health effects. In addition, since the health effects are translated into an equivalent social cost, I can compare these costs to other costs and benefits as well as evaluate the cost-effectiveness of options to mitigate any adverse effects.

For using installed backup generators for meeting peak electricity demand, I find that on a full (private and social) cost basis, properly controlled backup generators are more cost-effective for meeting peak electricity demand than building new peaking plants. The private costs are lower because the generators are already installed to address reliability concerns (e.g. to protect against blackouts). As a result, the capital costs do not need to be counted for the peak electricity application; hence, the installed generators operate at their incremental operational cost, mostly fuel costs, plus an additional cost for interconnections to allow the generator to operate in parallel with the electricity grid. Since emergency and backup generators do not generally require emission controls to be permitted, however, there is a high social cost from operating these generators in highly populated urban centers. To address health concerns, cost-effective emission controls are available, specifically a catalyzed diesel particulate filter (DPF) to control fine particulate matter ($PM_{2.5}$) and an exhaust gas recirculation (EGR) to control nitrogen oxides (NO_x). These results are robust across four urban centers (Atlanta, Chicago, Dallas and New York City) for a range of health endpoints and when accounting for uncertainties in the air quality modeling. Thus, I recommend that the relevant authorities reconsider their ban on using diesel generators to meet peak electricity demand, taking care to ensure that the

emission controls achieve their stated performance and that the generators are properly sited so as not to cause a nuisance in the immediate area.

Alternatively, a sodium sulfur (NaS) battery facility in New York City could supply electricity during the afternoon hours after charging from cheaper generation available at off peak hours from the rest of the state. For this application, emissions are displaced in the urban center but increase at the location of the plant used for charging the battery. Displacing dirtier peaking capacity results in benefits to New York City. Further, due to the large population in New York City, there is a net social benefit for most types of charging plants if a distillate fuel oil peaking plant is displaced. If a natural gas fueled peaking plant is displaced, however, there is a net social cost. In the short-term, this strategy involves a human health cost at the upstate charging locations. To mitigate these equity concerns, the electricity to charge the batteries must be obtained from renewable generation such as night time wind power. Interactions with the Renewable Portfolio Standards (RPS) and the Clean Air Interstate Rule (CAIR) could provide this cleaner generation. The available data, however, is insufficient to evaluate the types of base load plants that could be used for charging and the frequency that they would be employed. As a result, I recommend that the Federal Energy Regulatory Commission (FERC) task NYISO to provide this data to allow for a comprehensive analysis of the changes in air quality and human health before siting new battery facilities.

Since emissions by themselves do not provide sufficient information for this analysis, an important part of this work is transforming the emission into ambient concentrations. For this modeling, I employ the Particulate Matter Comprehensive Air Quality Model with extensions ($PMCAM_x$) and evaluate the ability of $PMCAM_x$ and the available emission files to provide robust results for policy analysis. For the backup generator application, I find that in cases where there are large changes in the gaseous precursors to $PM_{2.5}$, the changes in secondary $PM_{2.5}$ can have a large influence on the resulting human health costs. Known problems with the representation of these formation mechanisms in $PMCAM_x$, however, reduce confidence in these results. To address this issue, I separate the changes in concentrations into individual species and cost the human health effects

from different species combinations, including costing only concentration enhancements. While this does not directly address the uncertainty, it creates a "worse case" scenario to test the robustness of the policy recommendations. In addition to issues with the mechanisms, there are also uncertainties related to the emissions files. For the backup generators, I find significant increases in particulate matter nitrate (PNO_3) in Atlanta. For the formation of PNO_3, there must be sufficient "free" ammonia (NH_3). There are known issues with NH_3 emission estimates and without better measurements of NH_3 emissions, it is difficult to assess whether the PNO_3 increases would actually be observed. A network for monitoring total NH_3 would provide the information required to evaluate these results.

By contrast to secondary $PM_{2.5}$, the mechanisms for the formation of ozone (O_3) are well understood and the changes in O_3 are consistent with the underlying volatile organic compound (VOC)/NO_x ratios in $PMCAM_x$. These ratios, however, depend on basecase emissions which are not static in time. Since new epidemiological evidence suggests that O_3 is linked to premature mortality, it is important that the modeled O_3 concentrations reflect present and near future ambient conditions for policy evaluation. As a result, I recommend additional sensitivity analysis on available emission files with timely updates as data become available.

6. References

1. Lave, L. B.; Seskin, E. P., Air Pollution and Human Health. *Science* **1970,** *169* (3947), 723-733
2. Pope, C. A.; Dockery, D. W.; Schwartz, J., Review of Epidemiological Evidence of Health-Effects of Particulate Air-Pollution. *Inhalation Toxicology* **1995,** *7* (1), 1-18
3. Krupnick, A. J., Valuing Health Outcomes: Policy Choices and Technical Issues. *http://www.rff.org/Publications/Pages/PublicationDetails.aspx?PublicationID=9556*, *Resources for the Future* **2004,** *Accessed April 9, 2009,*
4. Rabl, A.; Holland, M., Environmental assessment framework for policy applications: Life cycle assessment, external costs and multi-criteria analysis. *Journal of Environmental Planning and Management* **2008,** *51* (1), 81-105
5. Lovins, A. B., Energy Strategy - Road Not Taken. *Foreign Affairs* **1976,** *55* (1), 65-96
6. Russell, A., Regional photochemical air quality modeling: Model formulations, history, and state of the science. *Annual Review of Energy and the Environment* **1997,** *22*, 537-588
7. Gaydos, T. M.; Pinder, R.; Koo, B.; Fahey, K. M.; Yarwood, G.; Pandis, S. N., Development and application of a three-dimensional aerosol chemical transport model, PMCAMx. *Atmospheric Environment* **2007,** *41* (12), 2594-2611.DOI 10.1016/j.atmosenv.2006.11.034
8. Baumol, W. J.; Oates, W. E., *The theory of environmental policy*. 2nd ed.; Cambridge University Press: Cambridge [Cambridgeshire] ; New York, 1988; p x, 299 p.
9. Sundqvist, T., What causes the disparity of electricity externality estimates? *Energy Policy* **2004,** *32* (15), 1753-1766.Doi 10.1016/S0301-4215(03)00165-4
10. Rabl, A.; Spadaro, J. V., Public health impact of air pollution and implications for the energy system. *Annual Review of Energy and the Environment* **2000,** *25*, 601-627
11. ExternE, ExternE: Externalities of Energy. *http://www.externe.info/* **1995,** *Accessed April 2009,*
12. United States Environmental Protection Agency, *The Benefits and Costs of the Clean Air Act, 1970 - 1990*. Washington DC, 1997;
13. United States Environmental Protection Agency, *The Benefits and Costs of the Clean Air Act, 1990 - 2010*. 1999;
14. Stevens, G.; Wilson, A.; Hammitt, J. K., A benefit-cost analysis of retrofitting diesel vehicles with particulate filters in the Mexico City metropolitan area. *Risk Analysis* **2005,** *25* (4), 883-899
15. United States Environmental Protection Agency, AP - 42, Compilation of Air Pollutant Emission Factors, Volume 1: Stationary Point and Area Sources, 5th Edition. *http://www.epa.gov/ttn/chief/ap42/* **2005,** *Accessed January 15, 2009,*
16. Berkenpas, M. B.; Rubin, E. S.; Zaremsky, C. J., User Manual: Integrated Environmental Control Model. *http://www.iecm-online.com/PDF files/2007/2007ra Rubin et al, IECM User.pdf* **2007**,
17. Frey, H. C.; Li, S., Methods for quantifying variability and uncertainty in AP-42 emission factors: Case studies for natural gas-fueled engines. *Journal of the Air & Waste Management Association* **2003,** *53* (12), 1436-1447

18. United States Environmental Protection Agency, SPECIATE, Version 4.0. *http://www.epa.gov/ttn/chief/software/speciate/index.html* **2007,** *Accessed April 9, 2009*,
19. Gery, M. W.; Whitten, G. Z.; Killus, J. P.; Dodge, M. C., A Photochemical Kinetics Mechanism for Urban and Regional Scale Computer Modeling. *Journal of Geophysical Research-Atmospheres* **1989,** *94* (D10), 12925-12956
20. Carter, W. P. L., Development of an Improved Chemical Speciation Database and Software for Processing VOC Emissions for Air Quality Models. *http://www.cert.ucr.edu/~carter/emitdb* **2005,** *Accessed January 2007*,
21. Federal Energy Regulatory Commission, Form 714 - Annual Electric Balancing Authority Area and Planning Area Report. *http://www.ferc.gov/docs-filing/eforms/form-714/overview.asp* **2009,** *Accessed January 2009*,
22. United States Environmental Protection Agency, Emissions & Generation Resource Integrated Database (eGRID2006) *http://www.epa.gov/cleanenergy/energy-resources/egrid/index.html* **2006,** *Accessed August 2007*,
23. United States Environmental Protection Agency, National Electric Energy Data System (NEEDS). *http://www.epa.gov/airmarkt/progsregs/epa-ipm/index.html#needs* **2006,** *Accessed January 2009*,
24. Ventyx, Velocity Suite. *http://www.ventyx.com/velocity/vs-overview.asp* **2009**,
25. Chang, J. S.; Brost, R. A.; Isaksen, I. S. A.; Madronich, S.; Middleton, P.; Stockwell, W. R.; Walcek, C. J., A 3-Dimensional Eulerian Acid Deposition Model - Physical Concepts and Formulation. *Journal of Geophysical Research-Atmospheres* **1987,** *92* (D12), 14681-14700
26. Capaldo, K. P.; Pilinis, C.; Pandis, S. N., A computationally efficient hybrid approach for dynamic gas/aerosol transfer in air quality models. *Atmospheric Environment* **2000,** *34* (21), 3617-3627
27. Gaydos, T. M.; Koo, B.; Pandis, S. N.; Chock, D. P., Development and application of an efficient moving sectional approach for the solution of the atmospheric aerosol condensation/evaporation equations. *Atmospheric Environment* **2003,** *37* (23), 3303-3316.Doi 10.1016/S1352-2310(03)00267-X
28. Odum, J. R.; Hoffmann, T.; Bowman, F.; Collins, D.; Flagan, R. C.; Seinfeld, J. H., Gas/particle partitioning and secondary organic aerosol yields. *Environmental Science & Technology* **1996,** *30* (8), 2580-2585
29. Nenes, A.; Pandis, S. N.; Pilinis, C., ISORROPIA: A new thermodynamic equilibrium model for multiphase multicomponent inorganic aerosols. *Aquatic Geochemistry* **1998,** *4* (1), 123-152
30. Grell, G. A. D., J.; Stauffer, D.R., A Description of the Fifth Generation Penn State/NCAR Mesoscale Model (MM5). *http:/www.mmm.ucar.edu/mm5/documents/mm5-desc-doc.html* **1995**,
31. LADCO, BaseE Modeling Inventory, Midwest Regional Planning Organization. *http://www.ladco.org/tech/emis/BaseE/baseEreport.pdf* **2003**,
32. Karydis, V. A.; Tsimpidi, A. P.; Pandis, S. N., Evaluation of a three-dimensional chemical transport model (PMCAMx) in the eastern United States for all four seasons. *Journal of Geophysical Research-Atmospheres* **2007,** *112* (D14), -.Artn D14211 Doi 10.1029/2006jd007890
33. Briggs, G. A. *Diffusion estimation for small emissions*; NOAA Report ATDL-106: 1973;

34. Abt Associates Inc., Environmental benefits mapping and analysis program (version 2.4), http://www.epa.gov/air/benmap/, Bethesda, MD: . *Prepared for US Environmental Protection Agency, Office of Air Quality Planning and Standards, Innovative Strategies and Economics Group, Research Triangle Park, NC* **2005,** *Accessed January 2009*,
35. Farrow, S. R.; Wong, E.; Ponce, R. A.; Faustman, E. M.; Zerbe, R. O., Facilitating regulatory design and stakeholder participation: The FERET template with an application to the Clean Air Act. *Improving Regulation: Cases in Environment, Health and Safety* **2001,** *Washington, DC.* (Resources for the Future),
36. United States Environmental Protection Agency, Health Assessment Document for Diesel Exhaust. *http://cfpub.epa.gov/ncea/cfm/recordisplay.cfm?deid=29060* **2002,** *Washington, DC: Office of Research and Development*,
37. Office of Environmental Health Hazard Assessment, Air Toxics Hot Spots Progam Risk Assessment Guidelines. Part II: Technical Support Document for Describing Available Cancer Potency Factors. *http://oehha.ca.gov/air/hot_spots/may2005tsd.html* **2005,** *Accessed January 2009*,
38. National Research Council, Estimating Mortality Risk Reduction and Economic Benefits from Controlling Ozone Air Pollution. *http://www.nap.edu/catalog.php?record_id=12198* **2008,** *Washington DC: National Academies Press*,
39. Matthews, H. S.; Lave, L. B., Applications of environmental valuation for determining externality costs. *Environmental Science & Technology* **2000,** *34* (8), 1390-1395
40. Boardman, A. E. G., David H.; Vining, Aidan R.; Weimer, David L., *Cost-Benefit Analysis: Concepts and Practice*. Second ed.; Prentice Hall: Upper Saddle River, NJ, 2001;
41. Krupnick, A.; Morgenstern, R., The future of benefit-cost analyses of the Clean Air Act. *Annual Review of Public Health* **2002,** *23*, 427-448
42. Northeast States for Coordinated Air Use Management (NESCAUM), Stationary Diesel Engines in the Northeast: An Initial Assessment of the Regional Population Control Technology Options and Air Quality Policy Issues. *www.nescaum.org/documents/rpt030612dieselgenerators.pdf* **2003**,
43. Meyer, J. F., John; Troester, Dennis, Standby Generation: A New Proposition. *Public Utilities Fortnightly* **2002,** *140* (11),
44. Greene, N.; Hammerschlag, R., Small and clean is beautiful: exploring the emissions from distributed generation and pollution prevention policies. *The Electricity Journal* **2000,** *13* (Jun), 50 - 60
45. Allison, J. E.; Lents, J., Encouraging distributed generation of power that improves air quality: can we have our cake and eat it too? *Energy Policy* **2002,** *30* (9), 737-752.Pii S0301-4215(01)00135-5
46. Heath, G. A.; Granvold, P. W.; Hoats, A. S.; Nazaroff, W. W., Intake fraction assessment of the air pollutant exposure implications of a shift toward distributed electricity generation. *Atmospheric Environment* **2006,** *40* (37), 7164-7177.DOI 10.1016/j.atmosenv.2006.06.023
47. Public Interest Energy Research Program, Air Quality Implications of Backup Generators in California. Volume One: Generation Scenarios, Emissions and

Atmospheric Modeling, and Health Risk Analysis. *http://www.energy.ca.gov/pier/final_project_reports/CEC-500-2005-048.html* **2005**,
48. Strachan, N.; Farrell, A., Emissions from distributed vs. centralized generation: The importance of system performance. *Energy Policy* **2006,** *34* (17), 2677-2689.DOI 10.1016/j.enpol.2005.03.015
49. Massahusetts Clean Air Task Force, Diesel Engines: Emission Controls and Retrofits. *http://www.catf.us/publications/factsheets/Diesel_Controls_and_Retrofits.pdf* **2003**,
50. Wien, S.; England, G. C.; Chang, O. M. C., Development of Fine Particulate Emission Factors and Speciation Profiles for Oil and Gas-Fired Combustion Systems. Topical Report: Test Results for a Diesel Fuel-Fired Compression Ignition Reciprocating Engine with a Diesel Particulate Filter at Site Foxtrot. *www.nyserda.org/programs/environment/emep/06_Foxtrot_R1-V2.pdf* **2004,** *Accessed April 9, 2009*,
51. United States Environmental Protection Agency, Aerodynamic Information Retrieval System (AIRS). *http://www.epa.gov/ttn/airs/airsaqs/detaildata/downloadaqsdata.htm* **2005**,
52. ESI International, Diesel Emission Control Strategies Available to the Underground Mining Industry. *http://www.deep.org/reports/esi_final_report.pdf* **1999**,
53. Washington State University Extension Energy Program, Diesel Particulate Filter. *http://www.energy.wsu.edu/pubs/default.cfm#RenewableReports* **2004**,
54. Levesque, C. J., Distributed generation: doomed by development details? . *Public Utilities Fortnightly* **2001,** *139* (3), 47-51
55. National Research Council, Rethinking the Ozone Problem in Urban and Regional Air Pollution. *http://books.nap.edu/catalog.php?record_id=1889* **1991,** *Washington, DC: National Academies Press*,
56. Kleinman, L. I.; Daum, P. H.; Imre, D. G.; Lee, J. H.; Lee, Y. N.; Nunnermacker, L. J.; Springston, S. R.; Weinstein-Lloyd, J.; Newman, L., Ozone production in the New York City urban plume. *Journal of Geophysical Research-Atmospheres* **2000,** *105* (D11), 14495-14511
57. California Air Resources Board, Emission reduction offsets transaction cost: Summary report for 2004. *http://www.arb.ca.gov/nsr/erco/ercrpt04.pdf* **2004**,
58. Lively, M. B., Saving California with Distributed Generation. *Public Utilities Fortnightly* **2001,** *139* (12),
59. NYISO Auxiliary Market Operations, Emergency Demand Response Program Manual. *http://www.nyiso.com/public/webdocs/products/demand_response/emergency_demand_response/edrp.mnl.pdf* **2008,** *Accessed February 2009*,
60. Gilmore, E. A.; Lave, L. B.; Adams, P. J., The costs, air quality, and human health effects of meeting peak electricity demand with installed backup generators. *Environmental Science & Technology* **2006,** *40* (22), 6887-6893.Doi 10.1021/Es061151q
61. Scott, J.; Silverman, I.; Tatham, S., *Cleaner Diesel Handbook (http://www.edf.org/article.cfm?contentid=3987)*. Environmental Defense Fund: 2005;
62. Blankinship, S., Conversion package aims at cleaning up stationary diesel gensets. *Power Engineering* **2002,** *106* (4), 52

63. Energy Information Administration, Weekly Retail Gasoline and Diesel Prices. *http://tonto.eia.doe.gov/dnav/pet/PET_PRI_GND_DCUS_NUS_W.htm* **2008,** *Accessed April 2009*,
64. Manufacturers of Emission Controls Association, MECA Independent Cost Survey for Emission Control Retrofit Technologies. *www.epa.gov/diesel/documents/meca1.pdf* **2000**,
65. Western Regional Air Partnership, Offroad Diesel Retrofit Guidance Document. *http://www.wrapair.org/forums/msf/offroad_diesel.html* **2005**,
66. Blankinship, S., Dual fuel conversion can offer big advantages. *Power Engineering* **2005,** *109* (8), 58
67. California Air Resources Board, Currently Verified Control Technologies. *http://www.arb.ca.gov/diesel/verdev/vt/cvt.htm* **2008,** *Accessed April 2009*,
68. Kassel, R. B., Diane, Cleaning Up Today's Dirty Diesels: Retrofitting and Replacing Heavy-Duty Vehicles in the Coming Decade. *Natural Resoures Defense Council: www.nrdc.org/air/transportation/retrofit/retrofit.pdf* **2004**,
69. Papagiannakis, R. G.; Hountalas, D. T., Combustion and exhaust emission characteristics of a dual fuel compression ignition engine operated with pilot Diesel fuel and natural gas. *Energy Conversion and Management* **2004,** *45* (18-19), 2971-2987.DOI 10.1016/j.enconman.2004.01.013
70. Laden, F.; Schwartz, J.; Speizer, F. E.; Dockery, D. W., Reduction in fine particulate air pollution and mortality - Extended follow-up of the Harvard six cities study. *American Journal of Respiratory and Critical Care Medicine* **2006,** *173* (6), 667-672.DOI 10.1164/rccm.200503-443OC
71. Pope, C. A.; Burnett, R. T.; Thun, M. J.; Calle, E. E.; Krewski, D.; Ito, K.; Thurston, G. D., Lung cancer, cardiopulmonary mortality, and long-term exposure to fine particulate air pollution. *Jama-Journal of the American Medical Association* **2002,** *287* (9), 1132-1141
72. Klemm, R. J.; Mason, R., Replication of Reanalysis of Harvard Six-City Study. . In *Revised Analyses of Time-Series Studies of Air Pollution and Health*, Health Effects Institute: Boston, MA, 2003; pp 165 - 172
73. Schwartz, J., Daily Deaths Associated with Air Pollution in Six US Cities and Short-Term Mortality Displacement in Boston. In *Revised Analyses of Time-Series Studies of Air Pollution and Health*, Health Effects Institute: Boston, MA, 2003; pp 219 - 226
74. Liao, K. J.; Tagaris, E.; Napelenok, S. L.; Manomaiphiboon, K.; Woo, J. H.; Amar, P.; He, S.; Russell, A. G., Current and future linked responses of ozone and PM2.5 to emission controls. *Environmental Science & Technology* **2008,** *42* (13), 4670-4675.Doi 10.1021/Es7028685
75. Meng, Z.; Dabdub, D.; Seinfeld, J. H., Chemical coupling between atmospheric ozone and particulate matter. *Science* **1997,** *277* (5322), 116-119
76. Tsimpidi, A. P.; Karydis, V. A.; Pandis, S. N., Response of Fine Particulate Matter to Emission Changes of Oxides of Nitrogen and-Anthropogenic Volatile Organic Compounds in the Eastern United States. *Journal of the Air & Waste Management Association* **2008,** *58* (11), 1463-1473.Doi 10.3155/1047-3289.58.11.1463
77. Ansari, A. S.; Pandis, S. N., Response of inorganic PM to precursor concentrations. *Environmental Science & Technology* **1998,** *32* (18), 2706-2714

78. Pinder, R. W.; Adams, P. J.; Pandis, S. N.; Gilliland, A. B., Temporally resolved ammonia emission inventories: Current estimates, evaluation tools, and measurement needs. *Journal of Geophysical Research-Atmospheres* **2006,** *111* (D16), -.Artn D16310 Doi 10.1029/2005jd006603
79. Zhang, J.; Chameides, W. L.; Weber, R.; Cass, G.; Orsini, D.; Edgerton, E.; Jongejan, P.; Slanina, J., An evaluation of the thermodynamic equilibrium assumption for fine particulate composition: Nitrate and ammonium during the 1999 Atlanta Supersite Experiment. *Journal of Geophysical Research-Atmospheres* **2002,** *108* (D7), SOS2.1-SOS2.11.Artn 8414
Doi 10.1029/2001jd001592
80. Nowak, J. B.; Huey, L. G.; Russell, A. G.; Tian, D.; Neuman, J. A.; Orsini, D.; Sjostedt, S. J.; Sullivan, A. P.; Tanner, D. J.; Weber, R. J.; Nenes, A.; Edgerton, E.; Fehsenfeld, F. C., Analysis of urban gas phase ammonia measurements from the 2002 Atlanta Aerosol Nucleation and Real-Time Characterization Experiment (ANARChE). *Journal of Geophysical Research-Atmospheres* **2006,** *111* (D17), D17308.Artn D17308 Doi 10.1029/2006jd007113
81. Pun, B. K.; Seigneur, C., Sensitivity of particulate matter nitrate formation to precursor emissions in the California San Joaquin Valley. *Environmental Science & Technology* **2001,** *35* (14), 2979-2987.Doi 10.1021/Es0018973
82. Donahue, N. M.; Robinson, A. L.; Pandis, S. N., Atmospheric organic particulate matter: From smoke to secondary organic aerosol. *Atmospheric Environment* **2009,** *43* (1), 94-106.DOI 10.1016/j.atmosenv.2008.09.055
83. United States Environmental Protection Agency, 2006 National Ambient Air Quality Standards for Particle Pollution - Regulatory Impact Analysis. *http://www.epa.gov/ttnecas1/ria.html* **2006**,
84. Bell, M. L.; McDermott, A.; Zeger, S. L.; Samet, J. M.; Dominici, F., Ozone and short-term mortality in 95 US urban communities, 1987-2000. *Jama-Journal of the American Medical Association* **2004,** *292* (19), 2372-2378
85. Bell, M. L.; Dominici, F.; Samet, J. M., A meta-analysis of time-series studies of ozone and mortality with comparison to the national morbidity, mortality, and air pollution study. *Epidemiology* **2005,** *16* (4), 436-445.DOI 10.1097/01.ede.0000165817.40152.85
86. Bell, M. L.; Peng, R. D.; Dominici, F., The exposure-response curve for ozone and risk of mortality and the adequacy of current ozone regulations. *Environmental Health Perspectives* **2006,** *114* (4), 532-536.Doi 10.1289/Ehp.8816
87. Levy, J. I.; Chemerynski, S. M.; Sarnat, J. A., Ozone exposure and mortality - An empiric Bayes metaregression analysis. *Epidemiology* **2005,** *16* (4), 458-468.DOI 10.1097/01.ede.0000165820.08301.b3
88. National Atmospheric Deposition Program (NADP), Passive Ammonia Monitoring Network. *http://nadp.sws.uiuc.edu/nh3Net/* **2009,** *Accessed May 15, 2009*,
89. Herzog, J. W., Current and near-term emission control strategies for diesel powered generator sets. *Telecommunications Energy Conference, 2002, INTELEC.* **2002,** *24th Annual International*, 394-399
90. EPRI, *EPRI-DOE Handbook of Energy Storage for Transmission and Distribution Applications*. EPRI & US Department of Energy: Palo Alto, CA, 2003;

91. Denholm, P.; Kulcinski, G. L.; Holloway, T., Emissions and energy efficiency assessment of baseload wind energy systems. *Environmental Science & Technology* **2005,** *39* (6), 1903-1911.Doi 10.1021/Es049946p
92. Walawalkar, R.; Apt, J.; Mancini, R., Economics of electric energy storage for energy arbitrage and regulation in New York. *Energy Policy* **2007,** *35* (4), 2558-2568.DOI 10.1016/j.enpol.2006.09.005
93. Schainker, R. B., Executive overview: energy storage options for a sustainable energy future. *Power Engineering Society General Meeting, IEEE* **2004,** *2* (2309 - 2314),
94. Denholm, P.; Holloway, T., Improved accounting of emissions from utility energy storage system operation. *Environmental Science & Technology* **2005,** *39* (23), 9016-9022.Doi 10.1021/Es0505898
95. Rodriguez, M. A.; Carreras-Sospedra, M.; Medrano, M.; Brouwer, J.; Samuelsen, G. S.; Dabdub, D., Air quality impacts of distributed power generation in the South Coast Air Basin of California 1: Scenario development and modeling analysis. *Atmospheric Environment* **2006,** *40* (28), 5508-5521.DOI 10.1016/j.atmosenv.2006.03.054
96. Carreras-Sospedra, M.; Dabdub, D.; Brouwer, J.; Knipping, E.; Kumar, N.; Darrow, K.; Hampson, A.; Hedman, B., Air quality impacts of distributed energy resources implemented in the northeastern United States. *Journal of the Air & Waste Management Association* **2008,** *58* (7), 902-912.Doi 10.3155/1047-3289.58.7.902
97. New York State Department of Environmental Conservation, New York State's largest coal plants to slash pollution levels. *Environment DEC,* *http://www.dec.ny.gov/environmentdec/19027.html* **2005,** *Accessed April 2009,*
98. United States Environmental Protection Agency, Clean Air Interstate Rule. *http://www.epa.gov/cair/* **2009**,
99. Farrell, A. E.; Lave, L. B., Emission trading and public health. *Annual Review of Public Health* **2004,** *25*, 119-138.DOI 10.1146/annurev.publhealth.25.102802.124348
100. New York State Public Service Commission, Retail Renewable Portfolio Standard. *http://www.dps.state.ny.us/03e0188.htm* **2009**,
101. Us Department of Energy, E. E. a. R. E., Database of State Incentives for Renewables and Efficiency. *http://www.dsireusa.org/* **2009,** *Accessed May 2009,*
102. New York State Reliability Council, L. L. C., NYSRC Reliability Rules for Planning and Operating the New York State Power Systems. *www.nysrc.org/pdf/NYSRCReliabilityRulesComplianceMonitoring/RRManuaRev2Ver18.pdf* **2007**,
103. United States Environmental Protection Agency, Facility Registry System. *http://iaspub.epa.gov/sor_internet/registry/facilreg/home/overview/home.do* **2008**,
104. Carnegie Mellon University (CMU), Integrated environmental control model (IECM). *http://www.iecm-online.com/publications.html* **2008**,
105. Energy Information Administration, Receipts and Quality of Coal by Rank Delivered for Electricity Generation. *http://www.eia.doe.gov/cneaf/electricity/epm/table4_15.html* **2005,** *Accessed April 2009,*
106. Graus, W. H. J.; Voogt, M.; Worrell, E., International comparison of energy efficiency of fossil power generation. *Energy Policy* **2007,** *35* (7), 3936-3951.DOI 10.1016/j.enpol.2007.01.016
107. LADCO, BaseE Modeling Inventory, Midwest Regional Planning Organization. *http://www.ladco.org/tech/emis/BaseE/baseEreport.pdf* **2003,** *Accessed April 2006,*

108. CIESIN, Gridded Population of the World. *http://sedac.ciesin.columbia.edu/gpw/* **2008**,
109. European Commission (EC) *ExternE: Externalities of Energy, Vol 7-10*; Luxembourg, 1999;
110. Ventyx, Velocity Suite. *http://www.ventyx.com/velocity/vs-overview.asp* **2009,** *Acccessed April 2009*,
111. US Department of Energy: Energy Efficiency and Renewable Energy, New York Commission Approves Deal Doubling Wind Power, Oct 6 2008. *http://apps1.eere.energy.gov/states/news_detail.cfm/news_id=12035* **2008,** *Accessed April 2009*,
112. Newcomer, A.; Blumsack, S. A.; Apt, J.; Lave, L. B.; Morgan, M. G., Short run effects of a price on carbon dioxide emissions from US electric generators. *Environmental Science & Technology* **2008,** *42* (9), 3139-3144.Doi 10.1021/Es071749d
113. Energy Information Administration, Electric Power Annual. *http://www.eia.doe.gov/cneaf/electricity/epa/epa_sum.html* **2007**,
114. Energy Information Administration, Historical energy price data. *http//:tonto.eia.doe.gov* **2007,** *Accessed April 2009*,
115. New York Independent System Operator (NYISO), Load data. *http://www.nyiso.com/public/market_data/load_data.jsp* **2005,** *Accessed April 2009*,
116. Walawalkar, R., Emerging Electric Energy Storage Technologies and Demand Response in Deregulated Electricity Markets: http://wpweb2.tepper.cmu.edu/ceic/phd.htm#Walawalkar. *Thesis, Carnegie Mellon University* **2008**,